RISK ANALYSIS AND DECISION MAKING FOR AUTONOMOUS UNDERWATER VEHICLES

By

© Xi Chen

A Thesis submitted to the School of Graduate Studies

in partial fulfillment of the requirements for the degree of

Doctor of Philosophy

Faculty of Engineering and Applied Science

Memorial University of Newfoundland

July 2023

St. John's Newfoundland Canada

Abstract

Risk analysis for autonomous underwater vehicles (AUVs) is essential to enable AUVs to explore extreme and dynamic environments. This research aims to augment existing risk analysis methods for AUVs, and it proposes a suite of methods to quantify mission risks and to support the implementation of safety-based decision making strategies for AUVs in harsh marine environments. This research firstly provides a systematic review of past progress of risk analysis research for AUV operations. The review answers key questions including fundamental concepts and evolving methods in the domain of risk analysis for AUVs, and it highlights future research trends to bridge existing gaps. Based on the state-of-the-art research, a copula-based approach is proposed for predicting the risk of AUV loss in underwater environments. The developed copula Bayesian network (CBN) aims to handle non-linear dependencies among environmental variables and inherent technical failures for AUVs, and therefore achieve accurate risk estimation for vehicle loss given various environmental observations. Furthermore, path planning for AUVs is an effective decision making strategy for mitigating risks and ensuring safer routing. A further study presents an offboard risk-based path planning approach for AUVs, considering a challenging environment with oil spill scenarios incorporated. The proposed global Risk-A* planner combines a Bayesian-based risk model for probabilistic risk reasoning and an A*-based algorithm for path searching. However, global path planning designed for static environments cannot handle the unpredictable situations that may emerge, and real-time replanned solutions are required to account for dynamic environmental observations. Therefore, a hybrid risk-aware decision making strategy is investigated for AUVs to combine static global planning with dynamic local re-planning. A dynamic risk analysis

model based on the system theoretic process analysis (STPA) and BN is applied for generating a real-time risk map in target mission areas. The dynamic window algorithm (DWA) serves for local path planning to avoid moving obstacles. The proposed hybrid risk-aware decision-making architecture is essential for the real-life implementation of AUVs, leading eventually to a real-time adaptive path planning process onboard the AUV.

Acknowledgements

This thesis is written with tremendous support and assistance from the people who accompanied me during my doctoral research period.

I would like to first thank my supervisory committee. My deepest gratitude goes to Dr. Neil Bose. Thank you for providing me this valuable opportunity to conduct research on risk analyses for autonomous underwater robotics. You have been giving me boundless encouragement and unconditional support all the time during my PhD journey. Your kindness, generosity and humanity have always inspired me to move forward without fear. You are the perfect supervisor in my heart. I also want to thank my co-supervisors Dr. Faisal Khan (Texas A&M University), Dr. Mario Brito (University of Southampton), and Dr. Ting Zou. You have been my academic role models. You have always provided me significant guidance and support for my research with your extensive knowledge and broad vision. Thank you again everyone, I cannot emphasize enough my gratitude to my supervisors. I have no doubt that this challenging journey would not have been successful without them.

I would like to thank the company of my friends I met in St. John's, Yaomei Wang, Bo Thanyamanta, Craig Bulger, Gina Miller, Eonjoo Kim, Jimin Hwang, and Ginelle Nazareth. Thank you so much for your enormous support and warm accompany all the time, especially during the hard pandemic time. You are the brightening light in my dark times.

I gratefully acknowledge the following projects and sponsors. This research was funded by Fisheries and Oceans Canada through the "*Multi-partner Oil Spill Research Initiative (MPRI)*

1.03: Oil spill reconnaissance and delineation through robotic autonomous underwater vehicle technology in open and iced waters" and the NSERC Alliance Project "*Characterization and delineation of oil-in-water at the Scott Inlet seeps through robotic autonomous underwater vehicle technology 2021-2024*". I also acknowledge Memorial University and the School of Graduate Studies (SGS) for their component of fellowship support.

A special thanks to my family. I can never express how much I appreciate my parents. You always stand by me with the everlasting love. Thank you so much for your unconditional support for every decision I made. I believe it is the family full of love that gives me the courage to pursuit the doctoral degree, offers me the liberty to choose what I desired, and motivates me to achieve higher goals in the future. Last but not least, I want to thank my significant other, Yang Yang, my beloved and my best friend. You have always been there for me. You have embraced me just for who I am. Thank you for your continued and unfailing love, support and understanding during all the good and hard times.

Table of Contents

List of Tables

List of Figures

Nomenclature

Acronym	Definition
ABE	Autonomous Benthic Explorer
APF	Artificial potential field
AUGs	Autonomous underwater gliders
AUVs	Autonomous underwater vehicles
BBN	Bayesian belief network
BN	Bayesian network
CBN	Copula Bayesian network
DAG	Directed acyclic graph
DBN	Dynamic Bayesian network
DRA	Dynamic risk analysis
DWA	Dynamic window approach
DVL	Doppler velocity log
ETA	Event tree analysis
FBN	Fuzzy Bayesian network
FMEA	Failure mode and effects analysis
FTA	Fault tree analysis
FuSDRA	Fuzzy system dynamics risk analysis
GPS	Global positioning system
IMR	Inspection, maintenance, and repair
IMU	Inertial measurement unit
INS	Inertial navigation system
MASS	Maritime autonomous surface ships
OAT	One-at-a-time
RIFs	Risk influencing factors
RMP	Risk management process
RRT	Rapidly-exploring random trees
SD	System dynamics

STP	State transition probability
STPA	Systems theoretical process analysis
UCAs	Unsafe control actions
USV	Unmanned surface vessels
VFH	Vector field histogram

Chapter 1. Introduction

1.1 Background and motivation

Autonomous underwater vehicles (AUVs) are effective platforms for navigating underwater or under-ice to provide automated measurements without human intervention (Xu et al., 2013; Brito and Griffiths, 2016). The high level of autonomy of AUVs makes them an ideal tool for multiple data-gathering applications in scientific (Wadhams et al., 2006; Dowdeswell et al., 2008; Jenkins et al., 2010), commercial (Kleiner et al., 2011), military (Rothrock and Wensnahan, 2007), and geopolitical (Brito et al., 2012) areas. Equipped with various advanced sensors, AUVs can deliver high spatial and temporal resolution subsurface measurements (Rudnick et al., 2004b). However, operating in harsh marine environments with dynamic underwater conditions, poor visibility, and potential corrosion will inevitably pose the risk of vehicle damage or loss. Therefore, it is essential to conduct an effective risk analysis to ensure the safe deployment of AUVs. Hence, this study aims to provide systematic risk analysis approaches and safety-based decision making strategies for AUVs in challenging marine environments.

This thesis addresses risk analysis and risk-based decision making for AUVs. The following subsection defines the research questions and objectives that underlie this thesis.

1.2 Research questions and objectives

The overall research topic is risk-based decision making for navigation of AUVs. To achieve this core research objective, four subquestions need to be answered. The four subquestions and subobjectives of this thesis are presented in Fig. 1.1. Details of the research questions and objectives are elaborated in the following subsections.

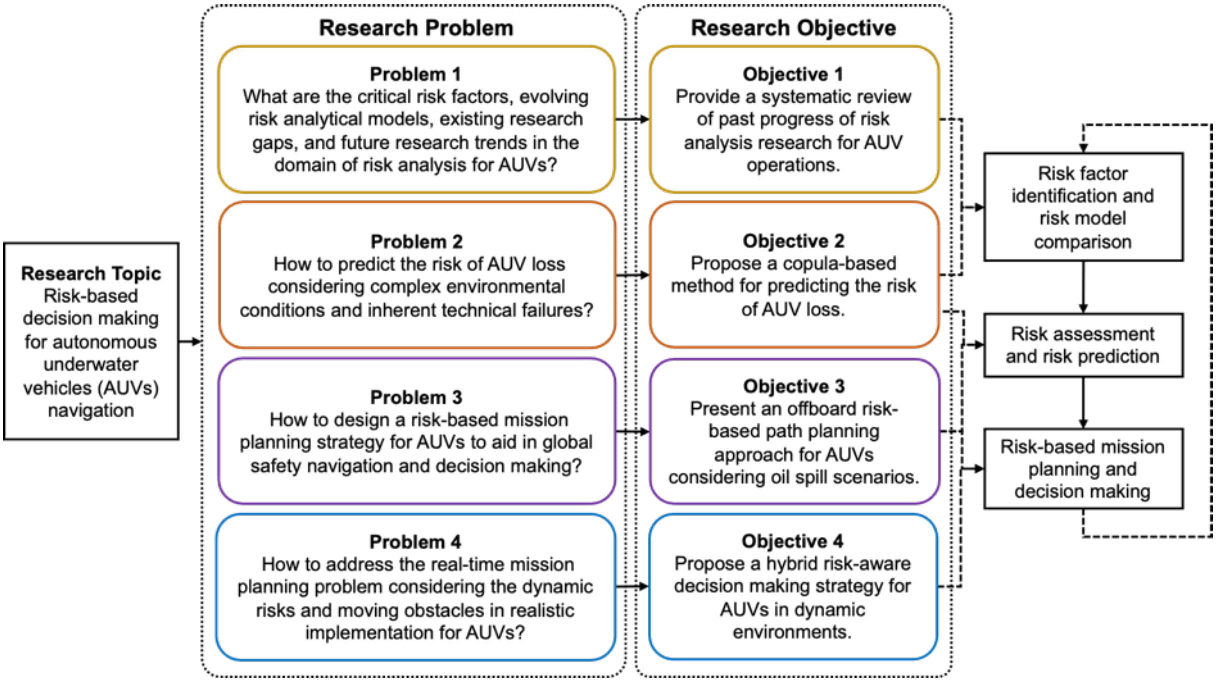

Fig. 1.1. Framework of the research problems and objectives

1.2.1 The first research question and objective

As AUV technologies have gradually matured, risk analysis for AUVs has become essential to ensure safer operations and assist decision making. A number of past efforts regarding risk analysis have been undertaken to improve the safety performance of AUVs. However, a systematic review and analysis of past studies has not yet been reported. As a thorough review will enable researchers to gain a better understanding of AUV risk analysis and benefit future development, a critical review of the state-of-the-art is timely.

In light of the above, the first objective of this study was to provide a structured review of risk analysis research regarding AUV operations. It aimed to answer four key questions arising from historical developments and to highlight future trends in this domain. The main contribution of the literature review was to help researchers and AUV stakeholders obtain comprehensive insights about fundamental concepts and evolving methods for the risk analysis of AUVs. Meanwhile, it was also intended to indicate directions for future research to bridge existing gaps.

1.2.2 The second research question and objective

Autonomous underwater gliders (AUGs) are a type of autonomous underwater vehicles (AUVs), which are characterized by long endurance, slow speed, low energy consumption, and a wide survey range (Roper et al., 2021; Wang et al., 2021b; Wang et al., 2022b). AUGs can operate in multiple types of underwater environments, such as in open water, under sea ice or ice shelves, and near coastal areas (Brito et al., 2008). However, complex underwater conditions and the long cruise endurance of AUGs could expose them to an increased risk of loss. The main limitation of current studies for AUGs is the lack of a tailored method for risk analysis considering both dynamic environments and potential functional failures of the vehicle.

Hence, the second objective of this study was to propose a coupla-based approach for risk prediction of AUGs in dynamic underwater environments. Both open water and coastal water environments were considered in this study, while conditions of under ice or under ice shelves were not within the scope. The developed coupla Bayesian network (CBN) aimed to capture non-linear environmental impacts on the functional failures of AUGs, thereby estimating the risk of vehicle loss given various environmental conditions. The contribution of this research was twofold. Firstly, the proposed method was tailored for AUGs. It captured the synergies between AUGs′ inherent functional failures and influential environmental factors, whilst considering the dynamic nature and non-linear dependencies among their relationships. The predicted risk profile can assist further decision making and risk mitigation during real AUG missions. Secondly, this study not only added details to risk analysis for AUGs, but also extended the application of the CBN model into a broader AUV domain. The present model is not restricted to an AUG system but can be flexibly adapted to other AUV platforms by incorporating the vehicle′s specifications to enhance safety performance.

1.2.3 The third research question and objective

An oil spill is one of the major accidents in the ocean that can damage the marine ecosystem, social economy, and human health (Hwang et al., 2020; Zhu et al., 2021). Due to hazardous effects of oil spills, it is essential to detect and track the oil during or after a spill for environmental impact assessment and response decision-making (White et al., 2016). Compared with traditional survey tools such as ships or unmanned aerial vehicles, AUVs coupled with multiple sensors are superior in providing high-resolution sampling data of submerged oil plumes, achieving communication of spill information in near real-time, as well as preventing personnel exposure to hazardous oil spill environments (Pereira et al., 2013; Vinoth Kumar et al., 2020). Therefore, it is beneficial to deploy AUVs to search and delineate subsurface oil plumes, capturing oil behaviors, and improving the efficiency of oil spill response. However, operating in an oil spill environment could expose AUVs to the risk of loss due to the effects of ocean currents, surface waves, potential underwater obstacles, and oil contamination on sensors. Hence, it is essential to minimize the risk of loss presented by these factors and enhance their safety navigation during spill response missions. Risk-based path planning is one of the critical techniques for mitigating risks and ensuring AUVs′ safe deployment before a mission. It refers to planning an optimal path for the vehicle from its initial state to the goal state of a mission considering the risk involved, which is under certain criteria (e.g., shortest path length, minimal cruise time, minimal risk profile), and as the same time, avoiding obstacles along a path (Zeng et al., 2015; Lefebvre et al., 2016; Guo et al., 2021).

While previous studies have explored different risk-based path planning methods for mitigating AUV risks, limitations were observed from them. Firstly, most of the former research only addressed risks in a general marine environment with impacts of a single environmental variable, for example, underwater currents (Pereira et al., 2013). However, to the authors knowledge, there are no former studies considered the scenario of AUVs navigating in complex oil spill environments with interactions of multiple risk variables, and accordingly provided the mission planning strategy from a safety perspective. Secondly, limited past works have applied a probabilistic model for quantifying the risk state of AUVs given varied environmental observations. While probabilistic reasoning could enhance the accuracy of risk prediction and further improve the efficiency of decision making, therefore, a rigorous method that integrates a probabilistic risk model into the path planning problem for AUVs is needed.

Therefore, the third objective of this study was to propose a risk-based path planner for AUVs to improve their safety performance and enhance autonomous capabilities in oil spill environments. Specifically, hazardous impacts of potential risk variables in oil spill regions were analyzed. A risk analysis model based on the Bayesian network (BN) was then developed for probabilistic reasoning over current risk states of vehicle loss, which considered various environmental conditions and potential underwater obstacles. This risk model was extended to assist in generating a risk map of a gridded mission area. In order to avoid high-risky regions while achieving a relatively shorter path length, the A* algorithm was employed to search for a Risk-A* solution. The performance of the proposed planner was demonstrated in a simulated case study with a spill area in Baffin Bay.

1.2.4 The fourth research question and objective

Global path planning designed for static environments cannot handle the unpredictable situations that may emerge, and re-planned solutions are required to account for dynamic environmental observations. Hence, the last objective of this study was to explore a hybrid risk-aware architecture for AUVs′ autonomous mission planning to combine static global planning and dynamic local re-planning, which is essential for the real-life decision making of AUV missions. Specifically, a risk model based on the STPA-BN was adopted to predict the risk of vehicle loss given varied environmental conditions. The A* algorithm was applied for global path planning to generate a global path for AUVs to reach the target. Then the dynamic window algorithm (DWA) was used for local path planning to avoid dynamic obstacles.

1.3 Research contributions

The research outcomes of this thesis represent original contributions to the domain of risk analysis and safety-based decision making for AUVs navigation. The contributions of this thesis mainly contain four aspects.

(i) This research presented a comprehensive review of past progress of risk analysis research for AUV operations. This review addressed questions related to basic concepts and developing methods within the field of risk analysis for AUVs, while also emphasizing potential trends for future research. The underlying risk factors were identified, and the evolving risk analysis methods were comparatively analyzed. The main contribution of this review is beneficial for domain researchers to obtain comprehensive insights about risk analysis of AUVs. Meanwhile, it is expected to indicate directions for future research to bridge existing gaps.

(ii) This study contributed a potential approach of risk prediction tailored for AUGs in complex underwater environments. It captured the synergies between AUGs′ inherent functional failures and dynamic environmental conditions, whilst achieving updated risk prediction for AUG loss both temporally and spatially. The developed model can be extended to applications for other types of AUVs by incorporating the vehicle′s inherent specifications. The present work can potentially improve the safety performance of AUGs and assist risk mitigation in decision making.

(iii) This study provided a rigorous global path planning method for AUVs from a safety perspective. The integrated BN-based risk model can predict the risk states of AUVs while intuitively presenting spatial risk distributions in a complex oil spill environment. The probabilistic reasoning can enhance the effectiveness and accuracy of further risk-based decision making. Furthermore, the developed Risk-A* planner can avoid potential risky regions and obstacles, and meanwhile, it achieved a trade-off between risk mitigation and mission efficiency. It is expected that the proposed strategy can serve as a worthwhile precomputing policy to prevent AUV loss at the path planning stage, and therefore enhance the safety decision-making capability of AUVs for safer navigation.

(iv) This research developed a risk-ware hybrid path planning strategy for AUVs operating in challenging environments. The risk factors of vehicle loss were identified from a control perspective using the STPA framework. The risk state of the vehicle during navigation was rigorously estimated based on an online STPA-BN model. The predicted risk index was integrated into a hybrid path planning module to achieve real time risk-aware decision making. The proposed risk-aware path planning strategy that considers the risk cost during cruising exhibited better performance in avoiding risky regions along a path. It helped to select safer waypoints in real time, and at the same time, it mitigated the risk level within a tolerable threshold to ensure safe navigation.

1.4 Thesis outline

This thesis consists of six chapters and is organized in a manuscript format. Four of the chapters include parts that have been submitted or accepted for publication. The thesis abides by 'A thesis by peer-reviewed research publication' strategy. The overview of each chapter is provided as follows.

Chapter 1 introduced the background, motivation, research questions, research objectives, contributions, and outline of this thesis.

Chapter 2 provided an extensive literature review of risk analysis research regarding AUV operations. It aimed to answer key questions covering historical developments and future trends in this research domain. By retrieving and analyzing former literature, this chapter identified critical risk factors of AUV operations, summarized the evolving risk analysis models, and highlighted the existing limitations and future directions. This chapter provided the research foundation for the following chapters.

Chapter 3 proposed a copula-based approach for risk prediction of AUV loss in dynamic underwater environments. The developed CBN model aimed to handle non-linear dependencies among environmental variables and inherent technical failures for AUVs. In the constructed CBN structure, a Bayesian Belief Network (BBN) model was firstly applied for identifying potential risk variables and their causal relationships to vehicle loss. Copula functions were then incorporated to quantitatively capture the dependencies among risk variables and predict the risk level. The effectiveness of the proposed method was demonstrated in a case study, which considered deploying a Slocum G1 Glider in a real water region. Risk mitigation measures were also provided according to case study results. This chapter has proved that the BBN model can serve as a basic risk model for AUVs. Therefore, the following chapters mainly applied the BBN model for risk-based decision making.

Chapter 4 proposed an offboard risk-based path planning strategy for AUVs considering the complex oil spill environment. A risk model based on the BN was developed for probabilistic reasoning of risk states given varied environmental observations. This risk model further assisted in generating a spatially-distributed risk map covering a potential mission area. A Risk-

A* searching algorithm was then employed to plan a Risk-A* path through the constructed risk map. The proposed planner was applied in a case study with a Slocum G1 Glider in a real-world spill environment around Baffin Bay. This chapter was the foundation for the next chapter to propose a hybrid path planner combining both static global planning and dynamic local re-planning.

Chapter 5 proposed a hybrid risk-aware decision making strategy for AUVs, which aimed to bridge risk identification from a control perspective, real-time risk modelling, and risk-aware path planning to achieve more intelligent and safer deployment of AUVs. Specifically, the risk state of the vehicle during navigation was rigorously estimated based on an online risk model. The predicted risk index was integrated into a hybrid path planning module to achieve real time risk-aware decision making.

Chapter 6 summarized the overall thesis and discussed the key research findings of each chapter. A comprehensive conclusion was derived from the thesis outcomes. As the closing chapter of this thesis, limitations and future work were also highlighted in this chapter.

Chapter 2. Literature Review

Preface

A version of this chapter has been published as: ***Chen X, Bose N, Brito M, et al. A review of risk analysis research for the operations of autonomous underwater vehicles [J]. Reliability Engineering & System Safety 2021, 216: 108011****. I am the primary author along with the Co-authors, Neil Bose, Mario Brito, Faisal Khan, Bo Thanyamanta, and Ting Zou. I developed the conceptual framework for the review of risk analysis research for the operations of autonomous underwater vehicles. I prepared the first draft of the manuscript and subsequently revised the manuscript based on the co-authors′ and peer review feedback. Co-authors Neil Bose, Mario Brito, and Faisal Khan provided support in implementing the concept development, reviewing, and revising the manuscript. Co-authors Bo Thanyamanta and Ting Zou provided assistance in reviewing and correcting the results. The co-authors also contributed to the review and revision of the manuscript.*

Abstract: This chapter presents a comprehensive literature review of past progress of risk analysis research for AUV operations. It answers key questions including fundamental concepts and evolving methods in the domain of risk analysis for AUVs, and it highlights future research trends to bridge existing gaps. Forty-two domain articles are retrieved and analyzed in this chapter. Through this literature review, critical risk factors and causal relationships of AUV operations were identified. A comparative analysis of evolving methods and models was performed by categorizing them as qualitative, semi-quantitative, and quantitative. Future trends of research in this field were also outlined. This chapter plays a key role to provide

fundenmental knowledge and comprehensive understanding of the research of AUV risk analysis.

2.1 Introduction

AUVs are untethered and unmanned platforms to provide automated measurements in dangerous, distant, and dynamic ocean environments (Caress et al., 2008). They have been increasingly applied in various oceanic observations, such as seawater sampling (Hwang et al., 2019), oil spill detection (Wang et al., 2022c), seafloor mapping (Zwolak et al., 2017), pipeline inspection (Xiang et al., 2010), and so on. The expanded applications of AUVs are in parallel with significant improvements in cruise endurance, range, and payload sensor advancement (Zhang et al., 2011). In recent research, AUVs are increasingly deployed in harsh environments such as under sea ice or ice shelves in the Antarctic (Jenkins et al., 2010; Williams et al., 2015; Gwyther et al., 2020) and the Arctic regions (Wadhams et al., 2006; Dowdeswell et al., 2008; Salavasidis et al., 2016). Operating in such extreme conditions, including thick ice cover, permafrost, fragile material integrity, unpredictable climatic changes, and poor visibility, will inevitably pose a higher risk to both the physical vehicle and the onsite AUV supervisors (Loh et al., 2020c). Hence, it is essential to conduct effective risk analysis before a mission to ensure the safe deployment of AUVs.

Table 2.1, which is adapted from a former study (Hu et al., 2013), summarizes potential accident types of AUV operations and their severity according to the level of damage to the vehicle itself, where AUV loss could be regarded as the most severe accident. AUV loss usually refers to the complete loss of the physical vehicle or an AUV being damaged and unrepairable for future missions. It is not only financially costly due to the higher insurance premium and acquisition costs of the vehicle (Griffiths et al., 2007a), furthermore, it may also cause time delays or even the termination of research projects, lead to the loss of valuable gathered data, and potentially harm fragile polar environments (Griffiths and Collins, 2007; Brito et al., 2010).

Table 2.1. Classification of the consequence severity of AUV operations, adapted from (Hu et al., 2013).

Level	Consequence	Severity
I	AUV loss	Catastrophic
II	Severe damage, mission failure, mission abort	Critical
III	Mitigable damage, mission degraded, mission delayed	Moderate
IV	Minor damage	Marginal
V	Minimal damage or no damage	Negligible

Over the years, there have been a number of formally reported accidents of AUV losses during deployment, as shown in Fig. 2.1. For example, the AUV Autosub2 was lost under the Fimbulisen ice shelf in Antarctica in February 2005. A formal accident inquiry concluded that this accident was equally likely to have been caused by an abort command or a loss of power. Such technical failures could be most likely introduced during the manufacturing and assembly phases (Strutt, 2006). Another lost vehicle, SeaBED, which was designed to scan the seafloor below overhanging sea ice, became trapped under the Antarctic ice during a mission and was almost crushed by an iceberg before it was rescued (Waters, 2015). The Autonomous Benthic Explorer (ABE) was lost in March 2010, during its 222nd research dive off the coast of Chile. Researchers believed that the loss of the ABE was also caused by a technical failure. More specifically, the ABE may have suffered a catastrophic implosion of a glass sphere used for providing buoyancy, causing instant destruction of the on-board systems. Consequently, the ABE failed to send fail-safe commands for helping itself float to the surface for recovery (Lippsett, 2010). An underwater glider, Seaglider SG522, lost communication in the Antarctic in February 2012 after having completed 156 dives. The inquiry panel identified that the root cause was an erroneous command, which resulted in this glider continuously diving and eventually being lost (Brito et al., 2014b). In April 2014, the Autosub Long Range AUV lost communication during a mission near the Irish coast. Luckily, it re-transmitted its position signal and was recovered after three months. More recently, a Hugin AUV was lost during its first under ice mission in the Antarctic in January 2019, and it was recovered four days later. Pre-dive checks had been reviewed for this vehicle without any irregularities. Technicians believed the vehicle was trapped below an ice floe, causing the Iridium signal for the AUV position failing to be received (Bound, 2019).

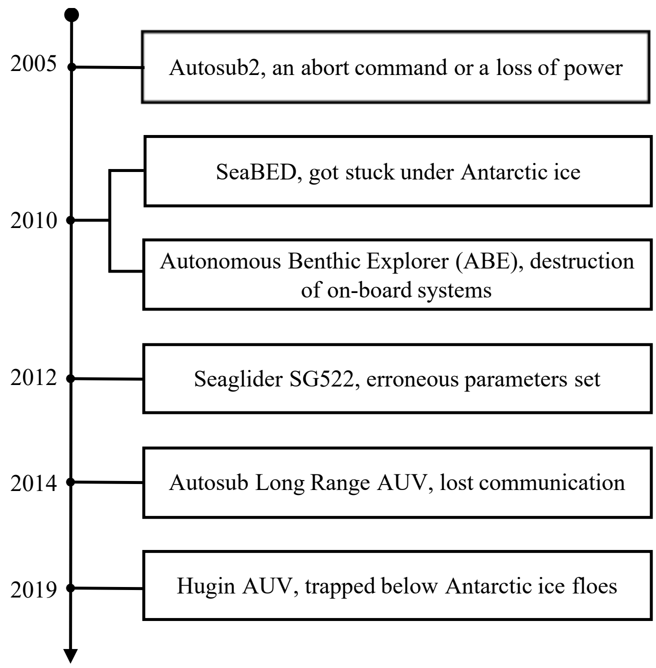

Fig. 2.1. Timeline and potential causes of historical accidents of AUV loss.

From the overview of historical accidents of AUV loss, it can be observed that the potential causes of historical accidents show a wide variety, which confirms the unpredictable and uncertain features of AUV related accidents. This non-uniform accidental pattern and relatively severe consequences imply the vulnerability of AUV operations and reinforce the necessity of implementing effective risk analysis before an AUV mission.

Risk analysis is a proactive approach for hazard identification, consequence analysis, and risk estimation for potential accidents (Rausand, 2013). There is a long history of the development of risk analysis techniques that have been applied in multiple fields, including nuclear power, chemical process, aerospace, and offshore oil and gas industries (Paté-Cornell and Dillon, 2001; Khakzad, 2015; Yang and Haugen, 2016; Zhou et al., 2021). Currently, with the booming development of the maritime industry, applications of risk analysis methods are also stimulated in this area (Madsen et al., 2000; Thieme and Utne, 2017; Wróbel et al., 2018b; Du et al., 2020; Wang et al., 2021a). Since marine systems are becoming more autonomous, using the AUV is an ongoing trend in the maritime industry for ocean research, ocean monitoring, military and commercial data-gathering, and so on (Brito and Griffiths, 2016; Thieme and Utne, 2017). As AUV technologies have gradually matured, risk analysis for AUVs has rapidly become essential to ensure safer operations and assist decision making. A number of past efforts regarding risk analysis have been undertaken to improve the safety performance of AUVs. However, to the best knowledge of the author, a systematic review and analysis of past studies has not yet been done. As a thorough review will enable domain researchers to gain a better understanding of AUV risk analysis and benefit future development, the author believe that a comprehensive literature review is timely.

In light of the above, the objective of this chapter is to provide a structured review of risk analysis research regarding AUV operations. It aims to answer four key questions arising from historical developments and to highlight future trends in this domain. As listed in Table 2.2, the four key questions show the overall structure of this literature review from analyses of past studies. The main contribution of this chapter is to help researchers and AUV stakeholders obtain comprehensive insights about fundamental concepts and evolving methods for the risk analysis of AUVs. Meanwhile, it is expected to indicate directions for future research to bridge existing gaps.

Table 2.2. Research questions and corresponding sections.

Question	Description	Section
Q_1	What is risk analysis for AUV operations?	Section 2.1
Q_2	What is the benefit of risk analysis for AUV operation?	Section 2.1
Q_3	How is risk analysis implemented for AUV operations?	Section 2.2&2.3
	$Q_{3,1}$: What are the key risk factors identified in past studies?	Section 2.2
	$Q_{3,2}$: Which risk analysis method was adopted in past studies?	Section 2.3
	$Q_{3,3}$: What are the advantages and disadvantages of these methods?	Section 2.3
	$Q_{3,4}$: What trends can be observed regarding past studies?	Section 2.2&2.3
Q_4	What are the future challenges of risk analysis for AUV operations?	Section 2.4

The scope of this chapter is restricted to risk analysis for AUV operations. According to the objective and scope of this review, the literature retrieval was performed based on keywords searching including AUVs with the combination of risk identification, risk analysis, risk assessment, risk management, risk mitigation, risk modeling, safety measures, and emergency system. A total of forty-two articles with significant relevance to the research purpose and scope were retrieved. In addition, to better answer the research questions and facilitate further statistical analysis, the selected publications were classified into various aspects, including the type of identified risk factors, the type of adopted risk analysis methods, the type of mission forms, the area of operations, and the type of potential consequences. The dataset of selected literature is classified and summarized in the Appendix.

The chapter is structured as follows. In section 2.2, critical risk factors of AUV operations are analyzed by categorizing them into technical factors, environmental factors, and human factors. Section 2.3 compares the evolving methods or models applied for AUV risk analysis by classifying them as three types: qualitative methods, semi-quantitative methods, and quantitative methods. Section 2.4 outlines current research gaps and future directions. The summary and conclusion of this chapter are given in Section 2.5.

2.2 Risk factors identification for AUV operations

Risk factors identification is defined as the process of identifying potential risk factors, which is the first step of the risk analysis phases (Rausand, 2013). Based on past studies, risk factors related to AUV operations are identified and analyzed in this section by categorizing them into technical factors, human factors, and environmental factors. Fig. 2.2 presents the number and distribution of former publications regarding these three types of risk factors. As mentioned in Section 2.1, the publication counting for the statistical analysis is based on the Appendix table.

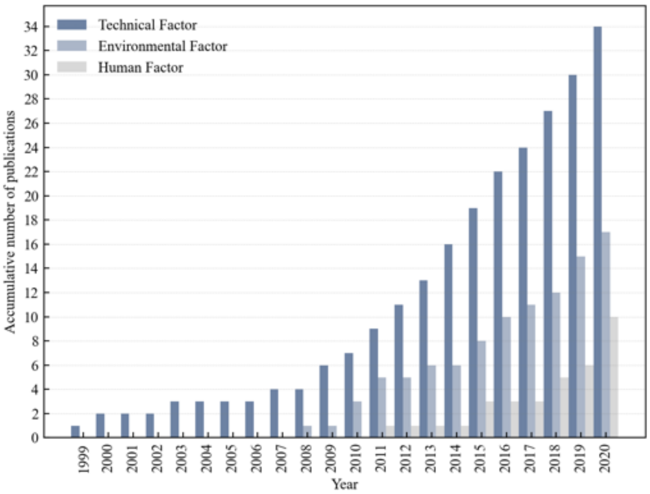

(a)

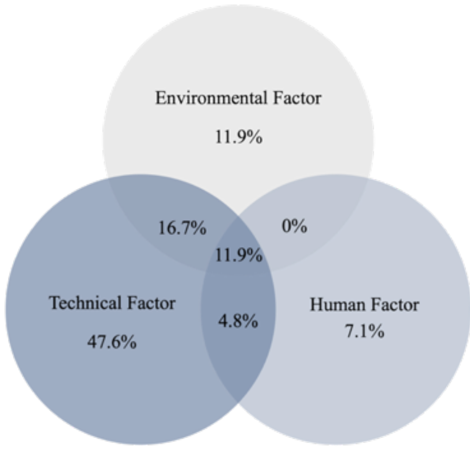

(b)

Fig. 2.2. Statistics of the research of three risk factors regarding (a) the accumulative number of publications and (b) the proportion of the publications.

From Figure. 2.2, it is observed that risk analysis research of AUVs regarding technical factors has been steadily increasing over the last two decades and surpasses the number of research regarding other two factors. By contrast, risk analysis research of AUVs regarding human factors, environmental factors, and interactive factors is emerging in recent years and receiving more attention. Each of the three risk factors is elaborated in the following subsections.

2.2.1 Technical Factors

Before the analysis of technical factors regarding an AUV system, it is important to understand different concepts between a failure, fault, and error. A failure refers to the inability of a component or system to perform a required function. A fault is defined as an abnormal condition, state, or defect, which may lead to a failure. An error refers to the discrepancy between a value, condition, or human behavior. It usually occurs when deviating from the target performance, which can also cause a failure (Rausand and Høyland, 2003).

A technical factor is defined as a risk contributor that is directly related to the AUV technical systems and components (Hegde et al., 2018). Previous studies have primarily focused on improving the technical performance of AUVs. As shown in Fig. 2.2(b), the number of studies related to technical factors accounts for 47.6% of the domain publications. With complex subsystems and components of an AUV, a technical failure can easily occur with electromechanical equipment, and then cause functional failures of a certain subsystem. Since an AUV works mainly depending on the cooperation of their subsystems, once a subsystem fails to work, there is a high risk of the overall mission failure. In particular, as a self-contained submarine robot, there is limited scope for calibrating and testing each component or subsystem thoroughly before a mission. Therefore, technical factors are most fundamental and paramount for the safe deployment of AUVs.

To better identify technical factors of AUVs, it is important to understand the main functions of AUV subsystems and key components, which are summarized in Table 2.3. The major subsystems of an AUV consist of the propulsion system, navigation system, communication system, power system, sensor system, and others.

A propulsion system is responsible for providing the propulsive force and, in the case of gliders, for changing the buoyancy. In general, AUVs can be classified into two types according to their different propulsion systems. The first type is actively-propelled AUVs with traditional propellers or thrusters to empower propulsion behavior, including horizontal and vertical movement. Another type is passively-propelled AUVs, such as traditional underwater gliders, which employ variable-buoyancy propulsion without any propellers or thrusters. Traditional gliders can ascend and descend underwater purely controlled by a buoyancy changing system. Simultaneously, they use wings to convert the vertical motion into horizontal motion, thereby achieving a sawtooth pathway in the water column. Currently, hybrid-driven gliders were born combining both propulsion and buoyancy systems. The hybrid gliders, such as the Slocum glider, Seaglider, Sea Explorer, and Folaga glider, are more maneuverable compared to traditional gliders, as they can fulfill both the depth-keeping cruise and saw-tooth gliding (Alvarez et al., 2009).

A navigation system enables an AUV to follow a predefined trajectory by measuring its position, attitude, and velocity. Among several kinds of navigation systems of AUVs, the inertial navigation system (INS) is widely used. The INS typically contains an inertial measurement unit (IMU) including accelerometers and gyroscopes. For inertial navigation, the linear acceleration is measured by accelerometers, and the angular velocity is measured by gyroscopes, and these parameters are combined to calculate the instantaneous velocity and position of the vehicle (Paull et al., 2014; Bao et al., 2020). In addition, some additional components, such as a Doppler Velocity Log (DVL), compass, pressure sensor, or global positioning system (GPS), are usually combined with the INS to provide integrated navigation. Among these auxiliary components, a DVL is an acoustic sensor that measures the velocity and position of the vehicle relative to both the sea bottom and sea flow, which can only function when the seabed is within the range of the instrument; a compass is used for orientation that provides the heading direction for the vehicle; a pressure sensor is used to measure the external pressure of the vehicle, from which the water depth can be estimated; GPS is a satellite-based positioning system, which enables an AUV at the water surface to acquire its position information, and GPS signals are input to the INS to correct the position measurement.

A communication system is used for transferring the mission instructions and monitoring the vehicle′s state, and it is particularly crucial during multi-vehicle missions. This system includes two parts: underwater communication is achieved by an acoustic modem, and above-water communication is achieved by local radio or satellite communication with an antenna.

A power system provides electrical energy by lithium-ion batteries or alkaline batteries (Griffiths et al., 2007b). Former studies have proved that more than 50% of AUV loss accidents are related to a power failure (Meng and Qingyu, 2010; Yu et al., 2017). In particular, an early study analyzed 63 mission abort incidents from a total of 205 glider missions (Brito et al., 2014a). As shown in Fig. 2.3, among the identified 19 failure modes of gliders, power failure was ranked as the second most common failure mode. Since the power system provides energy for all electrical motors, sensors, and the central computer, it is critical for the normal functioning of AUVs. In addition, it impacts the mission endurance, which is influenced by the available energy storage and the energy consumption rate.

An environmental recognition system generally processes sensor data to perceive the surrounding environment, detects the forward obstacles, and prevents the AUVs from colliding with the seafloor.

An emergency system ensures safety in emergency situations. It overrides the navigation system by employing low-risk path planning during the collision avoidance maneuver (Hegde et al., 2018). In addition, it also predominates the propulsion system in dangerous situations. For example, it can provide fail-safe measures by releasing the drop-weight, aborting the mission, and floating the vehicle to the water surface for rescue.

Table 2.3. Identification of AUV subsystems and risk factors.

AUV Subsystem	Functionality	Main Component	Risk Factor	Reference
Propulsion System	Provide the propulsive force Change the buoyancy	Propeller or thruster (active-propelled AUV) Variable-buoyancy system (passive-propelled AUV)	Thruster failure Buoyancy pump failure Bladder leak Fin actuator failure Rudder broken	(Griffiths et al., 2003; Bian et al., 2009a, b; Xu et al., 2013; Aslansefat et al., 2014a; Yu et al., 2017; Hegde et al., 2018)
Navigation System	Measure the position, attitude, and velocity data Provide dead-reckoning navigation Follow the predefined trajectory	DVL On-board GPS receiver Attitude sensor Depth sensor Altimeter	DVL failure Depth sensor failure Altimeter failure Inertial navigation failure GPS module failure	(McPhail, 1998; Griffiths et al., 2003; Bian et al., 2009a, b; Xu et al., 2013; Aslansefat et al., 2014a; Yu et al., 2017; Hegde et al., 2018)
Communication System	Underwater communication Above water communication Transfer and control the mission instruction	Acoustic sensor Radio transceiver module	Underwater acoustic sensor failure Radio communication failure Signal transmission failure Host computer failure	(Bian et al., 2009a, b; Aslansefat et al., 2014a; Brito et al., 2014b; Yu et al., 2017; Hegde et al., 2018)
Power System	Provide electrical energy	Lithium-ion battery	Energy depletion	(Bian et al., 2009a, b; Xu et

		Alkaline battery	Fail to charge Overcharging Battery detection failure Voltage and current monitoring failure	al., 2013; Aslansefat et al., 2014a; Allotta et al., 2017; Yu et al., 2017; Hegde et al., 2018; Locorotondo et al., 2021)
Environmental Detection System	Perceive the surrounding environment Avoid the forward obstacles Prevent colliding with the seafloor	Camera Forward-looking sonar	Underwater camera failure Light sources failure Sonar suite failure	(Bian et al., 2009a, b; Xu et al., 2013; Aslansefat et al., 2014a; Yu et al., 2017; Hegde et al., 2018)
Emergency System	Ensure safety in an emergency Alternate the low-risk path planning Jettison weight for fail-safe	Drop-weight	Hermetic hull broken Leak detection sensor failure Jettison device failure Mission aborting command failure	(Ortiz et al., 1999; Bian et al., 2009a, b; Xu et al., 2013; Yu et al., 2017; Hegde et al., 2018)

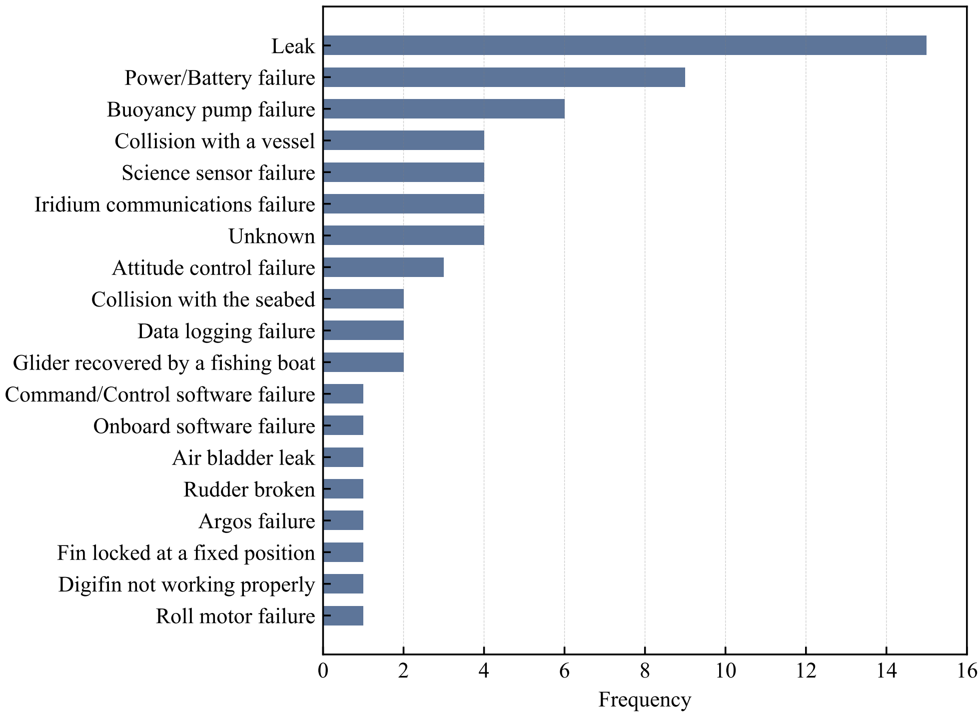

Fig. 2.3. Failure modes and their frequency during 63 abort incidents from 205 glider missions (Brito et al., 2014a).

There are various strategies to improve the technical performance of an AUV. Redundancies of key components can be adopted from the hardware level (Yu et al., 2017). For example, the redundancy of the propulsion system plays a key role in enhancing the safety of the vehicle. In case of a propulsion failure, a backup propulsion system could assure that the vehicle completes the mission and safely returns to the base, without losing any degree of freedom (Pugi et al., 2018). In another word, this backup functionality makes the vehicle more tolerant to a single failure. Therefore, the redundant solution not only achieves improved maneuverability but also enhances the failure robustness of the vehicle. From the software level, online monitoring and repairing could serve as effective risk mitigation measures (Aslansefat et al., 2014a). In addition, as most failures occur in the early phase of a mission, an endurance test can be performed in the operational configuration to monitor key subsystems before a mission (Kaminski et al., 2010). A mission can then proceed only when the vehicle operates properly during the endurance test. Otherwise, the vehicle should be recovered for onboard fault checking. Moreover, since AUVs might periodically return to a docking station for recharge, the problem of improper manipulation and positioning of electrical connections during recharging should be noticed. To address this problem, a current work provided a valid solution of underwater wireless power connection for the recharge (Allotta et al., 2017). This wireless recharging strategy could significantly simplify recharge operations in the underwater environment and protect the vehicle from the power failure as well. Another solution to prevent the power failure is to assure the safe state of batteries. A real-time diagnostic method was proposed to assess and monitor the state of health of lithium batteries (Locorotondo et al., 2021). A fast impedance measurement was applied to provide accurate diagnostic detecting of the operating conditions of the battery, which is simple to be implemented for AUVs.

2.2.2 Human Factors

The maturing of AUV technologies has fostered a gradual shift to risk analysis of human operators. To comprehensively control the risk of AUV deployments, human factors, which are critical but relatively difficult to quantify, are receiving more attention in the AUV risk management process. Human intervention influences the autonomy of AUVs. It should be noted that the autonomy is defined as the capability of a system to make decisions independently, which can be measured by six levels, namely (i) human operated, (ii) human assisted, (iii) human delegated, (iv) human supervised, (v) mixed initiative, and (iv) fully autonomous

(Thieme et al., 2015b). The level of autonomy denotes the involvement of human operators, i.e., a higher level of autonomy refers to less human intervention. Current AUV systems can be categorized into levels (ii), (iii), and (iv), while future AUVs may reach the level (v) and level (vi). Therefore, although an AUV system in the current state has a certain level of autonomy, human operators still play a vital role as a supervisor. The main intervention of human operators includes determining mission plans in the design phase, performing the launch and recovery of the vehicle, making decisions when encountering emergencies, and so on (Wróbel et al., 2017; Loh et al., 2020c). Noticeably, human errors may lead to the AUV being susceptible to failure. During the four-year missions of the Autosub3 AUV from 1996 to 2000, most of the faults were notably identified as a result of human errors rather than technical failures, as shown in Fig. 2.4 (Griffiths et al., 2003). This former study proved that human factors play a key role for AUV risks.

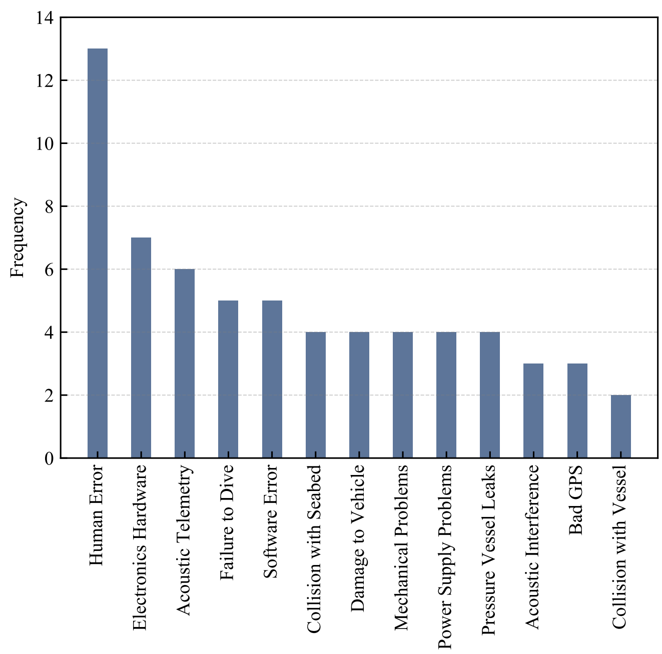

Fig. 2.4. Failure modes and their frequency during missions 1-240 of the Autosub3 AUV from 1996 to 2000 (Griffiths et al., 2003).

Other researchers have begun to recognize the importance of human factors contributing to the overall risk of AUV operation (Manley, 2007; Ho et al., 2011; Akhtar and Utne, 2014). A risk management framework incorporating human and organizational factors was established (Thieme et al., 2015a). This study proposed a structured approach to assess the risk of AUV loss and mission aborts resulting from human factors. Potential risk mitigation measures were provided, including procedures improvement, mission planning, and fault recognition. A case study involving the operation of the REMUS 100 AUV was conducted, which proved that risk analysis should consider not only the technical system itself but also the human interaction with the system. Extended studies assessed human factors in risk monitoring of AUV missions (Thieme et al., 2015b; Hegde et al., 2018). Detailed information of human factors, such as the level of training, operator experience, operator fatigue, and situation awareness, were analyzed in these studies. Furthermore, a system-based risk analysis framework was proposed for an in-depth analysis of the impact of human factors (Loh et al., 2019; Loh et al., 2020a; Loh et al., 2020b; Xu et al., 2020). Based on these former studies, identified human factors are summarized in Table 2.4. Several key findings were demonstrated as follows. Firstly, the risk level of AUV loss will gradually drop in the initial years of the formation of an AUV team, reaching a minimal level before rising again in later periods. In addition, the incident rate of human errors was proven to decline with the overall increase of the experience of an AUV team. Therefore, increasing the experience of AUV operators can be an effective way for risk mitigation, which can be achieved by safety training, human resources allocation, recruitment, and staff retention.

Table 2.4. Identified human factors in previous literature.

Human Factor	Description	Reference

Supervisory error checking	Ability of the operator to timely identify errors and contingency situations during a mission.	(Loh et al., 2020c)
Supervisory handling	Ability of the human supervisor to take required actions.	(Hegde et al., 2018; Loh et al., 2020c)
Wrong configuration setting	Wrong configuration parameters of a sensor are set which might lead to incorrect measurement.	(Loh et al., 2020c)
Workload	Number of tasks that the operators are required to execute.	(Parasuraman and Miller, 2004; Ho et al., 2011; Thieme et al., 2015b)
Experience of operators	Level of experience of the operators with the deployment mission.	(Manley, 2007; Loh et al., 2020a; Loh et al., 2020c, b)
Human fatigue	Inability to function at the desired level due to incomplete recovery from the demands of prior work and other working activities.	(Akhtar and Utne, 2014; Loh et al., 2020c)
Training of operators	Level of required operational and safety training for a human supervisor.	(Thieme et al., 2015b; Hegde et al., 2018)
Situational awareness	Ability to monitor the system, comprehend the information and take the right decisions.	(Ho et al., 2011; Johnson and Lane, 2011)
Communication of operators	Level of communication effectiveness among operators and the crew.	(Thieme et al., 2015b)
Trust in the system	Level of the operator's belief in the autonomous capabilities of the AUV.	(Parasuraman and Miller, 2004; Johnson et al., 2007; Ho et al., 2011)

2.2.3 Environmental Factors

AUVs operate in several typical subsea environments, such as under open water (Brito et al., 2008; Brito et al., 2014a), under sea ice or shelf ice (Griffiths and Brito, 2008; Brito and Griffiths, 2016), and along with coastal areas (An et al., 2001; Oliver et al., 2013), as shown in Fig. 2.5. Due to the dynamic and hazardous nature of subsea environments, ensure safe deployment is challenging. Therefore, it is vital to identify underwater environmental factors and understand how they can cause risks to AUVs. Based on former studies, this section has analyzed four critical risk-related environmental factors, namely, sea ice or shelf ice, underwater currents, ambient temperature, and water density.

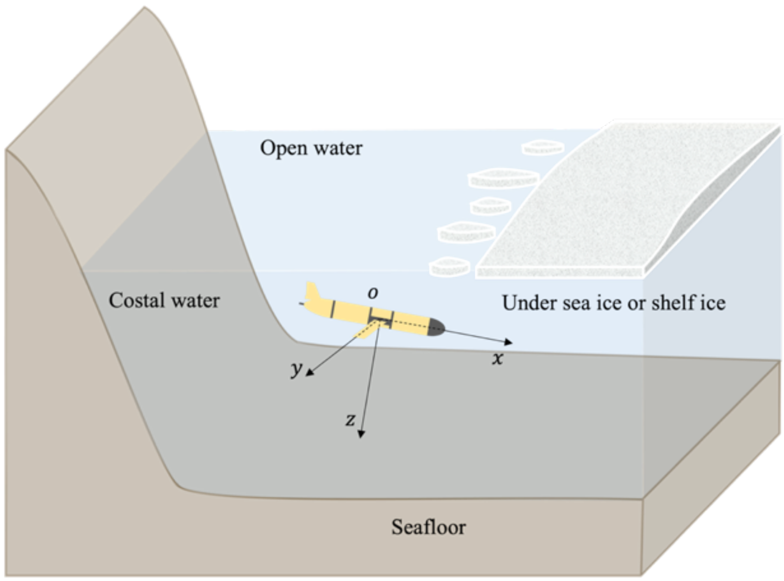

Fig. 2.5. Typical operating environments of AUVs.

2.2.3.1 Underwater current

Underwater currents result from the surface winds, gravitational tides, water density, and water pressure (Hegde et al., 2018; Ullah et al., 2020b). Underwater currents are critical for the dynamic motion control of AUVs, especially for the relatively slow-moving underwater gliders with a typical velocity below 0.5 m/s (Griffiths et al., 2007b; Petillo and Schmidt, 2012). Without external thrusters, a glider is easily subjected to environmental disturbances (e.g., strong currents). For example, strong currents may deviate it from a planned path, and as a result, a glider cannot reach its target position.

Various strategies have been proposed to improve AUV control against underwater currents, such as increasing the surfacing frequency to reduce positioning errors resulting from the currents (Bachmayer et al., 2006), and optimizing the navigation system by integrating current models (Smith et al., 2012).

2.2.3.2 Water density

Water density has a critical influence on the buoyancy control of AUVs. Basically, water density is decided by the combination of water depth, water temperature, and salinity (Hegde et al., 2018).

It is noted in Section 2.2.1 that some passively-propelled AUVs, such as underwater gliders, usually control their buoyancy either by filling an external bladder or by pushing seawater in or out of an internal reservoir (Griffiths et al., 2007b). However, in some mission regions, for instance, near melting glaciers, seawater density can change significantly due to the salinity dilution. As a result, decreasing water density will require more buoyancy for the vehicle′s rising motion (Bachmayer et al., 2006; Dowdeswell et al., 2008). On the contrary, in other areas where the water density is relatively high, redundant buoyancy could be provided and consequently compromises the vehicle's diving motion. In conclusion, once the water-density gradients exceed the compensating range of the vehicle, the buoyant-control failure will occur. Consequently, the vehicle may become trapped in a neutrally buoyant water-layer and fail to float to the surface, or the vehicle is unable to dive to the target depth. Thus, pre-measurement of the water density is necessary before an AUV mission to prevent the buoyant-control failure.

2.2.3.3 Sea ice

Deploying an AUV in the polar regions has a higher risk than in other areas, since sea ice is a risky contributor. Specifically, a former study proved that the median probabilities of AUV loss in under sea-ice and ice-shelf missions are 4.9 and 9.4 times higher than in open water missions, respectively (Brito et al., 2010).

Sea ice, which is characterized by ice thickness and ice concentration, can affect the operational risk of AUVs in multiple ways. Firstly, sea ice with modest thickness may pose a collision risk and poor visibility in the recovery phase or the fail-safe phase, as it could form a rigid lid and cause the AUV being trapped under the ice when floating to the surface. Moreover, sea ice may damage components such as the antennas and propeller blades during the floating process or crack the vehicle hull and cause leakage. Secondly, the occurrence probability of these collision incidents will increase with ice concentration. Moreover, the communication efficiency can be affected by both ice thickness and concentration (Brito and Griffiths, 2016). Consequently, the ability to receive satellite signals will be compromised under ice, and poor communication will in turn increase the difficulties for vehicle relocation.

To prevent the collision with ice, risk mitigation measures have been provided, such as attaching a tether to the vehicle (Doble et al., 2009; Forrest et al., 2012), mounting a locating beacon inside the vehicle (Kukulya et al., 2010), temporarily parking the vehicle in a safe location (Ferguson, 2008; Kaminski et al., 2010), and optimizing the obstacle avoidance system (Pebody, 2008; Eichhorn, 2009).

2.2.3.4 Ambient temperature

Another key environmental factor for AUVs is the ambient temperature. Low ambient temperature, especially in polar regions, can cause large temperature gradients between the air and the water column. Consequently, the vehicle or component may suffer integrity failure and the leakage problem (Ferguson, 2008). For instance, the CTD sensor may suffer cracks at low ambient temperatures, and therefore seawater will penetrate and freeze inside, eventually causing sensor failure (Kaminski et al., 2010). Additionally, low temperature also forces ice formation on the equipment. One example found that the GPS of an AUV was unable to acquire satellite signals when working in the Arctic, possibly due to a thin layer of ice that formed on the antenna (Bellingham et al., 2008). Another potential challenge caused by low temperature is the degradation of the power system. As introduced in Section 2.2.1, lithium batteries are widely used for AUVs. However, the battery capacity may drop significantly especially when the ambient temperature is below -20°C. As a result, poor battery performance could further lead to the premature of power depletion and a mission abort (Bandhauer et al., 2011). Apart from the impact on the vehicle itself, low temperature will cause harsh working conditions for the AUV operators both physically and psychologically.

According to the above analysis, the impacts of various subsea environmental factors and their interacting relationships are topologically represented in Fig. 2.6, where the arrows point to the functional failures caused by environmental factors. It is evident that distinct environmental factors may interact with each other and cause different functional failures. Hence, when conducting the risk analysis of AUVs in a certain environment, the operator must be aware of this and update the environmental factors according to local configuration.

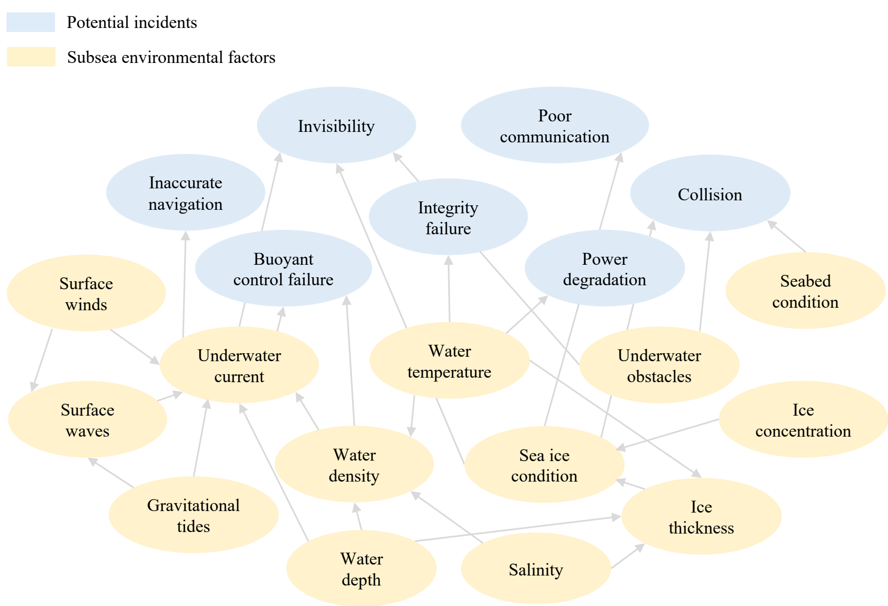

Fig. 2.6. Risk identification of subsea environmental factors.

2.3 Risk analysis methods for AUV operations

This subsection provides an overview of existing methods for risk analysis of AUV operations. It aims to outline the evolution of the developed methods and models, critically analyze the progress and limitations of past research, and highlight future research trends in this domain. This subsection is expected to help researchers gain a better understanding of historical developments for AUV risk analysis methods and bridge the existing research gaps in future work. In this subsection, the reviewed methods are categorized into qualitative, semi-quantitative, and quantitative methods. The classification of major risk analysis methods regarding AUV operations is shown in Table 2.5. Related to the three types of methods, Fig. 2.7 shows the accumulative number of publications of each type over the last two decades. It is observed that research using quantitative methods has rapidly increased in recent years, which implies that quantitative representation is becoming more widespread in the risk analysis of AUVs. In the following subsections, typical methods relating to the risk analysis of AUVs will be elaborated.

Table 2.5. Classification of typical risk analysis methods regarding AUV operations.

Risk Analysis Method		Reference
Qualitative	Safety layer method	(Ortiz et al., 1999)
	Tree diagram	(Madsen et al., 2000)
Semi-quantitative	Risk management process	(Griffiths and Trembanis, 2007; Brito et al., 2010; Griffiths and Brito, 2011; Thieme et al., 2015a)
	Failure Mode and Effects Analysis	(Hu et al., 2013; Harris et al., 2016)
Quantitative	Bow-tie model	(Yu et al., 2017)
	Kaplan-Meier survival model	(Brito et al., 2010; Brito et al., 2014a; Brito and Griffiths, 2016)
	Fault tree analysis	(Bian et al., 2009a, b; Hu et al., 2013; Xu et al., 2013; Aslansefat et al., 2014a; Thieme et al., 2015a; Brito, 2016; Harris et al., 2016; Xiang et al., 2017; Brito and Chang, 2018)
	Event tree analysis	(Thieme et al., 2015a; Brito et al., 2018)
	Bayesian network	(Griffiths and Brito, 2008; Brito et al., 2012;

	Thieme et al., 2015b; Brito and Griffiths, 2016; Brito and Griffiths, 2018; Hegde et al., 2018; Bremnes et al., 2019; Yang et al., 2020)
Markov chains	(Brito and Griffiths, 2011; Griffiths and Brito, 2011)
System dynamics	(Brito and Griffiths, 2012; Loh et al., 2020a; Loh et al., 2020c, b; Xu et al., 2020)

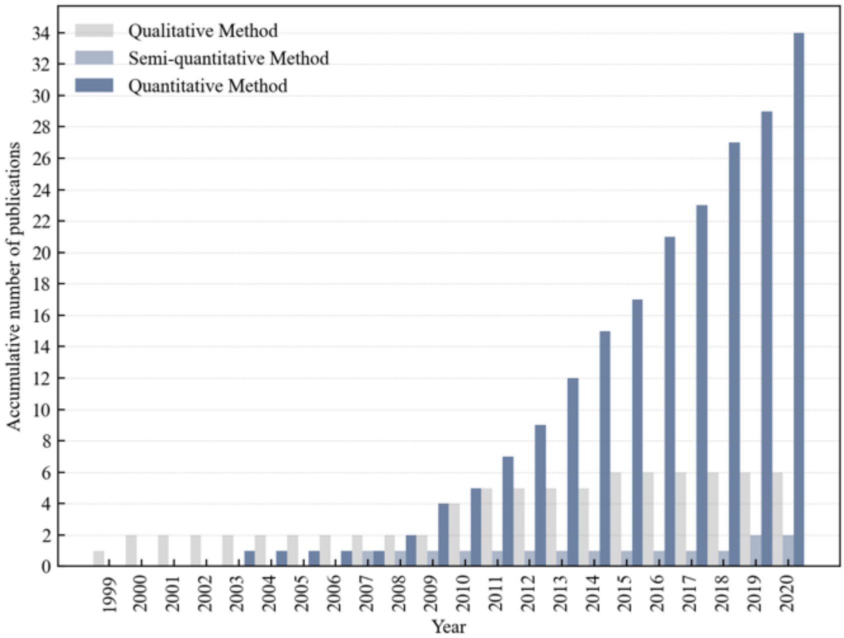

Fig. 2.7. Accumulative number of publications of the three types of risk analysis methods over the last two decades.

2.3.1 Qualitative methods

Qualitative risk analysis refers to a non-numerical representation to describe the frequency and the severity of a hazardous event. The representations include flow diagrams, graphs, sources of data, and other descriptive scales (Rausand and Høyland, 2003; Khan et al., 2015). Within the domain of risk analysis of AUVs, qualitative methods emerged in the early phase as shown in Fig. 2.7. A safety layer method was firstly proposed (Ortiz et al., 1999), which analyzed the technical reliability of AUVs, emphasizing that internal fault detection in the hardware structure is an essential step to achieve safe operations. Subsequently, a failure diagnosis layer was developed for AUV mission control (Madsen et al., 2000). A tree diagram was built to represent the potential causes of the mission failure.

The aforementioned qualitative research primarily used non-probabilistic models combining with expert knowledge. In the early development of AUVs, qualitative methods were ideal tools to analyze operating risks owing to a lack of available data. However, few of them explicitly capture the underlying risk contributors and complex causal relationships, and thereby the overall risk level cannot be determined accurately. Hence, qualitative methods can only offer general guidelines in the AUV risk analysis, and quantitative information is further required to handle the inherent uncertainties of AUV operational risk.

2.3.2 Semi-quantitative methods

Semi-quantitative methods fall in between qualitative and quantitative methods (Khan et al., 2015). They can roughly quantify probabilities and consequences and provide more detailed measurement than qualitative methods (Rausand and Høyland, 2003). Based on early research, a number of semi-quantitative approaches for risk analysis of AUVs have been successively proposed, including the risk management process (RMP) model and the failure mode and effects analysis (FMEA) method.

The RMP model was proposed to support decision making in extreme environments (Griffiths and Trembanis, 2007), as shown in Fig. 2.8. The proposed RMP model was the first systematic risk management approach to help an AUV team determine an acceptable risk level of deployment. It estimated the probability of AUV loss based on both expert knowledge and statistics. Applications of the RMP model have been discussed in subsequent studies (Brito et al., 2010; Griffiths and Brito, 2011; Thieme et al., 2015a).

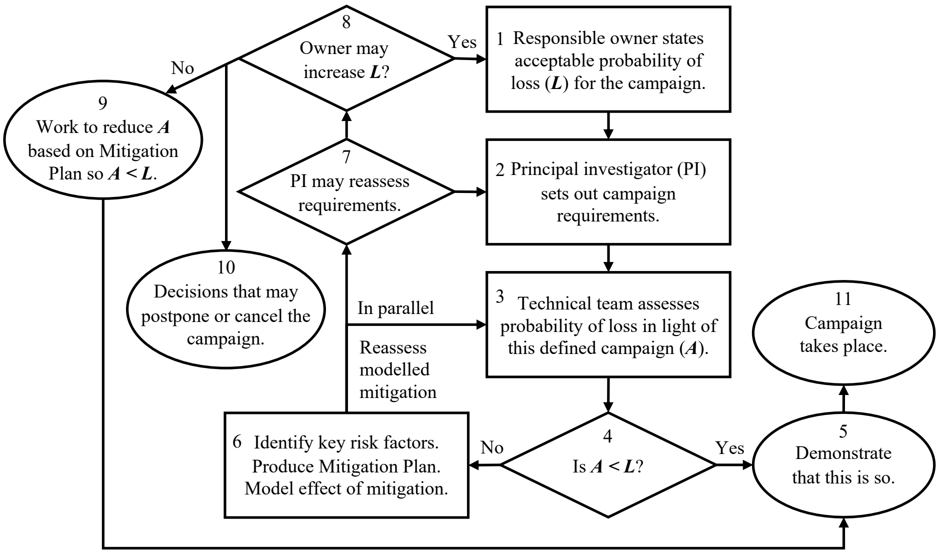

Fig. 2.8. The flow chart for the risk management process of AUVs (Griffiths and Trembanis, 2007).

FMEA is a systematic method for failure analysis. It is usually performed in the initial design phase of a system to analyze potential failure modes and their effects on the system. In another word, FMEA is particularly beneficial for preliminary risk analysis of a component or a system which has relatively constrained failure modes and simple causal relationships. Within the robotic industry, FMEA has been widely used to identify critical components and their effects on the robotic system (Harris et al., 2016). For instance, FMEA was applied to analyze different failure modes for an AUV mechanical system (Hu et al., 2013). Key components including the sealing elements and hermetic hulls were identified, which have the greatest impact on the failure of the overall mechanical system.

To sum up, semi-quantitative methods perform well in analyzing potential failure modes and consequences in the AUV domain. However, as the risk estimation in these methods mainly depends on experts rather than precise probabilistic calculation, bias and uncertainties are inevitably introduced. Thus, although semi-quantitative methods provide a valuable reference in initial risk analysis, quantitative methods are highly required to further reduce uncertainties and enhance the analysis accuracy.

2.3.3 Quantitative methods

Quantitative risk analysis provides a numerical estimation for probabilities, consequences, and severities (Rausand and Høyland, 2003). A remarkable benefit of quantitative methods is that they offer a reliable reference for tackling uncertainties and informing decision making (Khan et al., 2015). More recently, extensive studies have been carried out using quantitative risk analysis for AUVs.

Fault tree analysis (FTA) is a widely used quantitative method for risk analysis. It is a deductive, graphical, and structured tool which can capture the failure propagation between an undesired event and its potential causes with connection by logic gates (Khakzad et al., 2011). Currently, several advanced FTA methods have been developed. Fuzzy set theory was combined with FTA to address the uncertainty from expert judgement (Lin and Wang, 1997; Yazdi and Zarei, 2018). Dynamic FTA model was proposed to capture the time dependency among failures (Čepin and

Mavko, 2002; Ghadhab et al., 2019). In the domain of AUVs, the FTA method was also widely applied (Bian et al., 2009a, b; Xu et al., 2013). Among these studies, AUV mission failure was denoted as the top event, whereas the subsystem failure or component failure were identified as root causes. The fault tree was then built to depict the failure propagation and logical relationships between root causes and the top event. The Monte Carlo simulation was subsequently used in these studies to assist in the quantitative calculation for the probability of mission failure.

Event tree analysis (ETA) is an inductive and graphical method, which presents all potential outcomes and event sequences resulting from an initiating hazardous event (Rausand, 2013; Khan et al., 2015). It is widely used to identify possible accident scenarios and estimate the probability of the final outcome, considering the failure of installed safety barriers. Past studies have identified three consequences of AUVs using the ETA method, including AUV mission failure, mission abort, and AUV loss (Thieme et al., 2015a; Brito et al., 2018).

In addition to the FTA and ETA methods, another three advanced quantitative methods that applied in the AUV domain are comparatively analyzed in the following subsections, namely, Bayesian network, Markov chains, and the system dynamics method. Different characteristics between these methods are clarified by distinguishing their graphical models, advantages, and limitations as summarized in Table 2.6.

Table 2.6. Characteristics of the three risk analysis methods.

Risk Analysis Method	Graphical Model	Advantage	Limitation	Reference
Bayesian network	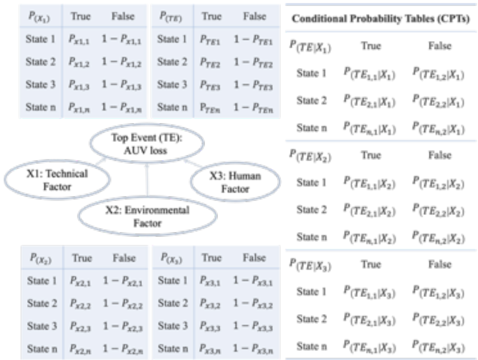 Adapted from (Brito and Griffiths, 2016)	Provides quantitative risk estimation, even when experimental data is limited. Risk factors and dependency relationships can be systematically identified and presented. Critical risk factors can be determined by BN inferences. Achieves updating risk estimation when new evidence is involved, which is specifically beneficial for AUVs in dynamic subsea environments.	The process of risk nodes identification, states definition, and CPTs computation may incorporate expert knowledge, which could induce uncertainties and biases. Constructing CPTs will become considerably complex as the number of variables increases. Unable to model complex non-linear correlations among variables.	(Khakzad et al., 2011; Khakzad, 2015; Brito and Griffiths, 2016; Hegde et al., 2018)
Markov Chains	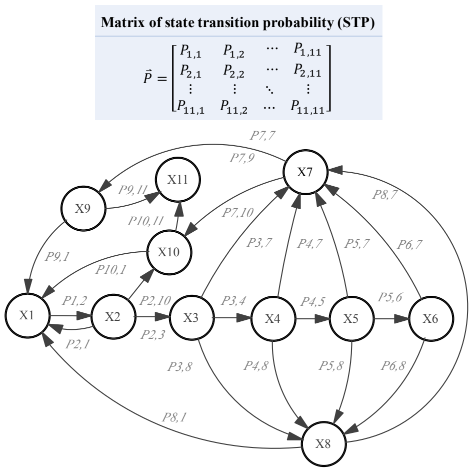	Identifies risks involved in distinct states and state transition processes, thereby can model the complete sequence of an AUV mission and facilitate risk analyses of each mission phase. A valuable tool for predicting the risk of AUV mission abort. It allows for quantifying the failure probability of each state by using STP, and it iteratively calculates the failure probability of the final mission goal.	Estimations of STP are usually derived from expert knowledge due to limited experimental data, which may lead to judgmental biases. Weak in representing the underlying risk factors and their causal relationships.	(Brito and Griffiths, 2011; Griffiths and Brito, 2011)

	Adapted from (Brito and Griffiths, 2011)			
System Dynamics	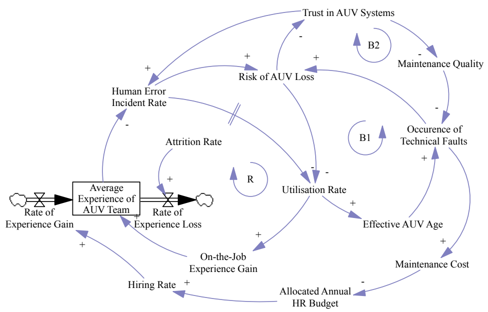 Adapted from (Loh et al., 2020b)	Complex causal relationships among risk factors can be captured effectively in the causal loop diagram. Dynamic behaviors of risk factors can be flexibly represented by stock and flow structures, which are particularly useful for dynamic AUV missions. Relatively easy to understand and apply without complex probabilistic computations.	Defining each risk variable and its correlation equation can be challenging and time-consuming. Constructing the SD model could become rapidly complex with the increase of the number of risk variables. Unable to address uncertainties in interrelationships of risk factors due to the deterministic nature of the SD model.	(Loh et al., 2019, 2020c, b)

2.3.3.1 Bayesian Network

Bayesian network (BN) is a robust method for risk analysis of multi-variable systems. Based on a well-defined Bayes theorem, BN is powerful to capture dependencies between variables in a probabilistic way (Hossain et al., 2019). It consists of a directed acyclic graph, in which nodes represent system variables, such as risk factors and potential consequences, while arcs denote causal relationships among nodes. The dependency degrees among nodes are specified using conditional probabilities, which can be defined by expert judgment or experiment data. With conditional probabilities and known prior probabilities of parent nodes, BN can provide both forward (predictive) and backward (diagnostic) inferences. In the forward reference, the probability of a child node can be predicted according to the law of total probability. While in the backward reference, the posterior probabilities of parent nodes are updated given new evidence of the child node, following Bayes theorem (Song et al., 2016).

BN can be combined with other risk analysis methods to enhance its accuracy and reduce uncertainty. By mapping the fault tree, event tree, or Bow-tie model into BN, it can help clearly represent dependencies between nodes (Yang et al., 2017a). To capture the time dependence of a system, the dynamic Bayesian network (DBN) is more advanced than the BN (Khakzad, 2015; Kammouh et al., 2020). The states and occurrence probabilities of variables in the DBN are updated over time, and the logic of the DBN is changed based on new observations. Therefore, the DBN can model the dynamics by using time series data (Khan et al., 2020). Although the classic BN is capable of handling the uncertainties through experts′ knowledge, it is still required to deal with incomplete data and vague information. A resulted fuzzy Bayesian network (FBN) was proposed to address this limitation by employing the fuzzy set theory. The FBN has been widely applied in multiple areas, such as maritime and offshore systems (Wan et al., 2019; Yu et al., 2021), process industries (Yazdi and Kabir, 2017), human reliability analysis (Zhou et al., 2018), and so on. Another limitation of the traditional BN is its inability to model complex correlations, such as non-linear dependencies among risk variables. To address this concern, a Copula Bayesian network was proposed by combining Copula functions with the BN (Elidan, 2010b). This integrated model acts as an excellent tool to measure non-linear dependencies among multivariate variables, and therefore it has been especially performed in complex systems and uncertain domains, such as the process system (Hashemi et al., 2016), the metro tunnel system (Pan et al., 2019), the complex electronic system (Sun et al., 2021a), and so on.

So far, within the domain of risk analysis of AUVs, the BN model is mainly used for estimating the risk of AUV loss (Griffiths and Brito, 2008; Brito and Griffiths, 2016) and monitoring the mission success (Thieme et al., 2015b; Hegde et al., 2018). It was first used for estimating the risk of loss of AUVs in a sea ice environment (Griffiths and Brito, 2008). Operations under sea ice or ice shelves may involve significant risks to AUVs. Earlier methods for assessing the risk were mainly based on expert judgment. However, subjective expert judgment can hardly provide accurate risk estimation. Thus, a solution using BN was proposed (Griffiths and Brito, 2008). The causal effects of the environments and the vehicle were captured in their study, and the expert judgment was included to provide conditional probabilities of the BN model. By quantitative calculation, the probability of vehicle loss was obtained. An extended study also applied BN for predicting the risk of AUV loss (Brito and Griffiths, 2016), where the ice concentration, ice thickness, environmental constraints, and vehicle types were highlighted as the main contributors to AUV loss.

Another application of the BN model for monitoring AUV mission success was proposed (Thieme et al., 2015b). The risk influencing factors (RIFs), which can cause the mission to abort, were modeled in their study. Although the BN model was proved as an effective method to assess risks before executing a mission, the study lacks quantitative estimations for the relationships among RIFs. To address this problem, an extended study presented a novel BN model to quantify the probability of the mission failure during the submarine operations of inspection, maintenance, and repair (IMR) (Hegde et al., 2018). Through this BN model, the RIFs that affect the failure of IMR missions were identified, including technical, organizational, and operational factors. The established BN model is relatively systemic and holistic, which can support the decision making of operators to achieve safer IMR operations.

Comparing to traditional risk analysis methods (i.e., FTA, ETA, and FMEA) for AUVs, BN outperforms in several aspects. Firstly, BN shows a clear structure to present causal relationships among risk variables. Secondly, with the forward and backward inference, BN can update the previous belief given new observing evidence, thereby it can reduce uncertainties and provide more accurate risk estimation. This characteristic is particularly beneficial for AUVs operating in dynamic underwater environments. Lastly, BN can be easily built by combining expertise, even when the historical information is incomplete. In another word, if the historical data are limited, using data-driven approaches to obtain conditional probabilities could be difficult, whereas involving expert judgment can be an effective solution in this case.

These advantages of BN broaden its range of applications. In addition to AUVs applied in the subsea oil and gas industry, the potential application of BN-based methods can be extended to other domains, such as deep-sea mining and aquiculture that may utilize AUVs for routine submarine operations.

2.3.3.2 Markov Chains

A Markov chain is a widely-used stochastic model for reliability analysis (Lisnianski et al., 2012). Here, a significant property should be noticed: finite discrete states of a system are considered in the Markov chain, and the state transition probability (STP) is only determined by the current state, rather than historical information. Therefore, the Markov chain is suitable for predicting the occurrence probability of a future state.

In an AUV mission, a complete deployment process comprises sequential phases from the initial predive test to the final recovery, where varied risks pertain to different phases. For instance, higher risks are associated with the launch and recovery phases (Griffiths et al., 2007a). Given that a Markov chain can identify system states and quantify the STP of a sequence of operations, it serves as an ideal method for the risk analysis of AUV deployment.

Former studies proposed a systematic Markov chain approach for modeling AUV risks in different phases and multiple scenarios (Brito and Griffiths, 2011; Griffiths and Brito, 2011). The developed Markov chain method consists of two steps. Firstly, a topological structure is established to present the sequential phases of AUV deployment. A total of 11 states are identified as shown in Fig. 2.9. The state descriptions and different risks which are involved in each phase are summarized in Table 2.7. Secondly, the STP is determined by embedding the extended Kaplan-Meier survival statistics. Hence, with the integration of the Markov chain and survival statistics, the failure probability of each state and of the overall mission goal can be quantified.

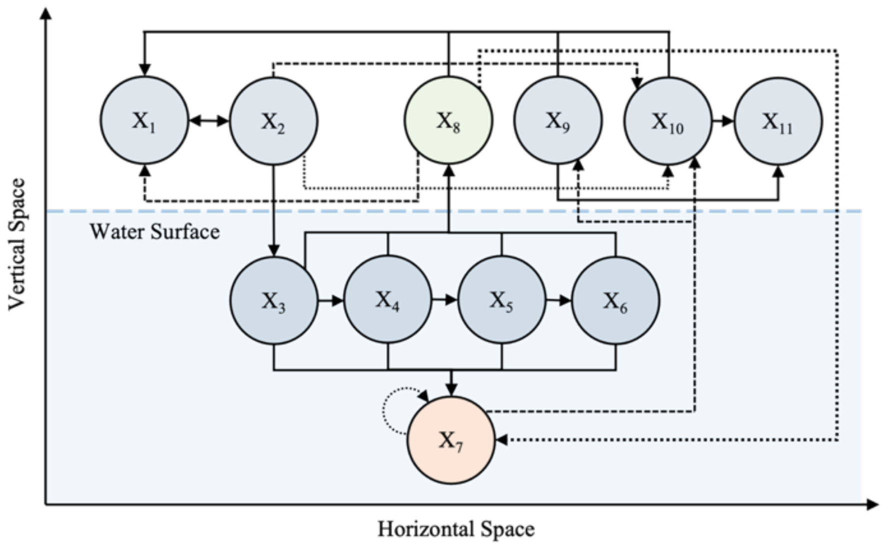

Fig. 2.9. Markov chain model capturing the sequential phases of the AUV deployment, adapted from (Brito and Griffiths, 2011).

Table 2.7. State description and risk involved in each phase of AUV deployment, adapted from (Brito and Griffiths, 2011; Griffiths and Brito, 2011).

State Number	State Name	State Description	Risk Involved
X_1	Pretest state	Fault identification and rectification	-
X_2	Post-test state	Ready to launch	-
X_3	Overboard state	Ready for predive checks	Loss risk next to a deployment platform
X_4	Diving	Proceed with the mission	Uncontrolled dive, Loss risk

X_5	Holding/test Pattern phase	Test during the first dive	Loss risk
X_6	Underway state	Proceed with the mission	Loss risk
X_7	Loss	Temporary or permanent loss of the vehicle	Loss risk
X_8	Recovery	Recover the vehicle	Loss risk, collision risk
X_9	Find	Find the vehicle	-
X_{10}	Salvage	Salvage the vehicle	Loss risk
X_{11}	Scrap	Scrap the vehicle as being beyond economical repair	-

The application of the Markov chain in their studies proved its efficiency for the risk analysis of multiple phases of AUV deployment. The clear graphical structure facilitates the risk estimation of each state and the overall mission achievement. However, a simple assumption is made in this method: the AUV risk is quantified as a function of the traveled distance. As the mission formats become more complex and dynamic in unpredictable environments, especially with the interaction of multiple vehicle platforms, an extended study based on the Markov chain is required as a suitable solution to provide updating STP in future studies.

2.3.3.3 System Dynamics

The system dynamics (SD) method was proposed for the analysis of dynamic complex systems (Forrester, 1997). It is an objective-oriented deterministic approach to understand non-linear behaviors of the system in real-time by using internal feedback loops, stock and flow structures, and time delays (Eusgeld et al., 2011). The central concept of the SD method is that it uses feedback control to represent how the system structure responds to dynamic behaviors (Loh et al., 2020c). Therefore, this method can effectively model both the dynamic nature and causal relationships among risk variables.

For the AUV system, the SD method was firstly used to analyze the risk influenced by multiple AUV deployments (Brito and Griffiths, 2012). The risk mitigation efforts were analyzed focusing on human resource management. Although that study lacks a structured framework and validation of the proposed SD method, it proves the potential capabilities of the method applied for risk analysis in the AUV domain. Furthermore, a system-based SD framework was firstly proposed for analyzing the risk of AUV loss (Loh et al., 2020c). Presented as a structured framework, this study mainly examined the human error in Antarctic AUV programs and provided measures for risk mitigation. The strength of the SD method is well recognized in this study: complex causal relationships between risk factors can be modeled, and the dynamic nature of these variables can be captured effectively by the stock and flow structures. However, solely applying the SD model for risk analysis has its drawbacks. Risk is often viewed as derived from uncertainties, which features the risk with a multi-dimensional, dynamic, and fuzzy nature (Haimes, 2009). However, such uncertainties cannot be effectively addressed by the classic deterministic SD model. This limitation has promoted the recent development of integrating the SD method with fuzzy logic (Loh et al., 2020a; Loh et al., 2020b; Xu et al., 2020). A resultant fuzzy system dynamics risk analysis (FuSDRA) method was proposed to achieve a more robust risk analysis for AUVs (Loh et al., 2020b). In the FuSDRA framework, the SD method can model the dynamic interrelationships among risk variables from different dimensions such as human and organizational factors, technical factors, and external commercial factors. At the same time, fuzzy logic is integrated to account for stochastic uncertainties of risk variables and their dependencies. An extended study used the FuSDRA approach to explore the relationships between the experience of operators and the risk of AUV loss (Loh et al., 2020a). It was the first time that the FuSDRA method was utilized for in-depth risk analysis of human factors. In a more specific application, the FuSDRA method was applied to analyze how the government support and technological obsolescence could influence AUV loss (Xu et al., 2020).

In conclusion, the hybrid FuSDRA approach leverages the strength while overcoming the constraints of both the SD method and fuzzy logic theory. Since it has been proved to be a powerful tool for risk estimation and decision making, it can be employed to offer more reliable measures of risk mitigation.

2.4 Future challenges of risk analysis for AUV operations

Based on the above analysis of past progress, section 2.4 identifies current research gaps and discusses future challenges in the domain of AUV risk analysis.

2.4.1 Dynamic risk analysis for AUV operations

In general, the dynamic risk of AUV deployment results from two factors. The first is the complexity of the AUV itself. The interaction between components and subsystems leads to complex functional dynamics. Secondly, AUVs usually operate in highly dynamic marine environments. Unsteady working conditions result in the dynamic nature that evolves with time and space. Thus, due to the dynamic nature, real-time risk analysis and decision making in uncertain underwater environments is challenging.

For now, the majority of risk analysis models applied to AUVs are traditional methods that have a static structure, which cannot capture dynamic uncertainties existing in the complex AUV system and the environment. Therefore, dynamic risk analysis (DRA) methods are required. DRA is defined as a method which is capable of updating the risk estimation dynamically. The key difference between the traditional risk analysis method and a DRA method is that DRA can monitor and assess abnormal conditions and update the overall risk level when new information is incorporated. In the AUV domain, tailored DRA methods are demanded to provide a dynamical way for risk estimation. Noticeably, effective and timely risk analysis is vital to predict an abnormal situation and prevent accidents. In particular, adopting DRA methods will help decision making based on the real-time situation, inform stakeholders to take early actions before incidents occur, and enable safer performances of AUVs operating in extreme environments

2.4.2 Risk analysis for AUVs with limited historical data

Historical data record fault information of AUV performances, which are the fundamental data required in many traditional risk analysis models (i.e., FTA, ETA, BN). Noticeably, historical data are essential for accurate risk estimation. However, in the early phase of employment of an AUV platform, fault data tend to be limited. In this case, the data basis for risk analysis models is insufficient, leading to the challenge of accurate risk estimation.

To address the concern of limited historical data, combining expert knowledge can be adopted. Specifically, incorporating expert judgments into the risk analysis process can provide qualitative reasoning and handle the missing data. However, merely relying on experts may lead to judgmental uncertainties, which indicates a need for more advanced methods to address the problem due to scarce data in future studies. Such advanced methods can compensate for missing data in a quantitative way and additionally use the data to predict in-situ risk estimation. Machine learning techniques have great potential to tackle data limitation problems. A number of studies have used machine learning algorithms to improve the quantification accuracy under scarce data conditions (Ramoni and Sebastiani, 2001; Rachman and Ratnayake, 2019), and provide valuable references to the AUV domain. Hence, machine learning based methods are effective tools for future research to reduce the dependence on historical data and expert judgments, and improve the accuracy and efficiency of risk estimation with incomplete data.

2.4.3 Intelligent risk analysis for AUV operations

Intelligent behaviors of an autonomous system are defined as onboard capabilities of decision-making, mission planning and re-planning, and fault tolerance (Seto, 2012). With the development of AUV technologies, risk analysis of AUV operations is broadening to an intelligent scope (Bremnes et al., 2019). Intelligent risk analysis in the AUV domain refers to performing risk analysis and decision making by the vehicle itself instead of human operators. More specifically, intelligent risk analysis enables the vehicle to process real-time data, assess in-situ risk levels, adapt path planning and motion control strategies according to current risk scenarios, and thereby assist the vehicle to accomplish a mission autonomously without much human intervention.

Most of the classic risk analysis methods applied in the AUV domain are based on the offline assessment before a mission. These methods aim to assist operators to estimate the current risk level, take necessary risk mitigation measures, and adapt their mission plans accordingly. However, traditional offline risk analysis relying on humans tends to be time-consuming. Time delays caused by manual analysis processes will result in real-time risk scenarios that cannot be precisely identified. Delayed risk identification will successively compromise the accuracy of current risk estimation and reduce the effectiveness of subsequent decision making. This leads to the consideration of changing the way of risk analysis from human offline prediction to autonomous online risk analysis.

Intelligent risk analysis can be a game-changer in future trends of risk analysis for autonomous vehicular systems. A potential solution is combining classic risk analysis models with machine learning techniques, and subsequently incorporating them into the online decision system. Currently, a number of studies have adopted machine learning methods to aid onboard risk analysis in the marine robotics domain (Hollinger et al., 2016; Xiang et al., 2017). The major advantage of machine learning algorithms is their self-learning capabilities to explore all possible interactions between non-linear input and output risk variables (Hegde and Rokseth, 2020). High computational speed enables them to achieve real-time risk prediction with much higher efficiency than human operators. In addition, a wide variety of data are continuously generated from sensor platforms. Machine learning techniques can process various forms of these data, including numerical data, textual data, and image data. The combination of data information is used to assess in-situ environmental and operational conditions, and thus achieve more systematic and accurate risk estimation. Therefore, the online decision system can take reasonable actions based on the current risk state. To sum up, in order to improve the autonomy level of AUVs and increase the efficiency of risk analysis, intelligent risk analysis is expected to be developed as an integral part of an AUV system.

2.4.4 Risk analysis for multi-AUVs collaboration

As the technology of AUVs gradually matures, the mission format of multi-AUVs is rapidly emerging (Harris et al., 2016). Multi-AUVs missions refer to the cooperative work of multiple AUVs to achieve a mission goal. As the mission format becomes more synergic, the multi-AUVs system can cruise larger areas and complete more difficult tasks than a single vehicle. At the same time, as the multi-vehicles operations are more interactive and dynamic, operational risks will inevitably become more complex, and thus effective risk analysis is required. However, most of the current risk analysis research has concentrated on traditional single-vehicle missions and cannot represent the interactive risk associated with multiple platforms. Therefore, novel methods are required in future research to facilitate the risk analysis for multi-AUVs collaboration.

When conducting risk analysis for a multi-AUVs scenario, the interactive impact among multiple vehicles is a key consideration. During the cooperation between multiple vehicles, reliable communication is needed for data updating and data transmission. This process requires consideration of the constraints of space and time for both vehicles within dynamic underwater environments whilst preventing collisions. On the other hand, the interaction between vehicles can influence the risk associated with vehicles. For example, if failures occur in the navigation system and the vehicle takes incorrect headings, the likelihood of colliding with nearby vehicles can be increased. Therefore, future studies of risk analysis for multi-AUVs collaboration should ensure cooperative efficiency whist improve the safety performance of involved platforms.

2.5 Summary and conclusion

The main objective of this chapter is to provide a systematic review of past progress of risk analysis research for AUV operations. This review answers key questions including fundamental concepts and evolving methods in the domain of risk analysis for AUVs, and it highlights future research trends to bridge existing gaps. The scope of this chapter is restricted to the research questions. Based on the aim and scope of this chapter, a total of forty-two articles with significant relevance to AUV-related risk analysis were retrieved. The underlying risk factors identified from selected literature are summarized into three categories: technical factors, environmental factors, and human factors. A comparative analysis was undertaken to provide a clear picture of the evolution process, advantages, and limitations of adopted risk analysis methods from qualitative, semi-quantitative, and quantitative aspects. Current research gaps and future challenges in this domain were briefly outlined.

In light of the review and analysis, three key conclusions can be drawn from this chapter. Firstly, systematic identification of risk factors and their causal relationships is vital for further risk analysis. Most of the early research focused on technical factors of AUVs, relying on historical performance data. Whereas in current trends, environmental factors, human factors, and their interactive impacts are increasingly receiving attention. Secondly, it is evident that quantitative methods have been rapidly implemented in recent years to enhance the accuracy and handle the uncertainties of risk analysis of AUVs. However, former studies still heavily rely on expert knowledge, which may introduce judgmental bias. Lastly, future challenges for risk analysis for AUVs may focus on addressing dynamic risk analysis, scarce historical data, intelligent risk analysis, and multi-vehicles risk analysis.

Chapter 3. A Copula-based Method of Risk Prediction for Autonomous Underwater Gliders in Dynamic Environments

Preface

A version of this chapter has been published as: ***Chen X, Bose N, Brito M, et al. A copula-based method of risk prediction for autonomous underwater gliders in dynamic environments [J]. Risk Analysis, 2023.*** *https://doi.org/10.1111/risa.14149. I am the primary author along with the Co-authors, Neil Bose, Mario Brito, Faisal Khan, and Ting Zou. I developed the conceptual framework for a copula-based method of risk prediction for autonomous underwater gliders in dynamic environments. I prepared the first draft of the manuscript and subsequently revised the manuscript based on the co-authors′ and peer review feedbacks. Co-authors Neil Bose, Mario Brito, and Faisal Khan provided support in implementing the concept development, reviewing, and revising the manuscript. Co-authors Ting Zou provided assistance in reviewing and correcting the results. The co-authors also contributed to the review and revision of the manuscript.*

Abstract: Based on the literature review results, this chapter aims to achieve the second research sub-objective, that is to provide a risk analysis model for risk prediction for AUVs in various environmental conditions. This chapter considers a certain type of AUVs, namely, autonomous underwater gliders (AUGs). AUGs are effective platforms for oceanic research and environmental monitoring. However, complex underwater environments with uncertainties could pose the risk of vehicle loss during their missions. It is therefore essential to conduct risk prediction to assist decision making for safer operations. The main limitation of current studies

for AUGs is lacking a tailored method for risk analysis considering both dynamic environments and potential functional failures of the vehicle. Hence, this chapter proposed a copula-based approach for evaluating the risk of AUG loss in dynamic underwater environments. The developed copula Bayesian network (CBN) integrated copula functions into a traditional Bayesian belief network (BBN), aiming to handle non-linear dependencies among environmental variables and inherent technical failures. Specifically, potential risk factors with causal effects were captured using the BBN. A Gaussian copula was then employed to measure correlated dependencies among identified risk factors. Furthermore, the dependence analysis and CBN inference were performed to assess the risk level of vehicle loss given various environmental observations. The effectiveness of the proposed method was demonstrated in a case study, which considered deploying a Slocum G1 Glider in a real water region. Risk mitigation measures were provided based on key findings. This chapter potentially contributes a tailored tool of risk prediction for AUGs in dynamic environments, which can enhance the safety performance of AUGs and assist in risk mitigation for decision makers.

3.1 Introduction

Autonomous underwater gliders (AUGs) are a type of autonomous underwater vehicles (AUVs), which are characterized by long endurance, slow speed, low energy consumption, and a wide survey range (Wang et al., 2021b; Wang et al., 2022b). They are buoyancy driven vehicles without any thruster, which can move vertically and horizontally with fixed wings, and thereby achieve a sawtooth pathway in the water column (Webb et al., 2001; Hwang et al., 2019). Currently, AUGs have been widely used in various oceanic observations such as oceanography sampling (Rudnick et al., 2022), ecosystem investigation (Reiss et al., 2021), oil spill detection (Dhont et al., 2019), underwater pipeline integrity monitoring (Zhang et al., 2021), and so on. AUGs can operate in multiple types of underwater environments, such as under open water, under sea ice or ice shelves, and near coastal areas (Brito et al., 2008). However, complex underwater conditions and the long cruise endurance of AUGs could expose them to the risk of loss. Therefore, effective risk prediction and risk mitigation are significant to enhance the safety performance of AUGs.

In the general domain of AUVs, considerable studies for risk analyses have been conducted to assist decision making and ensure their safer operations. A systematic review of typical methods for risk analyses of AUV operations was presented in (Chen et al., 2021b), covering both qualitative, semi-quantitative, and quantitative perspectives. However, different types of AUVs operate with various characteristics. For example, buoyancy-driven AUGs are more easily impacted by underwater currents and water depths compared to propeller-driven AUVs with a thruster (Fan and Woolsey, 2014; Loh et al., 2019). This implies that the potential risk factors leading to vehicle loss could differ widely given inherent features of different vehicle types. Hence, how to accurately identify the specific risk factors and propose a tailored risk analysis method for a certain type of AUVs remains to be addressed.

Recently, a number of studies have investigated risk analysis methods particularly for AUGs. Merckelbach (Merckelbach, 2013b) proposed a probabilistic model to analyze AUG loss due to a collision with a ship. Results proved that the probability of a collision between an AUG and a ship is proportional to the ship density in a mission region. Ship density is an indicator of the complexity of ship traffic, and it represents the number of ships in a given area. Pereira et al. (Pereira et al., 2013) developed a risk-aware path planner based on ocean current predictions, aiming to minimize the risk of collision between an AUG and underwater obstacles. Brito et al. (Brito et al., 2014a) summarized potential failure modes of AUGs based on 205 glider missions, where the leak problem, power failure, buoyancy pump failure, and collisions were observed as the most common failure modes of AUGs. Aslansefat et al. (Aslansefat et al., 2014b) utilized a fault tree method to conduct the risk assessment for AUG subsystems. The constructed fault tree enables designers to diagnose AUGs′ faults and their effects on subsystems′ functionality. Anderlini et al. (Anderlini et al., 2021) developed a remote fault detection system for Slocum gliders, which can diagnose a range of anomalies, such as wing loss, in near real time to improve safety performance. However, some limitations are observed in past research. Firstly, for an AUG operating in complex underwater conditions, multiple environmental factors could interact with each other to cause a technical failure and even further lead to vehicle loss. So far, limited studies have systematically identified potential environmental factors, internal functional failures, and their causal relationships to vehicle loss. Secondly, as a result of their long endurance, AUGs could experience different environmental conditions during a mission. Hence, compared to other types of AUVs, it is essential to apply a dynamic risk model for AUGs to capture the non-linear dependencies among multivariate risk factors, whilst continuously predicting the risk of vehicle loss given changing environmental observations.

A Bayesian belief network (BBN) is a robust method for risk analyses. It is powerful in capturing dependencies among risk variables in a probabilistic way, and thereby it is suitable for complex multi-variable systems (Yuan et al., 2015; Cai and Golay, 2022). Over the years, BBN has been widely applied for risk analyses in the AUV domain. Former applications of the BBN model mainly include estimating the risk of AUV loss (Brito and Griffiths, 2016; Bremnes et al., 2019; Yang et al., 2020) and monitoring the mission abort (Thieme et al., 2015b; Brito and Griffiths, 2018; Hegde et al., 2018). There are several advantages of using the BBN to assist risk analyses. Firstly, a topology structure of the BBN can clearly present the causal relationships among multiple risk variables. Secondly, with the predict inference and diagnose inference, BBN can achieve updating risk estimation given new observations, and this feature is particularly beneficial for an AUV system that operates in a dynamic underwater environment. In addition, despite a lack of historical accident data of the vehicle, BBN can provide quantitative risk prediction by incorporating expert knowledge, and therefore it well handles the uncertainties (Brito et al., 2022). However, despite the wide applications, limitations of the BBN are identified as follows: Most of the former studies applying the BBN for AUVs have used deterministic point-based probabilities rather than a continuous distribution, which could introduce uncertainties in probability estimations. In addition, conditional probability tables have been applied to measure the dependence degree among network nodes. However, constructing conditional probability tables could become considerably complex as the number of network nodes increases. Meanwhile, simply using conditional probability tables to describe the dependence structure is limited for modeling non-linear relationships among nodes.

In order to address the restrictions of the BBN model, Elidan (Elidan, 2010a) proposed a novel copula Bayesian network (CBN) by combining copula functions with a traditional BBN model. The copula function is a powerful tool to build joint distributions of multivariate variables with various marginals, which specializes in modeling non-linear dependencies (Bedford et al., 2016;

Bai and Lam, 2022). Therefore, the integrated CBN model can inherit strengths from both the copula functions in measuring multivariate dependencies and the BBN model in capturing causal relationships among random variables (Wang et al., 2016). A number of studies have applied the CBN model to conduct risk analyses for different multivariate systems. For instance, Hashemi et al. (Hashemi et al., 2019) and Guo et al. (Guo et al., 2019) used the CBN for multivariate safety analysis of process systems. They demonstrated the superiority of a CBN structure compared with a traditional BBN model. Zilko et al. (Zilko et al., 2016) utilized the CBN model to predict the lengths of railway disruptions, validating high computational efficiency of the CBN. Pan et al. (Pan et al., 2019) developed a hybrid CBN-based approach to model the structural health of an operational metro tunnel, which proved that the CBN is beneficial for real-time risk assessment. Sun et al. (Sun et al., 2021a) performed a reliability analysis for complex electronic systems using the CBN, realizing the dependent failure modeling of modules and components. Chen et al. (Chen et al., 2021a) applied the CBN to analyze the causality of a risky driving maneuver, which provided crash risk evaluation and assisted decision-making for traffic safety.

The objective of this chapter is to propose a CBN-based approach for risk prediction of AUGs in dynamic underwater environments. Both open water and coastal water environments are considered in this chapter, while conditions of under ice or under ice shelves are not within the scope. The developed CBN model aims to capture non-linear environmental impacts on the functional failures of AUGs, thereby estimating the risk of vehicle loss given various environmental conditions. The contribution of this research is twofold. Firstly, the proposed method is tailored for AUGs. It captures the synergies between AUGs′ inherent functional failures and influential environmental factors, whilst considering the dynamic nature and non-linear dependencies among their relationships. The predicted risk profile can assist further decision making and risk mitigation during real AUG missions. Secondly, this chapter not only adds details to risk analysis for AUGs, but also extends the application of the CBN model into a broader AUV domain. The present model is not restricted to an AUG system but can be flexibly adapted to other AUV platforms by incorporating the vehicle′s specifications to enhance safety performance.

The structure of this chapter is organized as follows. In Section 3.2, the background on the BBN model, the copula theory, and the CBN model is introduced. Section 3.3 describes the detailed process of the proposed CBN model, which mainly contains the CBN model development and the CBN model analysis. Section 3.4 provides a case study for applications of the proposed method, considering a Slocum G1 Glider operating in a real water region. Section 3.5 discusses the benefits, limitations, and future works of this chapter. Key findings are concluded in Section 3.6.

3.2 Theoretical background

3.2.1 Bayesian Belief Network

A BBN is defined as a directed acyclic graph (DAG) associated with a joint probability distribution, where the causal dependencies among variables can be captured by conditional probabilities (Pearl, 1986; Zarei et al., 2022). For a set of random variables $X = (x_1, x_2, \dots, x_n)$, the joint probability distribution of X can be calculated according to the chain rule of Bayes theorem in Eq. (3-1).

$$P(x_1, x_2, \dots, x_n) = \prod_{i=1}^{n} P\left(x_i \middle| x_{ipar}\right) \tag{3-1}$$

where n is the number of variables, x_{ipar} is the parent node of x_i, and $P\left(x_i \middle| x_{ipar}\right)$ is a conditional probability distribution.

3.2.2 Copula theory

Copula is a function that constructs the multivariate joint cumulative distribution of random variables which have various marginal distributions (Nelsen, 2006). Based on Sklar's theorem (Sklar, 1959), any multivariate joint distribution can be represented as a copula function of its marginals. Accordingly, let $\boldsymbol{x} = (x_1, x_2, \dots, x_n)$ be a finite set of random variables, and therefore the multivariate joint distribution function $F(x_1, x_2, \dots, x_n)$ can be expressed as:

$$F(x_1, x_2, \dots, x_n) = C\left(F_1(x_1), F_2(x_2), \dots, F_n(x_n)\right) \tag{3-2}$$

where $C(\cdot)$ indicates a copula function and $F_i(x_i)$ denotes the marginal distribution function of each variable. Assuming that the joint distribution function $F(x_1, x_2, \dots, x_n)$ has n-order partial derivatives, the joint density function can be obtained following the chain rule:

$$\begin{aligned} f(\boldsymbol{x}) &= \frac{\partial^n C\left(F_1(x_1), F_2(x_2), \dots, F_n(x_n)\right)}{\partial F_1(x_1) \partial F_2(x_2) \dots \partial F_n(x_n)} \prod_{i=1}^{n} f(x_i) \\ &= c\left(F_1(x_1), F_2(x_2), \dots, F_n(x_n)\right) \prod_{i=1}^{n} f(x_i) \end{aligned} \tag{3-3}$$

where $c(F_1(x_1), F_2(x_2), \ldots, F_n(x_n))$ represents the copula density function, and Eq. (3-3) can be used to construct a joint density function of multivariate variables.

3.2.3 Copula Bayesian Network (CBN)

Based on the copula theory, a CBN model is proposed by incorporating the copula function into a traditional BBN network (Amin et al., 2021). As a BBN model mainly uses conditional probabilities, similarly, the foundation of a CBN model is the conditional density function. Let $f(x|\boldsymbol{y})$, with $\boldsymbol{y} = (y_1, y_2, \ldots, y_k)$, be a conditional density function, and let $f(x)$ be the marginal density function of variable $\boldsymbol{x}$. Then, a copula density function $c(F(x), F(y_1), F(y_2) \ldots, F(y_k))$ can be specified that satisfies the following equation:

$$f(x|\boldsymbol{y}) = R_c(F(x), F(y_1), F(y_2), \ldots, F(y_k))f(x) \tag{3-4}$$

where $R_c(\cdot)$ is a scale factor which can be expressed as:

$$R_c(\cdot) = \frac{c(F(x), F(y_1), F(y_2), \ldots, F(y_k))}{\frac{\partial^k C(1, F(y_1), F(y_2), \ldots, F(y_k))}{\partial F(y_1)\partial F(y_2) \ldots \partial F(y_k)}} \tag{3-5}$$

According to Eq. (3-4) and Eq. (3-5), any copula density function $c(\cdot)$, together with a marginal density function $f(x)$, can be combined to construct a conditional density function $f(x|\boldsymbol{y})$. The detailed proof can be seen in Elidan's work (Elidan, 2010a).

3.3 Methodology

The proposed CBN model for risk prediction of AUGs in dynamic environments includes two major steps, as shown in Fig. 3.1. The first step develops the CBN structure, and the second step conducts the CBN model analysis. Details of each step are elaborated in the following subsections.

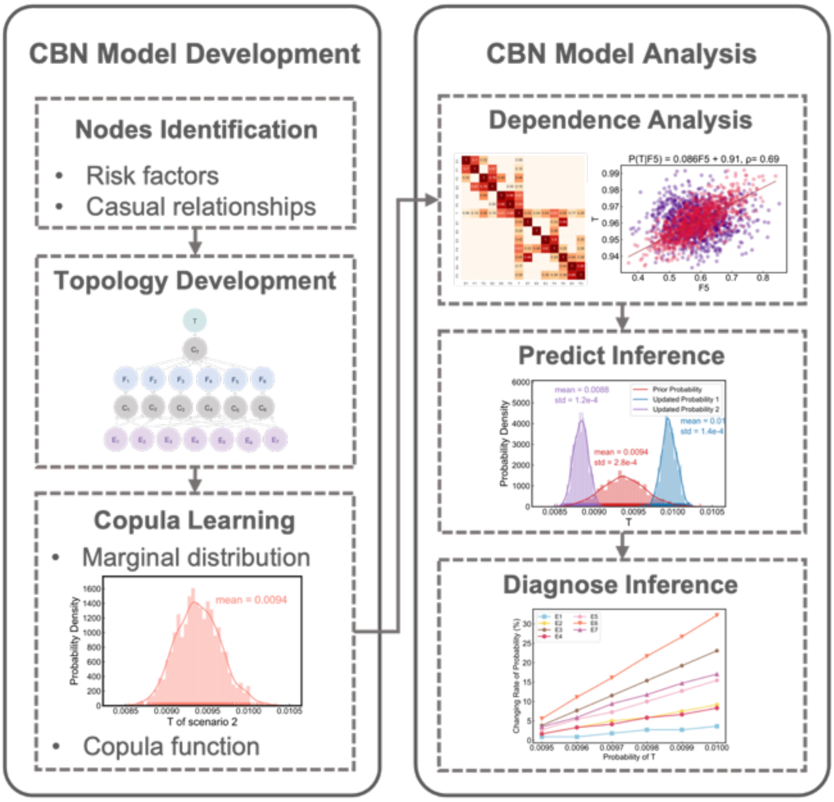

Fig. 3.1. Flowchart of the proposed CBN model.

3.3.1 CBN model development

In general, the development process of a CBN model mainly includes the identification of network nodes, the development of the network topology, and copula learning.

3.3.1.1 Identification of network nodes

The first step to construct a CBN model is the identification of network nodes. Three types of nodes are considered in this chapter, namely, root nodes, intermediate nodes, and leaf nodes.

The description of different network nodes is defined in Table 3.1.

Table 3.1. Three types of CBN nodes.

Node Type	Description	Example
Root node	Root causes that influence a system fault	Abnormal environmental conditions
Intermediate node	System faults that influence an undesirable event	Functional failures of AUGs
Leaf node	Undesirable abnormal events	AUG loss

3.3.1.2 Network topology development

The process of converting a BBN into a CBN structure is shown in Fig. 3.2. The BBN model is a graphical structure to present the causal relationships among network nodes. Similarly, the topology of a CBN model remains the same as the corresponding BBN structure (Hashemi et al., 2016). However, in contrast to a BBN that uses conditional probability tables, a CBN model adopts local copula functions to capture the dependency among system nodes. In addition, another key difference between these two models lies in that a CBN model replaces the prior probabilities of BBN nodes with marginal probability distributions.

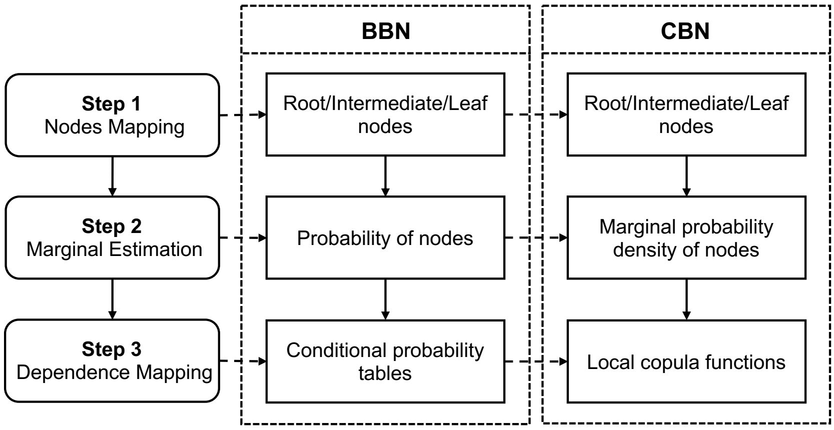

Fig. 3.2. Mapping a BBN into a CBN structure.

3.3.1.3 Copula learning

Copula learning of a CBN model mainly involves two steps. The proper marginal distributions of each network node can be firstly identified. Then, a suitable copula function modelling the dependencies among nodes should be determined.

3.3.1.3.1 Determine marginal distributions

Marginal distributions should be properly assigned for each network node. Different types of marginal distributions are not constrained by the CBN model. In this chapter, three widely used marginal distributions are selected to show the flexibility of the CBN model, namely normal, log-normal, and Beta distributions, which are summarized in Table 3.2.

Table 3.2. Three candidate marginal distributions.

Distribution	Probability Density Function	Mean	Variance
Normal	$f(x) = \frac{1}{\sigma\sqrt{2\pi}} exp\left(-\frac{(x-\mu)^2}{2\delta^2}\right)$	μ	δ^2
Log-normal	$f(x) = \frac{1}{x\sigma\sqrt{2\pi}} exp\left(-\frac{(lnx-\mu)^2}{2\delta^2}\right)$	$exp\,(\mu + \frac{\delta^2}{2})$	$(exp(\delta^2)-1)exp\,(2\mu+\delta^2)$

Beta	$f(x;\alpha,\beta)=\frac{x^{\alpha-1}}{B(\alpha,\beta)}(1-x)^{\beta-1}$	$\frac{\alpha}{\alpha+\beta}$	$\frac{\alpha\beta}{(\alpha+\beta)^2(\alpha+\beta+1)}$

3.3.1.3.2 Select the copula function

A Copula function is important to describe the dependency degree among CBN nodes, while different copula functions are varied in dependency characteristics (i.e., symmetry, tail dependence, and so on) (Pan et al., 2021). The Gaussian copula is a widely used symmetric copula, which is powerful in handling multi-variable problems (Sun et al., 2021b). The density function of the Gaussian copula is expressed as follows:

$$c_\rho^{Gauss}(x_1,x_2,\dots,x_n;\rho)=|\rho|^{-\frac{1}{2}}exp\left(-\frac{1}{2}\zeta(\rho^{-1}-I)\zeta^T\right) \quad (3\text{-}6)$$

where $\zeta=\left(\Phi^{-1}(x_1),\Phi^{-1}(x_2),\dots,\Phi^{-1}(x_n)\right)$, Φ^{-1} is an inverse function of the standard univariate normal cumulative distribution function, ζ^T is the transpose of the matrix ζ, I denotes the identity matrix, and ρ represents the matrix of correlation coefficients among nodes. The correlation coefficient in ρ measures the dependency degree between a pair of nodes, which is in the range of [-1, 1]. Specifically, two nodes are closely correlated when the absolute value of the correlation coefficient closes to 1. Oppositely, two nodes are mutually independent when the absolute value of the correlation coefficient closes to 0.

According to its definition, the Gaussian copula has *n*-dimensional generalizations, which can effectively capture the dependency degree among complex multi-variables. Thus, the Gaussian copula is applied in this chapter to construct the copula density function of the CBN model.

3.3.2 CBN model analysis

CBN model analysis is critical for exploring the dependency relationships among network nodes and assisting decision making. It mainly includes the dependence analysis, predict inference, and diagnose inference.

3.3.2.1 Dependence analysis

Dependence analysis can measure the dependence degree of a pair of variables, implying how two variables could change together. Key variables can be identified through the dependence analysis. Such variables normally have stronger impacts on the occurrence of an accident, and therefore they require more attention in risk mitigation and safety control. In this chapter, the dependence analysis was conducted based on the correlation coefficients, which were defined based on domain experts′ knowledge.

3.3.2.2 Predict inference

Predict inference aims to predict the probability distribution of an accidental event given observation of involved risk variables. As mentioned in Section 3.2, a CBN model can be applied to perform network inference by using the conditional density function. Assuming that A denotes an accidental event, $\boldsymbol{S}$ represents a series of influential risk variables. According to Eq. (3-4), the predict inference analysis of CBN can be specified as:

$$f(A|\boldsymbol{S}) = R_c\big(F(A), F(S_1), F(S_2) \ldots, F(S_k)\big) f(A) \tag{3-7}$$

where $f(A|\boldsymbol{S})$ presents the posterior probability of the event A given the observation of certain risk variables $\boldsymbol{S}$, $f(A)$ is the prior marginal probability distribution of the accident, and $R_c(\cdot)$ is the conditional copula density function that was defined in Eq. (3-5). Thus, the predict inference using Eq. (3-7) can achieve an updated probability of an accident based on new observations of risk variables.

3.3.2.3 Diagnose inference

Conversely, diagnose inference can estimate the posterior probability distribution of each risk variable given certain evidence of an accidental event, aiming to diagnose the most influential factor. The diagnose inference can be conducted according to Eq. (3-8). The variation between the prior distribution and the posterior distribution of a variable indicates its contribution to the observed accident, and greater variation implies larger criticality for this variable. In order to validate the diagnose inference of the proposed CBN model, a sensitivity analysis was conducted in Section 3.4.2.3.

$$f(S_i|A) = R_c\big(F(S_i), F(A)\big) f(S_i) \tag{3-8}$$

where $f(S_i|A)$ indicates the occurrence probability of the i-th risk factor given certain evidence of the accident A.

3.4 Case study

To validate the effectiveness of the proposed CBN model, a case study was conducted by evaluating the risk level of a Slocum G1 Glider that deploys in a real open water region. The basic specification of a Slocum G1 Glider is summarized in Table 3.3. In this case study, firstly potential risk factors causing vehicle loss were identified, which further assisted in constructing the CBN model. Then, the developed CBN model was utilized for dependence analysis, predict inference, and diagnose inference, respectively. Two risk scenarios considering AUG missions with dynamic time and space were separately analyzed. Accordingly, relative measures for risk mitigation were suggested in the case study.

Table 3.2. The specification of the Slocum G1 Glider (Wang et al., 2021c).

Parameter	Value
Weight in air	~52 Kg
Displacement	52 L
Depth Range	4-200 m
Speed	0.4 m/s horizontal
Range	1500 km

3.4.1 CBN model development

The CBN model was developed in this case study. Risk variables regarding AUG loss were systematically identified. Then, the BBN topology was presented to show their causal relationships. Copula learning was finally conducted to characterize network nodes and determine copula functions.

3.4.1.1 Identification of risk variables

As a premise to establish a CBN model, it is necessary to identify risk variables given AUG's inherent characteristics. Based on technical documents and domain experts' knowledge, seven environmental factors (E1-E7) and six functional failures (F1-F6) of an AUG system were extracted to describe AUG loss (T). To create the cause-effect links in the CBN model, environmental factors (E1-E7), functional failures (F1-F6), and AUG loss (T) were considered as root nodes, intermediate nodes, and the leaf node, respectively. The description of different nodes is provided in Table 3.4. To gain a better understanding of the mechanism that how the risk variables interact with each other, causal relationships among these nodes were elaborated as follows.

Table 3.4. Description of CBN nodes.

Node	Description	Node	Description
E1	Low temperature (°C)	F1	Integrity failure
E2	Large water depth (m)	F2	Power degradation
E3	Large ship density (routes/0.08km²/year)	F3	Invisibility
E4	High wave height (m)	F4	Collision
E5	Close to the seabed (m)	F5	Buoyancy control failure
E6	Large water density gradient (kg/m^3)	F6	Path deviation
E7	Large current speed (m/s)	T	Glider loss

3.4.1.1.1 Integrity failure (F1)

Integrity failure refers to a leak where water enters the pressure vessel of an AUG, which is a key failure mode leading to AUG loss. An early study analyzed 63 AUG incidents from a total of 205 missions (Brito et al., 2014a). Results showed that among the identified 19 failure modes of AUGs, integrity failure was ranked as the top common failure mode. In general, integrity failure can be caused by low ambient temperature (E1) and large water depth (E2).

Low ambient temperature (E1), especially in polar regions, can cause large temperature gradients between the air and the water column. Consequently, the vehicle or components may suffer integrity failure and leakage (Ferguson, 2008). For instance, a CTD sensor may suffer cracks at low ambient temperature, and seawater could therefore penetrate and freeze inside, eventually causing a sensor failure (Kaminski et al., 2010). Water depth (E2) also influences AUG′s integrity. A robust hull structure is required for the vehicle to resist external water pressure and protect internal electronics (Rudnick et al., 2004a). Since a larger water depth tends to generate higher water pressure, and such an exterior load will cause an adverse impact on the stability of the hull structure. Therefore, the large water depth will cause an AUG to suffer a higher risk of integrity failure.

3.4.1.1.2 Power failure (F2)

The amount of stored energy on an AUG affects its mission length and duration. Former studies have proved that more than 50% of AUV loss accidents were related to a power failure (Meng and Qingyu, 2010; Yu et al., 2017). Power failure is mainly affected by three influential factors, namely, low ambient temperature (E1), large water depth (E2), and a large water density gradient (E6).

Low ambient temperature (E1) can cause the energy degradation of batteries. The battery capacity may drop significantly especially when the ambient temperature is below -20℃ (Bandhauer et al., 2011). As a result, poor battery performance could further lead to premature energy depletion and a mission abort. In addition, since most of the available energy (~70%) is consumed to provide buoyancy across the pycnocline, the water depth of diving (E2) and the water density gradient (E6) are also critical factors influencing energy consumption (Meyer, 2016). Therefore, for an AUG, lower energy consumptions require deep dives in areas with low water density gradients.

3.4.1.1.3 Invisibility (F3)

Invisibility is mainly influenced by large ship density (E3) and high surface waves (E4). Intuitively, a large number of ships and high surface waves will cause poor visibility, especially in a recovery phase or a fail-safe phase of an AUG mission. They could cause difficulties for operators to find the vehicle when it is floating to the surface, and thereby the vehicle could be lost.

3.4.1.1.4 Collision (F4)

A collision accident includes colliding with ships, the seabed, and other underwater obstacles, which is a key contributor to the damage or loss of an AUG. The major factors causing collisions consist of large ship density (E3), close to the seabed (E5), and large current speeds (E7).

Operating in the surface regions could pose AUGs to the risk of collision with ships. A former study proved that the probability of collision between ships and AUGs is proportional to the shipping density in the mission region (Merckelbach, 2013b). Hence, operating the AUG in low-traffic regions would minimize the collision risk with ships. Colliding with the seafloor will potentially cause a hull leak, a broken antenna, a breakage in the external bladder, or a buoyancy engine problem. Since AUGs move at a relatively slow speed, fortunately, colliding with the seafloor could not cause extensive damages to AUGs unless the environment is energetic (e.g., strong near-bottom currents or dynamic underwater obstacles). Current speed could be another influential factor to the risk of collision. Low-speed AUGs could experience motion problems when the current speed exceeds its maximum forward speed (Claus et al., 2010). Consequently, the AUG might drift into shipping lanes or near-bottom water regions, causing collisions with ships, the seafloor, or other underwater obstacles.

3.4.1.1.5 Buoyancy control failure (F5)

Buoyancy control is a crucial function of AUGs. A buoyancy control failure could be a fatal contributor to AUG loss, which mainly has two influential factors, namely, large water density gradient (E6) and large water depth (E2).

A large water density gradient (E6) has a critical impact on buoyancy control. Generally, AUGs can control their buoyancy either by filling an external bladder or by pushing seawater in or out of an internal reservoir (Griffiths et al., 2007b). However, in some water regions (e.g., regions near melting glaciers), the seawater density can change significantly due to salinity dilution. As a result, decreasing water density will require more buoyancy for the vehicle′s rising motion. In this case, once the required buoyancy exceeds the compensating buoyancy provided by external bladders, a buoyancy control failure will occur. Consequently, the vehicle may be trapped in a neutrally buoyant layer and fail to return to the surface. Therefore, AUGs should be employed in regions with lower water density gradients to prevent buoyancy control problems. The buoyancy control of AUGs is also influenced by the large water depth (E2). In fact, both volumes of the external bladders and the pressure hull would become smaller with an increasing water depth (Yang et al., 2017b). Such deformation of the vehicle decreases buoyancy. If the vehicle cannot handle this decreasing buoyancy, it would also suffer buoyancy control failure.

3.4.1.1.6 Path deviation (F6)

High wave height (E4) and large current speed (E7) can affect the motion of an AUG by deviating the vehicle from its desired path.

High wave height (E4) could cause irregular external disturbances for the vehicle. For example, wave-induced forces can drag the vehicle toward the surface, and deviate it from its desired path (Fossen, 2012). Former research has shown that a higher wave height has a greater impact on the AUG's motion (Ullah et al., 2020a); specifically, when the wave height exceeds 1.5 m, the trajectory and pitch angle performance of a vehicle can be significantly affected. In addition, since AUGs are relatively slow-moving vehicles with a typical velocity below 0.5 m/s, they also tend to be easily influenced by large current speed (E7) (Petillo and Schmidt, 2012). A previous study has shown that an AUG could suffer difficulties in flying against currents that exceed 0.3 m/s (Bachmayer et al., 2006). Hence, strong currents may deviate an AUG from a planned path significantly, and as a result, the vehicle may not reach its target position, or even worse, could be lost.

3.4.1.2 Network topology development

Based on the above analysis, a BBN model was initially developed as shown in Fig. 3.3, which presents the relationships among environmental parameters (E1-E7), potential functional failures (F1-F6), and AUG loss (T). Conditional probability tables should be assigned among

BBN nodes. For simplicity, in this chapter, the assigned conditional probability employed a logical OR-gate, where values 1 and 0 represent the occurrence or non-occurrence of associated events respectively. According to Table V, the values of environmental nodes were divided into three levels: low, medium, and high, representing their severity degrees. The prior probability of each node was also provided in Table V. Ideally, the prior probability data should be obtained based on historical field data, technical documents, and statistical data. However, due to a lack of associated data, this chapter used the probability data based on domain expert knowledge and prior engineering experience. Considering the riskiest scenario according to Table 3.5, namely, all environmental nodes were at a high level, the occurrence probability of functional failure nodes (F1-F6) and AUG loss (T) can be predicted by applying Bayes' theorem in Eq. (3-1). The results were shown in Table 3.6. Different degrees of the probability value of AUG loss are defined in Table VII. It can be seen that when all environmental variables were at a high level, both predicted probabilities of functional failure nodes and AUG loss reached a "significantly high" level, which should be reduced by risk mitigation measures.

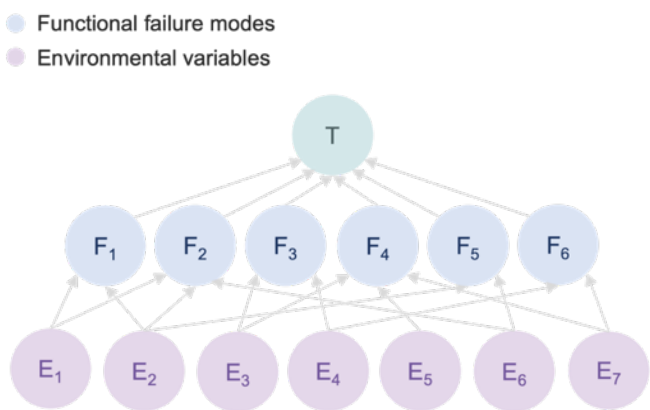

Fig. 3.3. The developed BBN topology.

Table 3.5. Value ranges and prior probability data of environmental nodes.

Node	Value Level	Value Range	Probability
	low	0-higher	0.0001
E1	Medium	(-10)-0	0.0011
	High	below (-10)	0.34
	low	0-50	0.0001
E2	Medium	50-150	0.0012
	High	150-higher	0.35
	low	0-30	0.0002
E3	Medium	30-100	0.0013
	High	100-higher	0.36
	low	0-0.6	0.0002
E4	Medium	0.6-1.2	0.0012
	High	1.2-higher	0.38
	low	10-higher	0.0001
E5	Medium	5-10	0.0011
	High	0-5	0.36
	low	0-4	0.0001
E6	Medium	4-8	0.0018
	High	8-higher	0.37
	low	0-0.15	0.0002
E7	Medium	0.15-0.3	0.0017

High	0.3-higher	0.39

Table 3.6. Predicted probability data of functional failures and glider loss, considering the riskiest scenario where all environmental nodes are at a high level.

Node	Probability
F1	0.57
F2	0.73
F3	0.60
F4	0.75
F5	0.59
F6	0.62
T	0.96

Table 3-7. Degrees of the occurrence probability of glider loss.

Degree of occurrence probability	Value range
Significantly high	10^{-1} - 1
High	10^{-2} -10^{-1}
Moderate	10^{-3} -10^{-2}
Low	<10^{-3}

The topology structure of the CBN model was transformed from the BBN model, as shown in Fig. 3.4, where C1-C7 represents local copula conditional density functions. In Fig. 3.4, similarly to the developed BBN in Fig. 3.3, causal relationships among nodes were identified, whereas the local copula functions assisted in modeling the dependence structure among nodes.

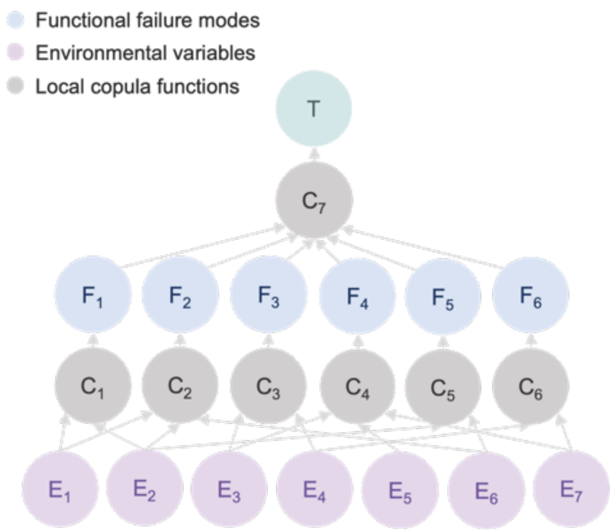

Fig. 3.4. The developed CBN model.

3.4.1.3 Copula learning

As described in Section 3.3.1.3, the process of copula learning includes determining marginal distributions to characterize each node and selecting local copula functions to describe the dependence relationships among nodes.

3.4.1.3.1 Determine marginal distributions

The marginal distribution of each environmental variable (E1-E7) was considered to follow three commonly used distributions (i.e., Normal, Log-normal, and Beta distributions) to test the flexibility of the CBN model. Table 3.8 summarizes the marginal distribution of each node. The principle of determining the parameters of each distribution is that the mean value of each distribution equals the probability of the associated node that was defined in Table 3.5, whereas an exact method for estimating each marginal distribution is not within the scope of this chapter.

Table 3.8. Probability distributions of environmental nodes (E1-E7) in the CBN model.

Node	Value Level	Marginal distribution	Parameters
	low	Normal	μ=0.0001, σ=0.00001
E_1	Medium		μ=0.0011, σ=0.0003
	High		μ=0.34, σ=0.10
	low	Log-Normal	μ=-9.22, σ=0.10
E_2	Medium		μ=-6.76, σ=0.25
	High		μ=-1.09, σ=0.28
	low	Beta	α=8.16, β=40799
E_3	Medium		α=18.75, β=14406
	High		α=7.93, β=14.11
	low	Normal	μ=0.0002, σ=0.00001
E_4	Medium		μ=0.0012, σ=0.0003
	High		μ=0.38, σ=0.10
	low	Log-Normal	μ=-9.22, σ=0.10
E_5	Medium		μ=-6.85, σ=0.27
	High		μ=-1.06, σ=0.27
	low	Beta	α=2.78, β=27771
E_6	Medium		α=20.21, β=11209
	High		α=8.25, β=14.06
	low	Normal	μ=0.0002, σ=0.00001
E_7	Medium		μ=0.0017, σ=0.0003
	High		μ=0.39, σ=0.10

Similarly, considering the riskiest scenario where all environmental nodes are at a high level, the marginal distributions of functional failures (F1-F6) and AUG loss (T) can be determined based on Table 3.6, and the results are shown in Table 3.9.

Table 3.9. Probability distributions of functional failures (F1-F6) and AUG loss (T), considering the riskiest scenario where all environmental nodes are at a high level.

Node	Marginal distribution	Parameters
F_1	Log-Normal	μ=-0.58, σ=0.17
F_2	Log-Normal	μ=-0.32, σ =0.10
F_3	Normal	μ=0.60, σ=0.09
F_4	Normal	μ=0.75, σ=0.07
F_5	Log-Normal	μ=-0.54, σ=0.13
F_6	Beta	α=29.19, β=17.89
T	Log-Normal	μ=-0.04, σ=0.01

3.4.1.3.2 Select the local copula function

As mentioned in Section 3.3.1.3, the Gaussian copula function is a widely used elliptical copula function, which outperforms in handling multi-variable dependencies and fast speed calculation. Therefore, the Gaussian copula was integrated into the established CBN model to measure the dependence relationships among variables.

3.4.2 CBN model analysis

Based on the above analysis, a complete CBN model was built. Then, the CBN model analysis, which includes the dependence analysis, predict inference, and diagnose inference, can be conducted to explore dependency relationships among risk variables and predict the risk profile of AUG loss given various environmental conditions.

3.4.2.1 Dependence analysis

Dependence analysis explores the dependency degree among risk variables, which aims to identify critical factors that impact AUG loss. Based on domain experts′ knowledge, the correlation coefficients among variables were determined. The strength of the correlation coefficients can be visualized using a heatmap, as shown in Fig. 3.5, where the color patch indicates the correlated strength from deep red (strong correlation) to light yellow (weak correlation). Accordingly, a hierarchical dendrogram divided all variables into six clusters with different colors in Fig. 3.5 (left side), and each cluster reveals an accidental pathway that results in AUG loss. For example, the node of AUG loss (T) is directly connected with the node of buoyancy control failure (F5), which is shown as the deepest color in the heatmap with the correlation coefficient of 0.69 compared to the other five functional failures. Subsequently, buoyancy control failure (F5) is further connected with the node of a large water density gradient (E6) and large water depth (E2), and therefore the first cluster (T, F5, E6, E2) is created. In other words, buoyancy control failure (F5) has greater influences on AUG loss than the other five functional failures, whereas a large water density gradient (E6) and large water depth (E2) are key environmental contributors to buoyancy control failure (F5). Therefore, F5 and its related environmental factors E6 and E2 require more attention to prevent AUG loss. Similarly, the accidental pathway of the other five functional failures and their related environmental factors can be identified as the first cluster.

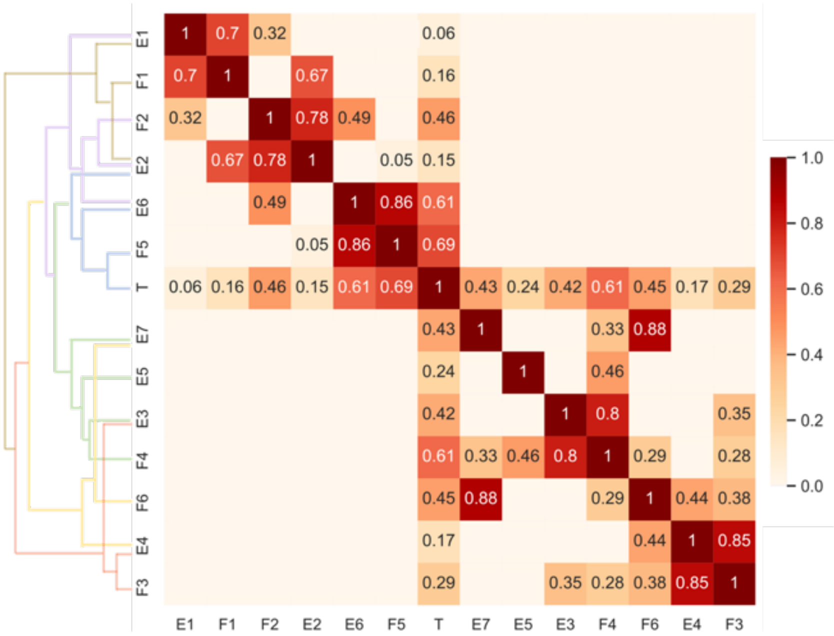

Fig. 3.5. Heatmap and dendrogram of correlation coefficients for pairs of CBN nodes.

After determining the correlation coefficients, the joint probability distributions among nodes can be determined using the Gaussian copula function. The scatter plots in Fig. 3.6 present examples of the joint probability distributions among different pairs of nodes, where Fig. 3.6 (a)-(d) present the dependencies between AUG loss (T) and its four most key functional failures, namely buoyancy control failure (F5), collision (F4), power degradation (F2), and path deviation (F6). Fig. 3.6 (e)-(h) exhibit the dependencies between AUG loss (T) and its four most critical environmental factors, including a large water density gradient (E6), large current speed (E7), large ship density (E3), and a short distance to the seafloor (E5). Noticeably, the blue points in Fig. 3.6 denote 1000 samples based on Table 3.8 and Table 3.9 without considering correlation coefficients, whereas the red points symbolize 1000 samples using the proposed CBN model with correlations incorporated. As can be seen, red points in Fig. 3.6 are more clustered and denser than blue points, and red points become denser with a larger correlation coefficient, which proves that a CBN model considering correlation coefficients can better describe dependency relationships among variables.

To intuitively show the degree of dependencies, assuming that two nodes are linearly related, and their dependency can be represented by linear regression lines, which are shown as the red lines in Fig. 3.6. To take Fig. 3.6 (e) as an example, the probability of AUG loss (T) can be roughly estimated when the probability of a large water density gradient (E6) is given according to the fitted linear regression function. By comparing Fig. 3.6 (e)-(h), it can be seen that Fig. 3.6 (e) presents stronger positive monotonicity with a greater slope due to a larger correlation coefficient (0.61), which indicates an obvious positive dependency among a large water density gradient (E6) and AUG loss (T). In other words, a great water density gradient (E6) is a dominant factor for causing AUG loss compared with the other six environmental variables. Nevertheless, in Fig. 3.6 (f)-(h), with the correlation coefficient decreasing from 0.43, 0.42, to 0.24, the slope of the regression line is gradually declining. At the same time, red sample points become more random. These findings indicate that a smaller correlation coefficient could lead to relatively weak dependency among variables. Similarly, by comparing Fig. 3.6 (a)-(d), the buoyancy control failure (F5) is also observed as the most important failure mode for AUG loss (T) due to its largest correlation coefficient (0.69) compared with the other functional failures, which deserves more attention in failure diagnosis and safety control during an AUG mission. Based on the above, results from linear regression analyses indicate that the dependencies modeled by the CBN are concordant with the defined correlation coefficients in Fig. 3.5.

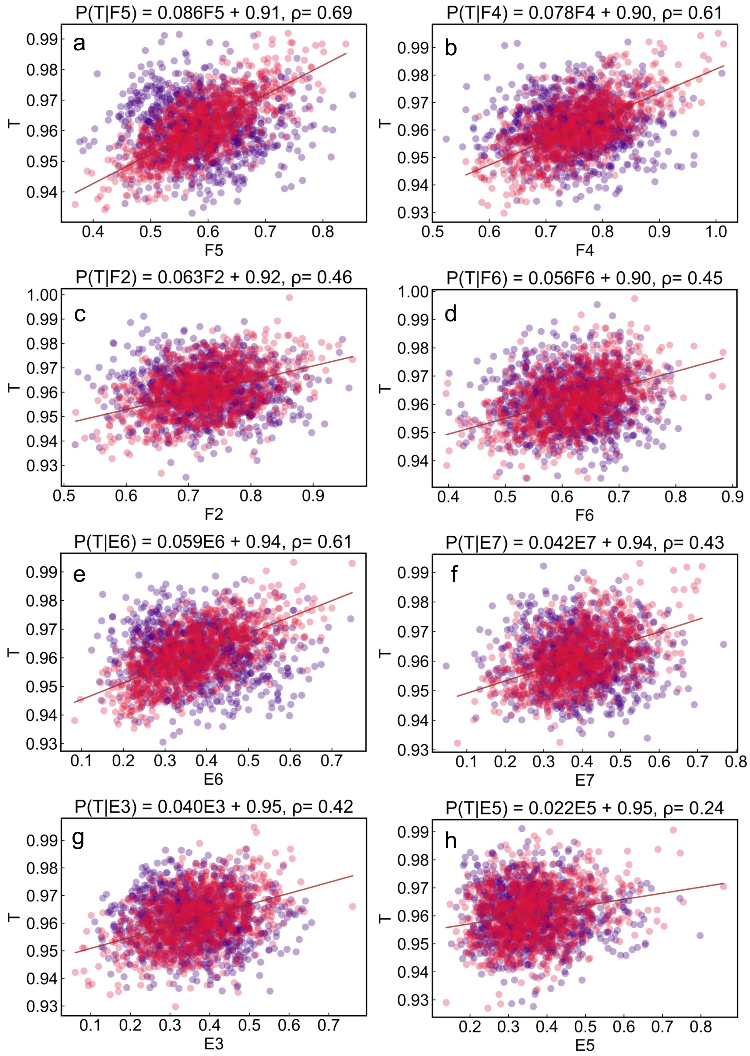

Fig. 3.6. The joint probability distribution and linear regression for pairs of CBN nodes.

3.4.2.2 Predict inference

Predict inference of the CBN model aims to update the probability distribution of AUG loss (T) given new evidence of involved risk variables. The developed CBN model can continuously predict the probability distribution of both functional failures (F1-F6) and AUG loss (T) using Eq. (7). Results of the predict inference are discussed as follows:

Changes in the probability distribution of environmental variables could lead to an updated distribution of both functional failures and AUG loss accordingly. Fig. 3.7 presents the updated probability when all environmental variables are at a low level, medium level, and high level, separately. Results show that updated mean probabilities of functional failures (F1-F6) and AUG loss (T) have a clear increase with the rising level of environmental variables. This indicates that a higher level of environmental factors is crucial to cause an increasing risk for both technical failures and vehicle loss. Specifically, the mean probability of AUG loss (T) increases largely from 0.0009, 0.0094 to 0.96. According to Table 3.7, the mean probability of AUG loss (0.96) reaches the “significantly high” range when all environmental variables are at a high level. In such a case, the risk of AUG loss should be effectively mitigated to an acceptable level by operating the vehicle in conditions where ambient environmental variables are at a relatively low level.

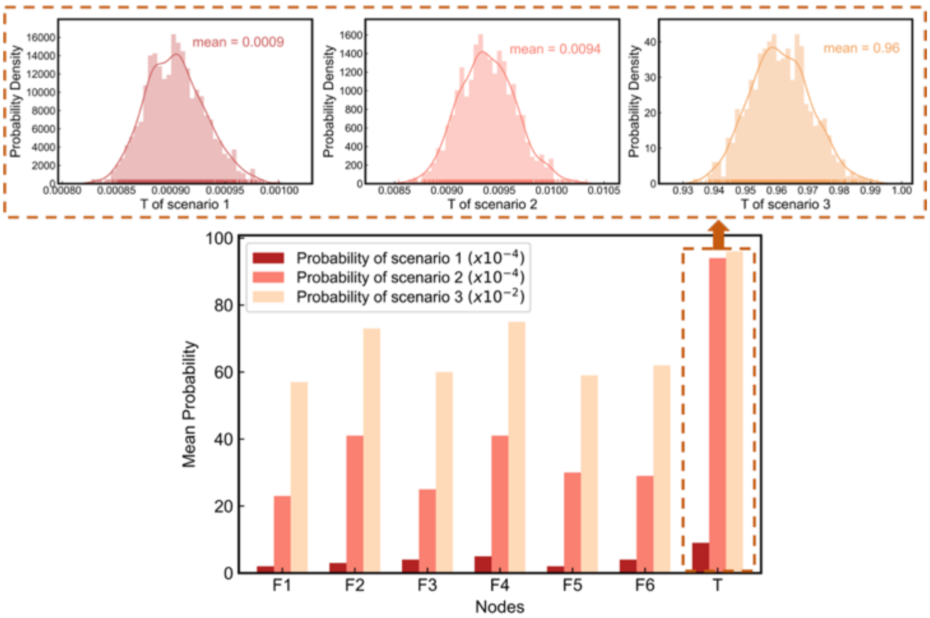

Fig. 3.7. Updated probability of functional failure nodes (F1-F6) and AUG loss (T) when all environmental variables are at a: low level (scenario 1), medium level (scenario 2), and high level (scenario 3), respectively.

As known in the former dependence analysis, a large water density gradient (E6), large current speed (E7), and large ship density (E3) were observed as the three most influential factors that affect AUG loss. A greater probability of these critical factors can cause an increasing risk of AUG loss. Considering all environmental variables are at a medium level initially, by limiting the probability of these three factors to new intervals, which is [0.0024, 0.0025] for a large water density gradient (E6), [0.0021, 0.0022] for large current speed (E7), and [0.0017, 0.0018] for large ship density (E3), respectively. The probability distributions of functional failures and AUG loss can be updated simultaneously, as shown in Fig. 3.8. By comparing the updated probability distribution (blue color) and the prior probability distribution (red color), it can be seen that updated probability distributions of both functional failure nodes and AUG loss have experienced obvious changes. Taking Fig. 3.8 (g) as an example, the main changes of the updated probability distribution of AUG loss (T) include the increasing mean value with the changing rate of 6.38% and the decreasing standard deviation with the changing rate of 53.33%, where the changing rate in this chapter is defined as Eq. (3-9). In other words, the risk level of AUG loss rises with the increasing probability of three key environmental factors. At the same time, the shape of the updated distribution becomes narrow with a reduced standard deviation, which denotes the decreasing uncertainty of the prediction. Similarly, Fig. 3.9 summarized the updated mean probability and standard deviation of all functional failure nodes, where most of the updated distributions experience an increase of the mean probability and a decrease of the standard deviation. Only the probability distribution of integrity failure (F1) exhibits no change because it is not correlated with the aforementioned three environmental factors, and therefore it is not influenced by the changes of these three factors. These findings proved that when narrowing the probability interval of key environmental factors into a relatively larger value range, the probability of both correlated functional failures and AUG loss will increase accordingly. Therefore, key risk variables should be monitored as the major checkpoints to mitigate the risk of AUG loss.

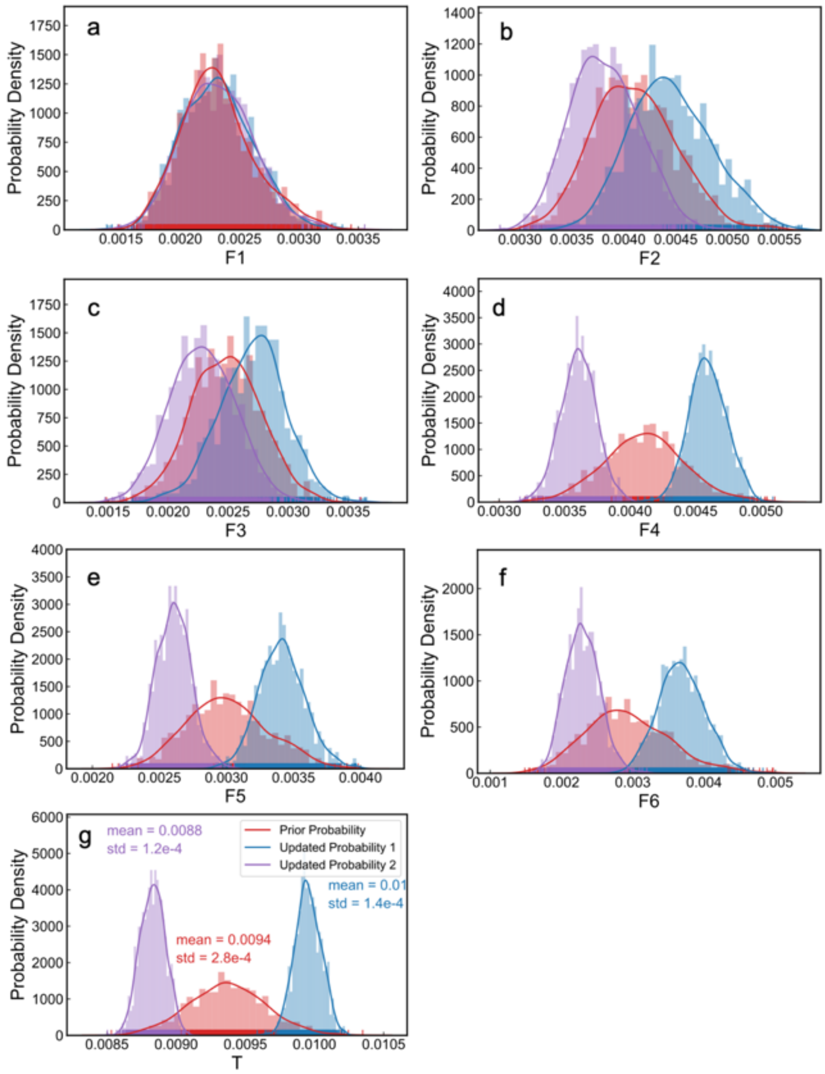

Fig. 3.8. Updated probability of: (a)-(f) functional failure nodes; and (g) AUG loss.

$$Changing\ Rate = \left|\frac{Updated\ Value - Prior\ Value}{Prior\ Value}\right| \times 100\% \tag{3-9}$$

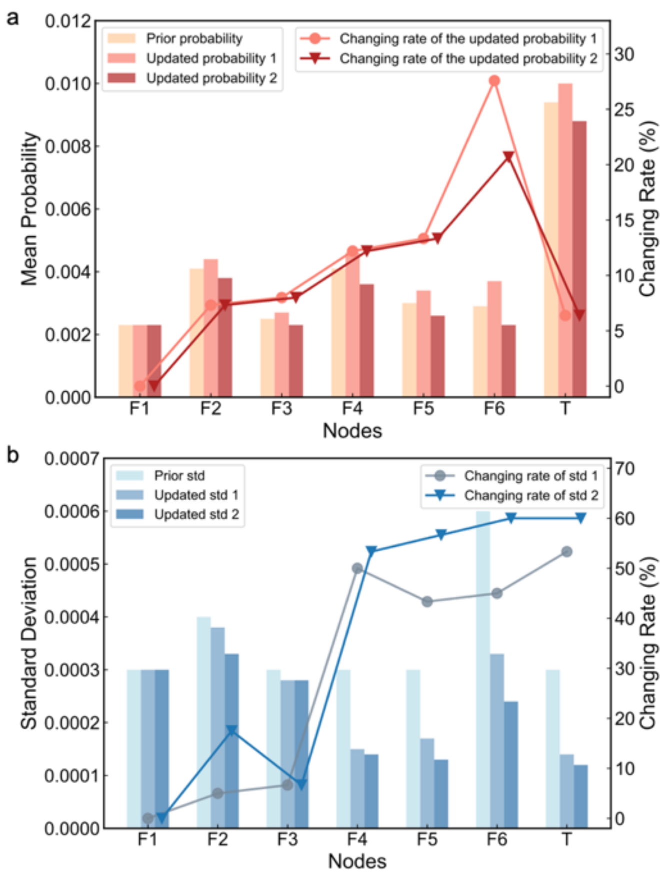

Fig. 3.9. Updated value and changing rate for: (a) mean probability; and (b) standard deviation.

On the contrary, a smaller probability of critical risk factors (i.e., a large water density gradient (E6), large current speed (E7), and large ship density (E3)) can effectively reduce the probability of AUG loss. Specially, modifying the probability of these three environmental variables into a relatively low interval, which is [0.0012, 0.0013] for E6, [0.0013, 0.0014] for E7, and [0.0008, 0.0009] for E3, respectively. As a result, the probability distribution of functional failure nodes and AUG loss can be updated accordingly, as shown in Fig. 3.8, where the purple color denotes the updated distribution. In Fig. 3.8 (g), the mean probability of AUG loss (T) decreases from 0.0094 to 0.0088, achieving a 6.4% reduction in the overall risk level. At the same time, the standard deviation also drops with a changing rate of 57.1%, which proves that the uncertainty of the prediction is also reduced. Similarly, Fig. 3.9 summarizes the updated mean probability and standard deviation of all functional failure nodes. Results show that only integrity failure (F1) remains no variation with the probability and standard deviation as it is not correlated with E6, E7, and E3 in the CBN model. However, the other five functional failures (F2-F6) experience various degrees of reduction in both the mean probability and the standard deviation, which in turn demonstrates that a decreasing probability of an environmental factor can effectively mitigate the probability of its correlated functional failures.

Former analyses proved that the predict inference of the established CBN model can effectively update the risk level of AUG loss given different environmental observations. Accordingly, risk mitigation of AUV operations can be achieved by controlling the occurrence probabilities of key risk factors. In addition, a narrow probability interval of risk factors is promising to reduce the prediction uncertainty. This means it is proper to operate an AUG in a relatively gentle environment, where the value of environmental parameters changes in a moderate range.

3.4.2.3 Diagnose inference

Diagnose inference of the CBN model aims to predict posterior probability distributions of each environmental variable given a certain state of AUG loss. Specifically, considering that the occurrence probability of AUG loss is known, the backward propagation from Eq. (3-8) can be carried out to diagnose the most likely environmental factors causing the accident.

A sensitivity analysis can be investigated to validate the diagnose inference of the proposed model. A sensitivity analysis identifies the variation of an output variable of a model by modifying the input variables, which is an effective method for performance validation of probabilistic models, such as BN-based models (Rositano et al., 2017). Through a sensitivity analysis, the most influencing factors can be determined for the diagnose inference, and this assists in suggesting specific safety measures for risk mitigation (Govender et al., 2022).

A sensitivity analysis based on the one-at-a-time (OAT) method was performed in this chapter. The OAT method is a classic method to investigate the effect of variation of parameters on posterior probabilities (Coupé et al., 1999). It works by changing one input variable and obtaining the variations of other output variables, and thereby determining the critical influential variables with high sensitivity (Riedmann et al., 2015).

In this chapter, assuming that the occurrence probability of AUG loss (T) is relatively high, which changed gradually from 0.0095 to 0.01. The posterior probabilities of each environmental variable can be obtained via diagnose inference, and the changing rates between their posterior probabilities and prior probabilities were calculated. Results of the sensitivity analysis are shown in Fig. 3.10. By comparison, the posterior probability of a large water density gradient (E6) experiences the greatest change with its mean probability rising by 32.22%. It validates that when the occurrence probability of AUG loss (T) is at a high level, a large water density gradient (E6) can be a dominant contributor. Similarly, the probabilities of a large current speed (E7) and a large ship density (E3) also show a large increasing rate of 23.08% and 17.06%, respectively. Therefore, these two nodes have a great influence on vehicle loss. Thus, in order to mitigate the risk of AUG loss from a higher level to an acceptable level, it is reasonable to give a priority to the probability mitigation of these critical influential factors.

Based on the sensitivity analysis, the diagnose inference was validated to achieve continuous updates of the posterior probability of environmental variables given different risk levels of AUG loss, and it assists in diagnosing the major contributors accordingly and providing reasonable safety measures. Therefore, once an acceptable risk level is determined by the decision maker, diagnose inference can be applied for targeted risk mitigation for AUG loss by adaptively controlling the key environmental variables until achieving the desired risk level.

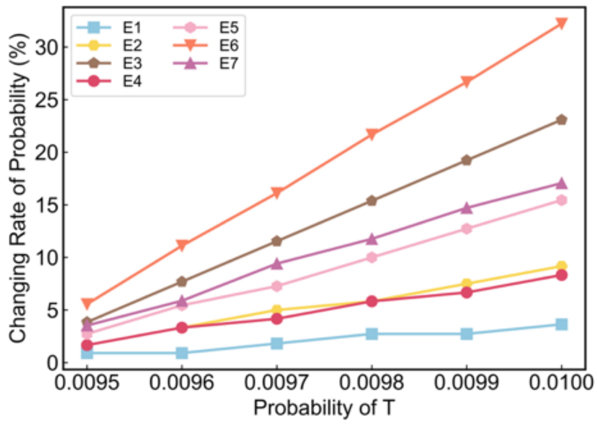

Fig. 3.10. Changing rates between posterior probabilities and prior probabilities of environmental nodes (E1-E7) given varying evidence of vehicle loss (T).

3.4.2.4 Application

Based on the above analysis, the proposed CBN model can be applied for risk prediction over time and space for a Slocum G1 Glider operating in a real water region. The area of Holyrood (47.4621-47.4624 °N, 53.1086-53.1083 °W) was selected as the target mission area. The data of each environmental variable on February 3rd, 2021 were collected from the website of Ocean Networks Canada (https://www.oceannetworks.ca/) and Marine Traffic (https://www.marinetraffic.com/), as shown in Fig. 3.11. In particular, Fig. 3.11 (a) displays the hourly changes of environmental variables of ambient temperature (E1), wave height (E4), water density gradient (E6), and current speed (E7), whereas Fig. 11 (b) roughly shows the ship density (E3) in the target area.

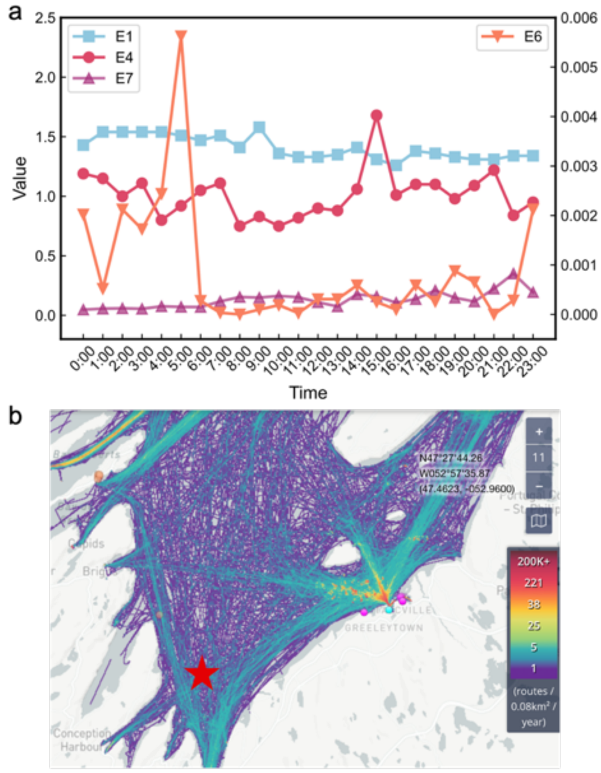

Fig. 3.11. Environmental data from the Holyrood area on February 3rd, 2021.

For simplicity, the value of each environmental variable was transferred to three levels according to Table 3.5, as shown in the top subplot in Fig. 3.12, where the value of water depth (E2) and distance to the seafloor (E5) was assumed to remain at a low level due to lack of data. Accordingly, the real-time occurrence probabilities of functional failures and AUG loss were predicted using the proposed CBN model, and the results are shown in the bottom subplot in Fig. 3.12. Noticeably, the probability of AUG loss (T) reached the “significantly high” level (>0.1) on three occasions, namely 15:00, 21:00, and 22:00. Specifically, at the time of 15:00 and 21:00, with the probability of high wave height (E4) rising to the high level, the probability of both visibility (F3) and path deviation (F6) experienced a clear increase. Consequently, the probability of AUG loss (T) further rose to 0.24 and 0.26, respectively. In addition, at the time of 22:00, a warning increase for the probability of large current speed (E7) occurred, as a result, the probability of collision (F4) exhibited an obvious increase in one hour reaching 0.34, which further caused a high probability of 0.24 with AUG loss (T).

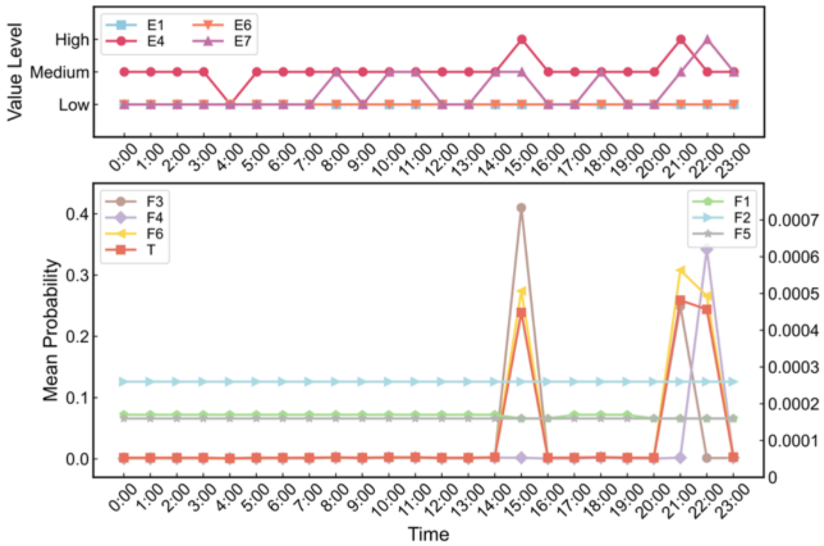

Fig. 3.12. Real-time risk prediction of functional failures and AUG loss with changes of environmental variables.

To explore the updating risk level over space, especially when an AUG operates at different water depths, the environmental variables of water depth (E2), ship density (E3), distance to the seafloor (E5), and water density gradient (E6) were mainly considered. A scenario can be assumed with the value level of these variables changing over water depth, as shown in the top subplot in Fig. 3.13. Results of the predicted probability of AUG loss and functional failures in various water depths are shown in the bottom subplot in Fig. 3.13, where the degree of probability changes from light yellow (lowest probability) to deep red (highest probability). As can be seen, in the surface water column (0-50 m), a high level of a large ship density (E3) can cause increases in the probability of invisibility (F3) and collision (F4), which further led to a higher probability (0.36) of AUG loss (T). As the water depth increases, the probability of E5 (close to the seafloor) and E6 (large water density gradient) also rose accordingly. As a result, probabilities of integrity failure (F1), power loss (F2), and buoyancy control failure (F5) grow accordingly. Once the water depth exceeded the maximum depth range (200 m) of the vehicle, the probability of AUG loss had a remarkable increase to 0.35. These findings revealed that the middle-water column was relatively safer than the surface and deep-water regions in this scenario. Therefore, risk mitigation measures can be taken accordingly. For instance, it is beneficial to reduce the surfacing times of AUGs in an area with busy shipping traffic. In addition, the risk of AUG loss can also be mitigated by avoiding deploying the vehicle in deep-water regions, especially with great water density gradients and high altitudes of the seafloor.

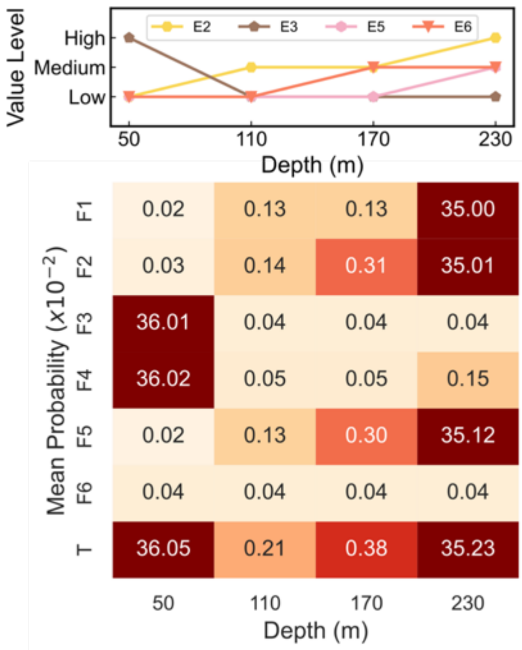

Fig. 3.13. Probability (×10-2) of functional failures and AUG loss under different water depth.

3.5 Discussion

Based on the case study analysis, the proposed CBN model was demonstrated to be a potential risk prediction method for AUGs operating in dynamic environments. In particular, the above applications proved that this model can effectively predict the risk of AUG loss given different observations of environmental factors. Correspondingly, a higher probability of environmental factors could lead to an increase of the probability of AUG loss. Hence, it is essential to operate in benign operating environments to enhance AUG safety. In summary, this chapter can be used to continuously update the risk level by monitoring different environmental conditions over time and space, and it can be implemented to minimize the risk of potential functional failures and AUG loss in advance of a mission. Therefore, this chapter can help decision-makers adaptively predict hazardous environmental conditions and provide insights for mitigating the risk level for safer operations. It should be noted that this chapter utilized the Slocum G1 Glider in the case study for model validation. Since different types of AUGs may have various characteristics, such as displacement, depth range, and cruise speed. Such inherent differences could cause the value level of risk variables to change as well. Therefore, a precondition of applying the proposed method or adapting it to risk analyses for other types of AUGs is considering their specifications.

Limitations of this chapter are recognized which should be addressed in future work. Firstly, this research only employed the Gaussian copula function to model the correlation relationships among risk variables. Future works will explore different kinds of copula functions (i.e., Archimedean copula functions) to describe the dependencies more accurately. Secondly, due to insufficient measured data, the case study combined measured environmental data with assumed environmental conditions, which could compromise the accuracy of risk prediction. In future work, real-time environmental data measured by multiple sensors should be incorporated to improve assessment accuracy. Lastly, this chapter provided an offline risk assessment method for AUGs, which could be extended to an online decision network for setpoint selection and path control given the current predicted risk level.

3.6 Conclusion

This chapter proposed a risk prediction method based on the copula Bayesian network (CBN) model for AUGs operating in dynamic underwater environments. In the constructed CBN structure, a BBN model was initially applied for identifying potential risk variables and their causal relationships to AUG loss. Copula functions were incorporated to quantitatively capture the dependencies among risk variables and predict the risk level of AUG loss. The potential application of the developed CBN model was demonstrated with a case study, which assisted in risk prediction for a Slocum G1 Glider deploying in a real open water region. Specifically, seven influencing environmental variables and six types of functional failures were identified. Three kinds of marginal distributions were applied to characterize each risk variable. The Gaussian copula function was then employed for modeling correlated dependencies among these variables. The CBN reference was finally conducted to evaluate the risk level for AUG loss both temporally and spatially.

Based on the results of the case study, four key findings are highlighted from this chapter: (1) Based on the dependence analysis, the most critical environmental variables contributing to

AUG loss were identified, including a large water density gradient (E6), large current speed (E7), and large ship density (E3), which deserve constant attention in the environmental monitoring and risk mitigation process. (2) Predict inference of the CBN model can continuously update the occurrence probability of AUG loss given new observations of environmental conditions. Results proved that the risk level of AUG operations can be mitigated by reducing the occurrence probabilities of key risk factors. Moreover, a narrow probability interval of these factors can minimize the prediction uncertainties, which gave insights into deploying the vehicle in a relatively gentle environment where the ambient conditions change moderately. (3) From the diagnose inference of the CBN model, the posterior probability of each risk variable can be obtained given a certain state of AUG loss. Hence, by defining an acceptable risk level of AUG loss, environmental conditions can be adaptively adjusted to achieve the safety requirement. (4) Applications considering a Slocum G1 Glider operating in the Holyrood water region validated that the proposed CBN model is effective for risk prediction both over time and space, which indicated that this chapter can be implemented to prevent risky occasions and areas in advance of a mission. In addition, risk mitigation measures can be provided according to the above findings, such as reducing the surfacing times for AUGs in the water column with busy shipping, and cruising away from deep-water regions with a large density gradient or with a close distance to the seafloor.

In conclusion, this chapter contributes a potential approach of risk prediction tailored for AUGs in complex underwater environments. It captures the synergies between AUGs′ inherent functional failures and dynamic environmental conditions, whilst achieving updated risk prediction for AUG loss both temporally and spatially. The developed model can be extended to applications for other types of AUVs by incorporating the vehicle's inherent specifications. The present work can potentially improve the safety performance of AUGs and assist risk mitigation in decision making.

Chapter 4. Risk-based Path Planning for Autonomous Underwater Vehicles in an Oil Spill Environment

Preface

A version of this chapter has been published as: ***Chen X, Bose N, Brito M, et al. Risk-based path planning for autonomous underwater vehicles in an oil spill environment [J]. Ocean Engineering, 2022, 266: 113077.*** *I am the primary author along with the Co-authors, Neil Bose, Mario Brito, Faisal Khan, Gina Millar, Craig Bulger, and Ting Zou. I developed the conceptual framework for the risk-based path planning for autonomous underwater vehicles in an oil spill environment. I prepared the first draft of the manuscript and subsequently revised the manuscript based on the co-authors′ and peer review feedbacks. Co-authors Neil Bose, Mario Brito, Faisal Khan, and Ting Zou provided support in implementing the concept development, reviewing, and revising the manuscript. Co-authors Gina Millar and Craig Bulger provided assistance in data investigation, reviewing and correcting the results. The co-authors also contributed to the review and revision of the manuscript.*

Abstract: This chapter aims to answer the third research sub-question: "How to design a risk-base decision making strategy based on the risk analysis model?" The applications of AUVs in complex environments have been hindered by the risk of vehicle loss. Path planning for AUVs is an effective technique for mitigating such risks and ensuring safer routing. Yet previous studies did not address path searching problems for AUVs based on probabilistic risk reasoning. This chapter aims to propose an offboard risk-based path planning approach for AUVs operating in an oil spill environment. A risk model based on the Bayesian network was

developed for probabilistic reasoning of risk states given varied environmental observations. This risk model further assisted in generating a spatially-distributed risk map covering a potential mission area. An A*-based searching algorithm was then employed to plan a Risk-A* path through the constructed risk map. The proposed planner was applied in a case study with a Slocum G1 Glider in a real-world spill environment around Baffin Bay. Simulation results proved that the Risk-A* planner outperforms in risk mitigation while achieving competitive path lengths and mission efficiency. The proposed method is not constrained to AUVs but can be adapted to other marine robotic systems.

4.1 Introduction

An oil spill is one of the major accidents in the ocean that can damage the marine ecosystem, social economy, and human health (Hwang et al., 2020; Zhu et al., 2021). Due to hazardous effects of oil spills, it is essential to detect and track the oil during or after a spill for environmental impact assessment and response decision-making (White et al., 2016). Although surface oil slicks can be detected and mapped by traditional survey methods (i.e., satellite imagery and ship-based sampling), subsurface oil detection could be more challenging due to the deep presence of oil and its spatial-temporal changes over time (Ji et al., 2020). AUVs are advanced marine robots that can be used for detecting, tracking, and assessing subsurface oil in deep water (Kinsey et al., 2011; Sahoo et al., 2019). Compared with traditional survey methods, AUVs coupled with multiple sensors are superior in providing high-resolution sampling data of submerged oil plumes, achieving communication of spill information in near real-time, as well as preventing personnel exposure to hazardous oil spill environments (Pereira et al., 2013;

Vinoth Kumar et al., 2020). Therefore, it is beneficial to deploy AUVs for searching and delineating subsurface oil plumes, capturing oil behaviors, and improving the efficiency of oil spill response.

Due to their ability to obtain in-situ data, some scientists have implemented AUVs for oil spill detection. During the Deepwater Horizon spill in the Gulf of Mexico, which was one of the largest oil spill accidents in history, a Sentry AUV was employed with underwater mass spectrometers to localize and track submerged oil plumes at approximately 1100 m depth (Camilli et al., 2010; Kinsey et al., 2011). A REMUS-600 AUV was deployed with a fluorometer at a natural oil seep off the coast of Santa Barbara, California, with a mission depth up to 35 m (DiPinto, 2019). A glider AUV coupled with a fluorometer was used to detect oils in Tallinn Bay in the Gulf of Finland, which proved that the glider is suitable to monitor the oil distribution over a larger sea area due to its long-endurance capability (Pärt et al., 2017). A Jaguar AUV was effectively used in the ice-mapping missions to detect the under-ice oil spills in the Northern Alaska coast (Maksym et al., 2014).

Yet none of the missions above have considered the risk of vehicle loss as part of their mission planning. However, operating in an oil spill environment could expose AUVs to the risk of loss due to the comprehensive effects of ocean currents, surface waves, potential underwater obstacles, and oil contamination on sensors. Therefore, it is essential to minimize such risks and enhance their safety navigation during spill response missions. Risk-based path planning is one of the critical techniques for mitigating risks and ensuring AUVs′ safe deployment before a mission. It refers to planning an optimal path for the vehicle from its initial state to the goal state of a mission considering the risk involved, which is under certain criteria (e.g., shortest path length, minimal cruise time, minimal risk profile), and as the same time, avoiding obstacles along a path (Zeng et al., 2015; Lefebvre et al., 2016; Guo et al., 2021).

A number of studies have investigated risk-based path planning methods for AUVs to realize safer operations. Pereira et al. (Pereira et al., 2011) proposed a minimum risk planner that minimized the cumulative surfacing risk for a glider AUV. Based on this work, an expanded study (Pereira et al., 2013) considered the effects of ocean currents on the vehicle for planning AUV paths and predicted ocean currents using a probabilistic model. The proposed planner effectively reduced the collision risk with ships and land. Hegde et al. (Hegde et al., 2016a) presented a method for developing collision risk indicators for AROVs. The proposed indicators (i.e., time to collision, mean time to collision, and mean impact energy) were used to identify risk prone waypoints for a given AROV path, which could further assist in mission path planning/replanning and provide risk reduction measures. Lefebvre et al. (Lefebvre et al., 2016) addressed the collision risk for AUV path planning using a hierarchical A* approach. To enhance the autonomy capability of the vehicle, the authors highlighted the integration of path planning in the AUV control architecture. However, that study only considered underwater obstacles while ignoring hazardous impacts of other environmental variables (e.g., underwater currents, ship density, etc.). Yan et al. (Yan et al., 2022) applied a whale optimization algorithm to tackle a three-dimensional planning problem for AUVs. The proposed planner can effectively avoid risky regions and achieve the shortest and safest path with minimal energy consumption. Zhang et al. (Zhang et al., 2022) addressed the AUV path tracking with real-time obstacle avoidance via a reinforcement learning technique. The risk constraints were adopted in reward functions to realize collision avoidance and ensure safety control.

While previous studies have explored different risk-based path planning methods for mitigating AUV risks, limitations are observed from them. Firstly, most of the former research only addressed risks in a general marine environment with impacts of a single environmental variable, for example, underwater currents. However, limited studies have considered the scenario of AUVs navigating in complex oil spill environments with interactions of multiple risk variables, and accordingly provided the mission planning strategy from a safety perspective. Secondly, limited past works have applied a probabilistic model for quantifying the risk state of AUVs given varied environmental observations. While probabilistic reasoning could enhance the accuracy of risk prediction and further improve the efficiency of decision making, therefore, a rigorous method that integrates a probabilistic risk model into the path planning problem for AUVs is needed.

The objective of this chapter is to propose a risk-based path planner for AUVs to improve its safety performance and enhance autonomous capabilities in oil spill environments. Specifically, hazardous impacts of potential risk variables in oil spill regions were analyzed. A risk analysis model based on the Bayesian network (BN) was then developed for probabilistic reasoning over current risk states of vehicle loss, which considered various environmental conditions and potential underwater obstacles. This risk model was extended to assist in generating a risk map of a gridded mission area. In order to avoid high-risky regions while achieving a relatively shorter path length, the A* algorithm was employed to search for a Risk-A* solution. The performance of the proposed planner was demonstrated in a simulated case study with a spill area in Baffin Bay.

The contribution of this chapter is twofold. Firstly, this chapter provided a rigorous path planning method for AUVs from a safety perspective. The integrated BN-based risk model can predict the risk states of AUVs while intuitively presenting spatial risk distributions in a complex oil spill environment. The probabilistic reasoning can enhance the effectiveness and accuracy of further risk-based decision making. Secondly, the developed Risk-A* planner can avoid potential risky regions and obstacles, and meanwhile, it achieves a trade-off between risk mitigation and mission efficiency. It is expected that the proposed strategy can serve as a worthwhile precomputing policy to prevent AUV loss at the path planning stage, and therefore enhance the safety decision-making capability of AUVs for safer navigation. The proposed method is not constrained to AUVs but can be adapted to other marine robotic systems.

The structure of this chapter is organized as follows. Section 4.2 defines the risk-based path planning problem and the solution of this chapter. Section 4.3 elaborates a BN-based model used for risk map generation and describes the A* algorithm used for path searching. Results of a simulated case study are discussed in Section 4.4, and Section 4.5 concludes this chapter.

4.2 Risk-based path planning: problem definition and solution

The proposed risk-based path planner in this chapter aims to find a Risk-A* path based on a probabilistic risk map. In this section, the general problem formulation was defined and the solved algorithm was described.

4.2.1 Problem definition

Generally, methods for AUV path planning can be broadly divided into two categories: global path planning and local path planning. Global path planning searches for a globally optimal path with known environmental information beforehand with an AUV mission, whereas local path planning finds a locally optimal strategy under unknown and dynamic environments (Cheng et al., 2021). This chapter mainly focused on the global path planning for AUVs, especially for a glider AUV, to plan an optimal risk path. The reason lies in that a local path planning algorithm would require an onboard implementation and consume more energy, while gliders consume low energy to secure high longevity of their missions. Therefore, real-time implementation of local path planning could be difficult considering energy consumption. In addition, environmental information for AUV missions, such as locations of large static obstacles (e.g., islands or rocks), could be obtained beforehand. In this case, it is worthwhile to conduct the offline global path planning prior to AUV missions as precomputing policies to ensure safe deployment.

In general, a global path planning problem can be formulated as an optimization problem, which can be defined as Eq. (4-1)

$$P^* = \underset{p_k \in P}{\operatorname{argmin}}\, g(p_k) \tag{4-1}$$

where $P = \{p_1, p_2, \dots, p_n\}$ is a set of feasible paths, p_k is the k^{th} path amongst the set P, and P^* denotes the optimal path that minimizes the cost function g. Through various cost functions, different optimal objectives can be realized, such as achieving the minimal involved risks, the minimal routing length, the minimal travel time, and so on.

The objective of this chapter is to search for a Risk-A* path for AUVs travelling from a given initial position to a goal position, whilst achieving a competitive path length. The risk state of an AUV can be specified by a risk index, which refers to the probability of vehicle loss. Hence, the objective function of this chapter can be modified as Eq. (4-2), and the cost functions of both the risk of vehicle loss and the path length are defined in Eq. (4-3) and Eq. (4-4), separately:

$$P^* = \underset{p_k \in P}{\operatorname{argmin}}[g_r(p_k) + g_l(p_k)] \tag{4-2}$$

$$g_r(p_k) = \sum_i r(w_i) \tag{4-3}$$

$$g_l(p_k) = \sum_{i-1} d(w_i, w_{i+1}) \tag{4-4}$$

where w_i is the *i^th^* waypoint to be reached along the path p_k, $r(w_i) \in [0, 1]$ denotes the risk index of the waypoint w_i, which is calculated using the Bayes theorem as Eq. (4-7) that is elaborated in Section 4.3.1; $g_r(p_k)$ represents the accumulative risk cost along the path p_k, which is under the constraint of the risk threshold that is defined in Eq. (4-5); $g_l(p_k)$ represents the accumulative length cost along the path, and $d(w_i, w_{i+1})$ denotes the Euclidean distance between the two adjacent waypoints.

$$r(w_i) < r_t \tag{4-5}$$

where r_t is a predefined risk threshold that specifies the maximum acceptable risk index for a waypoint.

4.2.2 Problem solution

To find a globally Risk-A* path, the A* algorithm was applied in this chapter. The A* algorithm, which is oriented from the Dijkstra′s algorithm, is an effective solution for searching the globally minimum-cost path in a static network, and it is widely applied to address low-dimensional path planning problems (Dijkstra, 1959; Hart et al., 1968). The evaluation function of this algorithm is defined in Eq. (4-6):

$$f(w_i) = g(w_i) + h(w_i) \tag{4-6}$$

where $g(w_i)$ is the actual cost from the start state w_s to the current waypoint w_i in the search network, $h(w_i)$ represents the estimated cost called a heuristic from the current waypoint w_i to the goal state w_g, and $f(w_i)$ is the total cost from the start state through the waypoint w_i to the goal state.

Therefore, A* calculates the total cost $f(w_i)$ of candidate nodes in the searching network, and it selects a node with the minimal value of $f(w_i)$ as the next traversal node until reaching the goal node. Meanwhile, A* relies on a heuristic $h(w_i)$ to fast drive the network exploration to the desired areas by exploring the fewest number of nodes. This exhibits its advantage in reducing the computational time and improving the path searching efficiency (Cheng et al., 2021). Another advantage of the A* algorithm is its flexibility to be adapted by modifying the heuristic and cost functions given various optimization objectives, which is particularly beneficial to AUV path planning considering different mission requirements in complex marine environments (Singh et al., 2018). Hence, the A* algorithm has been commonly used for planning global paths of AUVs with various optimization criteria, including the shortest path length (Wang et al., 2017; Wang and Pang, 2019), the minimal collision risk (Pereira et al., 2011; Lefebvre et al., 2016), the minimal energy consumption (Li et al., 2017; Yao et al., 2018), and the shortest searching time (Szczerba et al., 2000; Li and Zhang, 2020). Given its superiority in fast searching and flexible adaptation from the risk perspective, the A* algorithm was chosen as the path planning solution in this chapter.

4.3 Methodology

The flowchart of the proposed methodology is presented in Fig. 4.1. It can be broadly divided into three steps. A risk analysis model based on the BN was firstly established for probabilistic reasoning of waypoint risk indices. A risk map was then created based on the BN inference results. Through the generated risk map, an A*-based algorithm was employed to search for a Risk-A* path in the potential mission area. Details of the proposed approach were elaborated in the following subsections.

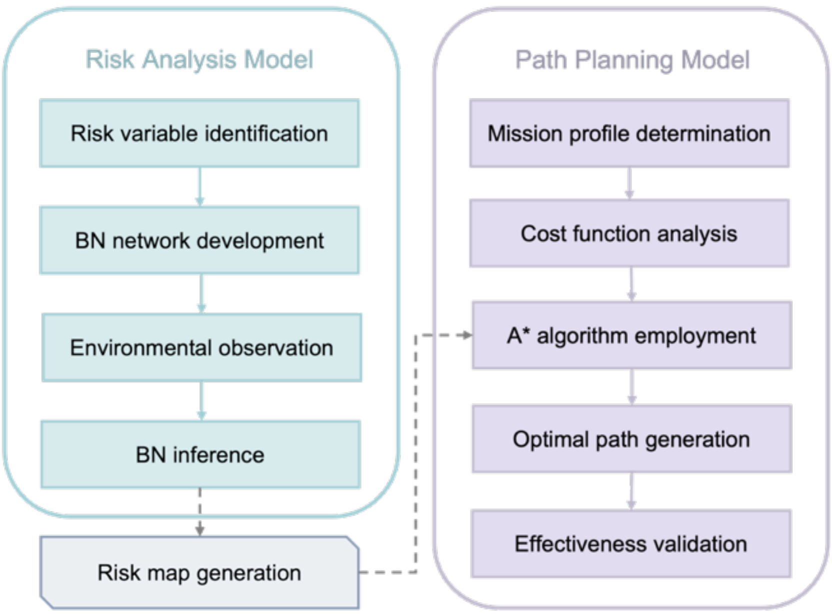

Fig. 4.1. Flowchart of the proposed method.

4.3.1 Development of the BN-based risk model

Risk variable identification is a premise to establish a BN-based risk model. Risk variables, which can potentially lead to AUV loss in an oil spill environment, should be firstly captured in this chapter. To facilitate further BN inference, identified risk variables can be discretized into three states according to their observed values, representing low, medium, and high severity, respectively.

BN is a probabilistic graphical model composed of vertices (nodes) and edges (arrows), where each node denotes a random variable and arrows represent causal relationships among nodes (Afenyo et al., 2017). Their dependency degrees can be captured mathematically using conditional probabilities with the Bayesian theorem. For each BN, there is a unique probability model. Assuming that X is a set of random variables: $X = (x_1, x_2, \dots, x_n)$, where n is the number of variables in the network. The joint probability $P(x_1, x_2, \dots, x_n)$ can be calculated according to the chain rule of the Bayes theorem using Eq. (4-7) (Jäger et al., 2018):

$$P(x_1, x_2, \dots, x_n) = \prod_{i=1}^{n} P(x_i | Pa(x_i)) \tag{4-7}$$

where $Pa(x_i)$ represents the set of parent nodes of x_i, and $P(x_i|Pa(x_i))$ is the conditional probability distribution.

Bayesian networks have been well applied for risk analyses in the AUV domain. Griffiths and Brito (Griffiths and Brito, 2008) firstly used a BN model for predicting the risk of AUV loss in a sea ice environment. An extended study based on it applied a BN model for AUV risk management in Polar regions (Brito and Griffiths, 2016). The proposed BN structure coped well with the uncertainties by eliciting expert judgement. Meanwhile, it captured the risk variables from both environmental factors (i.e., ice concentration and ice thickness) and the vehicle platform to produce an updated probability of vehicle loss. Hegde et al. (Hegde et al., 2018) presented a BN model for monitoring the mission abort during AUV operations of inspection, maintenance, and repair (IMR). This application of the BN model identified risk factors from technical, organizational, and operational perspectives, and it quantified the probability of the IMR mission failure. More recently, Bremnes et al. (Bremnes et al., 2019; Bremnes et al., 2020) proposed a Bayesian approach towards supervisory risk control of AUVs for under-ice operations. The BN reasoning was employed to predict the risk state for online risk modelling. The constructed risk model further assisted in decision-making for waypoint selections of the vehicle. Yang et al. (Yang et al., 2020) provided an approach for dynamic risk analyses of a long-range AUV based on a dynamic BN model. The risk state can be updated online when the vehicle experiences different operating environments, which automatically guides the AUV to avoid hazardous environmental conditions.

There are clear advantages of using the BN for AUV risk modelling. Firstly, due to the challenging operational environments of AUVs, multiple risk factors could interact to cause vehicle loss. BN contains a clear topological structure to present causal relationships among complex risk contributors, which facilities risk identification especially for a multi-variable system (Obeng et al., 2022). Secondly, BN is a probabilistic risk assessment tool. Adopting the conditional probability theory could enhance the accuracy of risk prediction and decrease uncertainties. In addition, based on its predictive reasoning, BN can update the current risk state of the vehicle given new environmental observations (Yazdi et al., 2021). This feature is particularly beneficial for an AUV platform which exposes to various operating environments during a mission, and thereby its spatial-temporal evolution of risk states can be timely predicted. Lastly, BN can be easily employed by combining expertise even when the historical data are limited (Brito et al., 2022). To our knowledge, the BN model has not been used for AUV path planning. This chapter extended the application of the BN model to the domain of AUV decision making.

4.3.2 Risk map generation

A risk map of a potential mission area can be generated based on BN reasoning results. The created risk map is represented in the form of probabilistic occupancy grids. Each grid evaluates the risk index $r(w_i) \in [0, 1]$, which is specified by the probability of the AUV loss given contained environmental conditions. As described in Section 4.2.1, the risk index $r(w_i)$ is calculated using the Bayes theorem as Eq. (4-7). Therefore, the risk map serves as a probabilistic measure of spatial risk states in the desired mission area. A trade-off should be considered when determining the grid resolution, as a relatively lower resolution could speed up the search progress but meanwhile sacrifice the accuracy of the planned vehicle's positions.

4.3.3 Development of the path planning model

Based on the constructed risk map, an A*-based path planning model can be then applied to obtain an optimal solution from the safety perspective. It firstly analyzes the cost functions of both risk indices and path lengths. Then, the objective function can be determined according to involved costs, and the A* algorithm is finally used to search for a Risk-A* path.

4.3.3.1 Cost function analysis

When considering the risk cost along a path, an actual risk cost $g_r(w_i)$ of the current waypoint w_i, which was originally defined in Eq. (4-3), can be adapted to Eq. (4-8). Moreover, an admissible heuristic $h_r(w_i)$ (i.e., an estimated risk cost) used for A* searching can be defined in Eq. (4-9). The method for heuristic estimation was adapted from former research (Pereira et al., 2011; Pereira et al., 2013; Lefebvre et al., 2016).

$$g_r(w_i) = r(w_i) \tag{4-8}$$

$$h_r(w_i) = N * r_{min} \tag{4-9}$$

where $r(w_i)$ denotes the risk index of the waypoint w_i, which was elaborated in Section 4.2.1. r_{min} is the globally minimum risk index among all grids in the risk map, and N is the minimal number of transitions from the current waypoint w_i to the goal w_g, which can be defined in Eq. (4-10):

$$N = \left\lfloor \frac{d(w_i, w_g)}{d_{max}} \right\rfloor \tag{4-10}$$

where $d(w_i, w_g)$ denotes the Euclidean distance between the current waypoint w_i and the goal w_g, and d_{max} is the maximum Euclidean distance between two adjacent waypoints.

When considering the length cost along a path, an actual length cost of the current waypoint $g_l(w_i)$, which was based on Eq. (4-4), can be adapted to Eq. (4-11). This actual length cost calculates the Euclidean distance $d(w_s, w_i)$ from the start point w_s to the current point w_i. We adopted an admissible heuristic $h_l(w_i)$ that was defined in Eq. (4-12), which estimates the Euclidean distance $d(w_i, w_g)$ from the current waypoint w_i to the destination w_g.

$$g_l(w_i) = d(w_s, w_i) \tag{4-11}$$

$$h_l(w_i) = d(w_i, w_g) \tag{4-12}$$

4.3.3.2 Objective function analysis

Based on Section 4.2.2, the objective function of this chapter combines the accumulative costs of both involved risks $f_r(w_i)$ and path lengths $f_l(w_i)$ along a path. Specifically, the risk cost $f_r(w_i)$ sums up the actual risk cost $g_r(w_i)$ and the heuristic risk cost $h_r(w_i)$. While the length cost $f_l(w_i)$ combines the actual length cost $g_l(w_i)$ and the heuristic length cost $h_l(w_i)$. Therefore, the objective function of the proposed Risk-A* planner can be specified in Eq. (4-13):

$$\begin{aligned} P^* &= \operatorname{argmin} \sum_i [f_r(w_i) + f_l(w_i)] \\ &= \operatorname{argmin} \sum_i \{[g_r(w_i) + h_r(w_i)] + [g_l(w_i) + h_l(w_i)]\} \end{aligned} \tag{4-13}$$

4.4 Case study

In this section, a simulated case study using a Slocum G1 Glider was performed in a real-world oil spill environment near Baffin Bay to validate the effectiveness of the proposed path planner. Firstly, the BN model was developed by incorporating various risk variables of a spill environment. A probabilistic risk map for vehicle loss was generated, presenting the spatial risk distributions in a selected mission area. Then, the searching A* algorithm was implemented to find a Risk-A* path based on the risk map. Comparative analyses with the other two classic planners were conducted to demonstrate the superiority of the proposed Risk-A* planner.

The employed AUV type in this chapter is Slocum G1 Glider. Its basic specification is summarized in Table 4.1. Although the actual motion of a glider AUV is in three dimensions, this case study only considered a two-dimensional trajectory of the vehicle in the horizontal plane for global path planning, which is particularly relevant in missions detecting an oil spill released by vessels without consideration of significant depth changes. However, this chapter can be expanded to a higher dimension by considering various mission depths, and the application scenario could be monitoring oil spills from reservoirs where the vehicle is required to dive much more deeply.

Table 4.1. The specification of the Slocum G1 Glider (Wang et al., 2021c).

Parameter	Value
Weight in Air	~52 Kg
Hull Diameter	0.213 m
Width including Wings	1.003 m
Vehicle Length	1.5 m
Minimum Turning Radius	~17 m
Displacement	52 L
Depth Range	4-200 m
Speed	0.4 m/s horizontal

Range	1500 km

4.4.1 Mission profile description

The mission area in this case study was selected as an open water area around Scott Inlet (71.10941 N, -71.10576 W), which is on the east coast of Baffin Island where oil seeps are naturally present. The satellite radar imagery has confirmed that large oil slicks over this region exceed 250 km^2, each representing over 50,000 barrels of surface oil (Oakey et al., 2012). Hence, with sufficient oil in the water, this region was chosen as a potential mission area. However, due to limited data for this area, we used information of oil concentrations in the region from a study following a hypothetical spill from an anthropogenic source. The size of the selected mission area was relatively small and set as 500 m × 500 m. The whole search space was discretized into grids and the resolution for each grid was 10 m × 10 m, namely, the minimum distance between two adjacent waypoints was 10 m. Fig. 4.2 illustrated the gridded mission area, where the start position and goal position were defined as (50 m, 20 m) and (450 m, 480 m) respectively in coordinates.

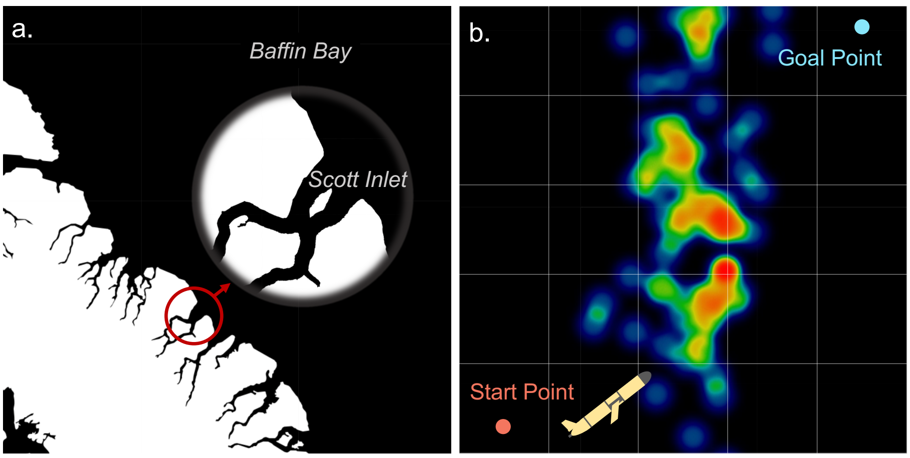

Fig. 4.2. Illustration of the selected mission area, where (a) shows the mission location near

Scott Inlet, Baffin Bay, and (b) shows an example of a gridded spill area with the start and goal positions.

4.4.2 Risk variable identification

As a precondition for the development of the BN model, in this case study, we mainly identified two types of risk variables that can lead to vehicle loss: environmental variables and mission complexity factors. In particular, we considered environmental variables including the current speed, wave height, ship density, and oil concentration. While mission complexity factors contain the mission depth and obstacle numbers. The description of identified BN variables is summarized in Table 4.2.

Table 4.2. Description and value ranges of the BN variables.

BN Variables	Description	Value Range		
		Low	Medium	High
E1	Current speed (m/s)	<0.05	0.05-0.15	>0.15
E2	Wave height (m)	<0.25	0.25-0.5	>0.5
E3	Oil concentration (ppb)	<50	50-100	>100
E4	Ship density (routes/0.08km^2/year)	<20	20-50	>50
M1	Mission depth (m)	<50	50-100	>100
M2	Obstacles	/	/	/

T	AUV loss	/	/	/

4.4.2.1 Environmental variables

A current speed can influence the motion of an AUV by deviating it from its planned path (Griffiths and Trembanis, 2007; Petillo and Schmidt, 2012). Such impacts could be more prominent for slow-moving AUVs, such as underwater gliders. In this case, the vehicle may not reach its target position, and as a result, it could collide with other vehicles or even get lost. Surface waves could cause the vehicle out of sight, and this may lead to difficulties especially for the recovery phase of an AUV mission. In addition, the wave-induced force can also drag the vehicle from its desired path. Oil in high concentration could cause contamination of optical sensors, and substantially degrade the sensor's ability to detect obstacles (Chen et al., 1987). In addition, if the oil coats the inside of a CTD sensor, it can possibly affect the sensor's calibration and thus cause false measurement. Ship density is another key factor and the probability of collision between ships and AUVs is proportional to the shipping density in a mission area (Merckelbach, 2013a).

4.4.2.2 Mission complexity factors

The number of underwater obstacles and the mission depth can influence the mission complexity. A large number of obstacles could cause higher requirements for the AUV's ability of obstacle avoidance, and they could also raise the possibility of collisions. The mission depth can affect both the vehicle's integrity, buoyancy control, and energy consumption (Chen et al., 2021b).

4.4.2.3 Data sources of risk variables

In this case study, environmental data in the mission area were collected based on the website of National Oceanic and Atmospheric Administration (https://www.ncei.noaa.gov/) and Marine Traffic (https://www.marinetraffic.com/). The oil concentration data used in the case study was randomly generated and referred from former research (Reich et al., 2016). Based on the above information, the collected environmental information can be visualized in Fig. 4.3, which presents the spatial distributions of the value of various risk variables. It should be noted that all the risk variables, except underwater obstacles, were assigned three discrete levels: low, medium, and high states, representing their severity. The expert elicitation method is a useful method to deal with limited historical data. In this chapter, we invited six domain experts to constitute the expert panel. The panel has sufficient experience in both the fields of AUV operations and risk assessment. The panel provided analyses and reviews including the identification of the risk variables, division of value ranges of the risk variables, assignment of prior probabilities and construction of the conditional probability tables (CPTs) for the proposed BN model. The detailed process of the expert elicitation method was adapted from previous studies (Brito and Griffiths, 2016; Huang et al., 2020; Wang et al., 2022a). The value ranges were divided as shown in Table 2 based on the judgements of domain experts, considering the specification of the Slocum G1 Glider. The mission depth in this study was assumed as 50 m, which is at the low level according to its severity division. According to Fig. 3 (d), the severity of ship density in the selected mission area was also indicated as a low level. Fig. 3 (e) presented 200 obstacles in the mapped area which were plotted in black. The obstacles inside the mission area were randomly generated to test the capability of obstacle avoidance of the proposed planner. For simplicity, only stationary obstacles (e.g., islands, buoys, rocks, and so on) were considered. Hence, the spatial distributions of severity states for the remaining three risk variables, namely, the current speed, wave height, and oil concentration, can be simplified according to the discretized value ranges in Table 4.2, which can be plotted in Fig. 4.4.

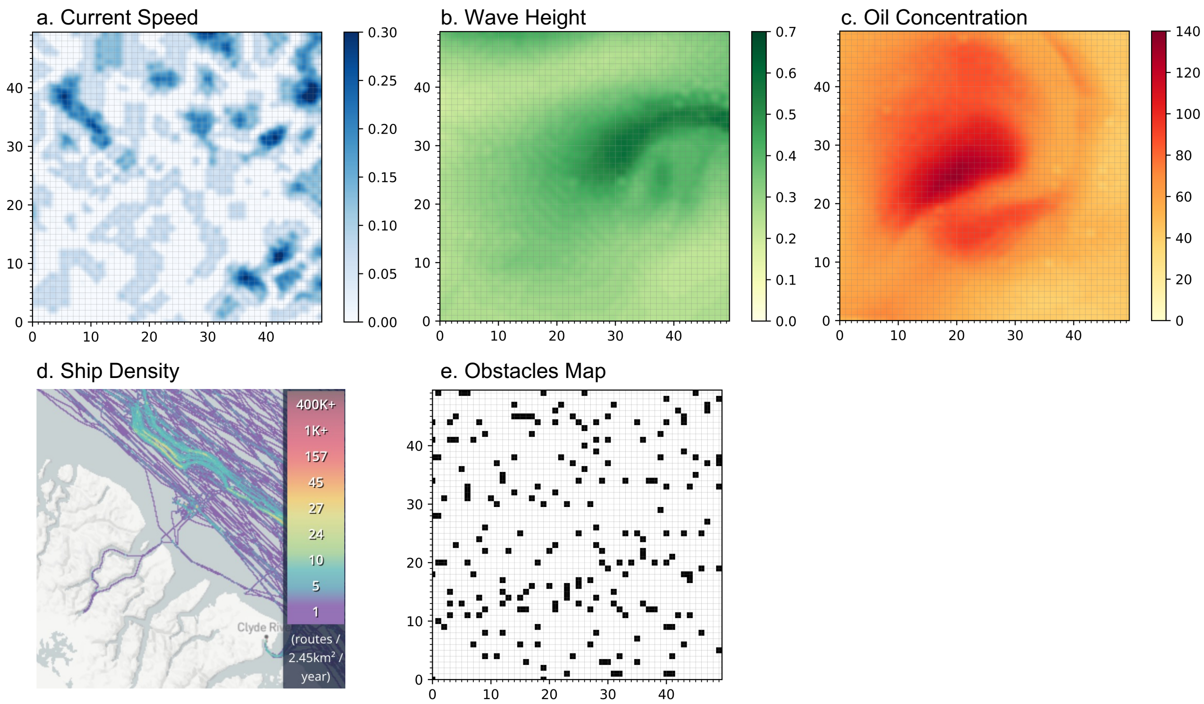

Fig. 4.3. Spatial data distributions of different risk variables in the selected mission area.

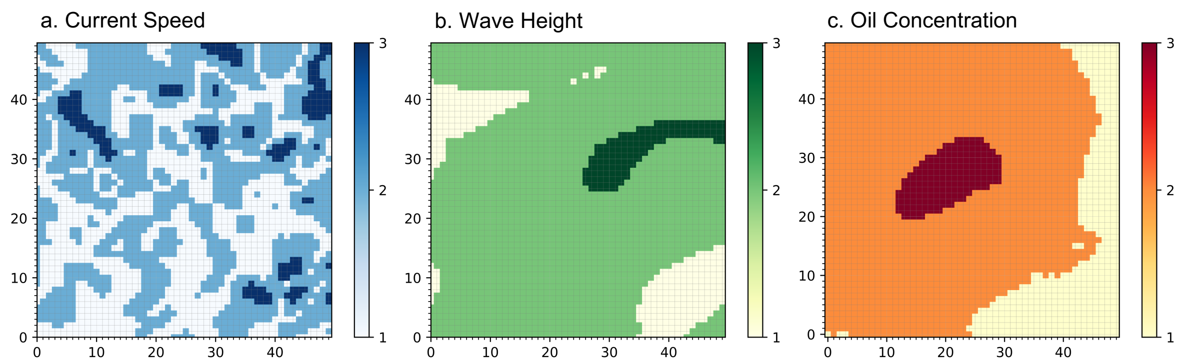

Fig. 4.4. Spatial distributions of severity states for the (a) current speed, (b) wave height, and (c) oil concentration.

4.4.3 BN development and risk map generation

Based on the above identification of potential risk variables and their causal relationships with vehicle loss, a BN model can be developed as shown in Fig. 4.5. The prior probability of each state of the risk variable and conditional probabilities among risk variables were determined according to domain experts' judgements.

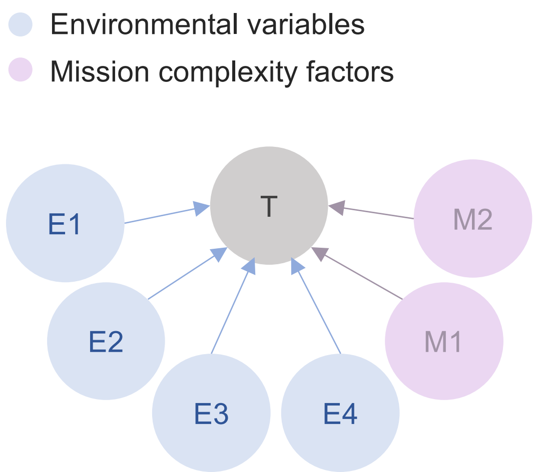

Fig. 4.5. Developed BN model.

On the basis of obtained environmental information and BN reasoning results, a risk map in terms of the probability of vehicle loss in the mission area can be generated and illustrated in Fig. 4.6. This risk map intuitively presents high-risky regions where the AUV should avoid, where the numbers on the scale represent risk indices. For instance, locations with obstacles have the highest risk index, which can always prevent the vehicle from selecting an obstacle as a waypoint. Other locations, for example, with large wave heights or with high oil concentration, also show relatively high risky in the risk map.

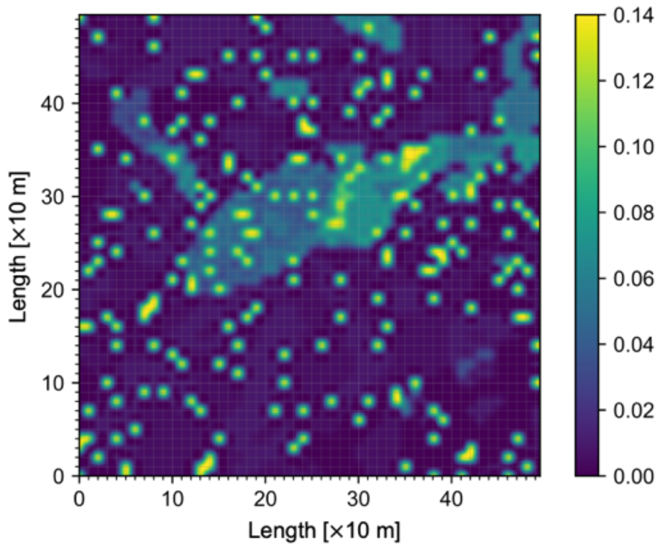

Fig. 4.6. Generated risk map in the mission area, where the numbers on the scale represent risk indices.

4.4.4 Simulation results and discussion

Based on the obtained risk map, an A* algorithm was employed for path planning. Effectiveness of the proposed Risk-A* planner was demonstrated by comparing it with the other two classic path planners: the minimal-length planner and the minimal-risk planner. Furthermore, influences of different risk thresholds on the Risk-A* planner were investigated. In realistic AUV operations, an acceptable risk threshold should be defined by stakeholders before a mission. In this study, the risk threshold was defined by the expert panel to forbid the vehicle from selecting a waypoint with an unacceptable risk index. According to the risk map in Fig. 4.6, the maximum risk index (i.e., the probability of vehicle loss) in the mission area is calculated as 0.14. A relatively low threshold of 0.05, which is around 36% of the maximum risk index, was used to rigorously test the vehicle′s ability to avoid obstacles and risky regions. It is noted that the predefined risk threshold can be tuned according to the willingness of risk tolerance.

4.4.4.1 Comparative analyses of the three path planners

We conducted simulations using the three path planners (i.e., minimal-length planner, minimal-risk planner, and the proposed Risk-A* planner) in the same risk map. The obtained paths were presented in Fig. 4.7 (left column), while their waypoint risk indices and accumulative risk indices along the path were compared in Fig. 4.7 (right column). The start and goal positions were arbitrarily set and depicted with red and blue dots, respectively. Searched paths of the three planners show obvious differences while both of them were observed to be able to successfully avoid obstacles. In Fig. 4.7 (a), the minimal-length planner finds the shortest path from the start position to the destination without considering the cost of waypoint risks. Hence, its obtained path is approximately straight and directly toward the target. But with this said, a number of waypoints′ risk indices along this path far exceed the predefined risk threshold of 0.05. For instance, the peak value (0.1) of the waypoint risk index occurs at the mission distance of 140 m, where the vehicle is directly passing through a high-risky area as shown in the risk map. On the contrary, Fig. 4.7 (b) shows that the minimal-risk path selects a set of waypoints with the lowest risk index, no matter how much path lengths cost. The resulted path is long and winding, which loiters to avoid any potential risky regions rather than making progress toward the goal. While the proposed Risk-A* planner, as shown in Fig. 4.7 (c), considers the costs of both the path length and waypoint risks. It searches a path with a moderate risk level and relatively shorter mission distance, and meanwhile, it satisfies the constraint of the risk threshold at each waypoint.

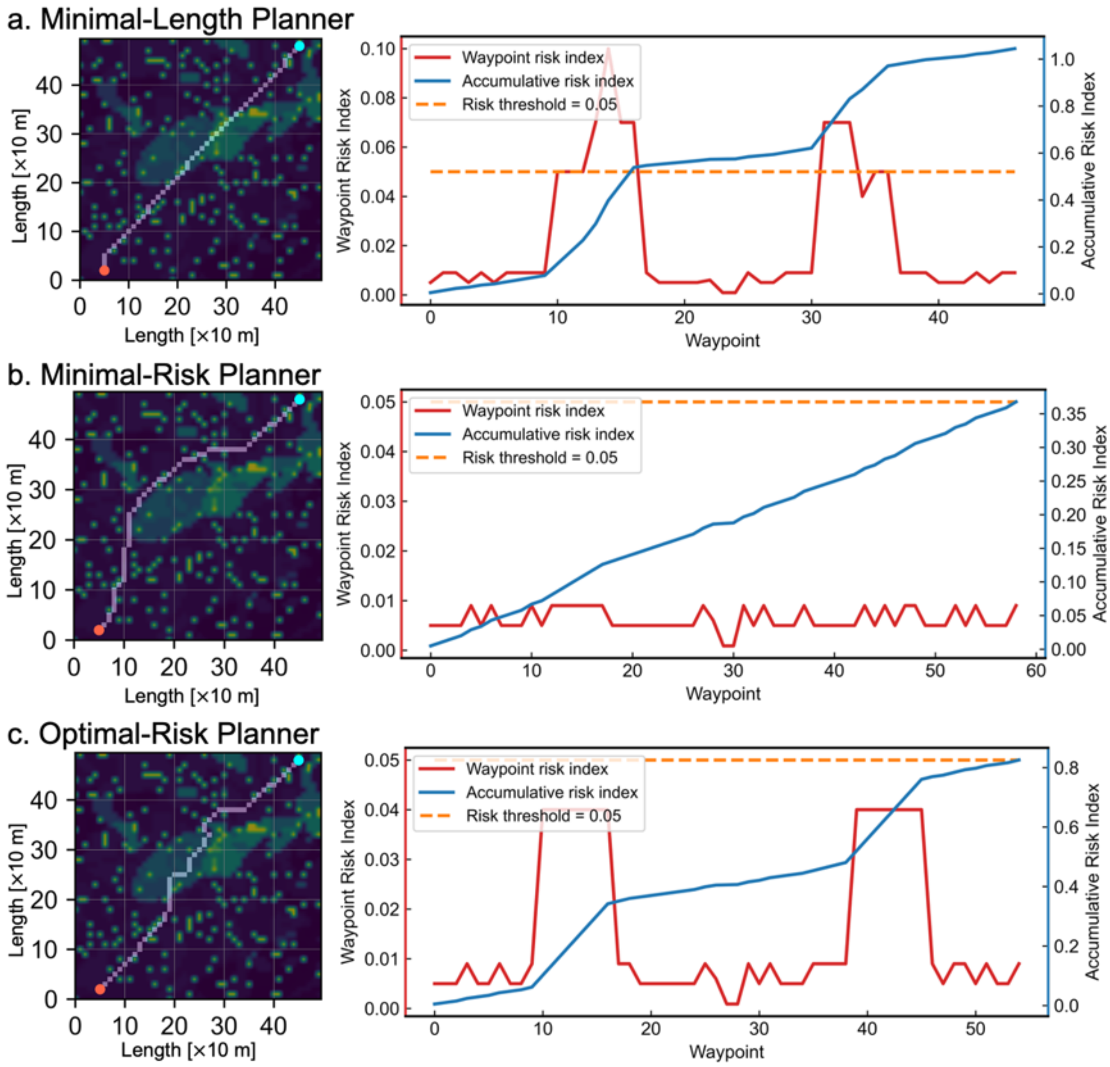

Fig. 4.7. Obtained paths, waypoint risk indices, and accumulative risk indices of the three path planners: (a) minimal-length planner; (b) minimal-risk planner; and (c) Risk-A* planner.

To provide additional comparisons, Fig. 4.8 compares the path length, max risk index (i.e., the maximum of waypoint risk indices), accumulative risk index, and computational time of three planners, respectively. The computational time of the three planners was normalized for comparison. The reference time, which was defined as 100%, was chosen as the computational time of the minimal-risk planner. Although this chapter mainly explored an offline global path planning approach for AUVs prior to a mission, computational time is still a key parameter to be considered. It impacts the efficiency of mission planning, which is important especially in dealing with large-scale planning problems with complex environmental conditions and long mission endurance. It can be seen from Fig. 4.8 (a) and (b) that the minimal-path length achieves the shortest path length of 627 m, however, its max risk index far exceeds the predefined risk threshold of 0.05, which is not acceptable for the safety requirement. On the contrary, the minimal-risk planner has the minimal max risk index among the three planners, which is only 0.009. In return, it has the largest path length, which is 12.6% higher compared with the minimal-length planner. As for the Risk-A* planner, its max risk index is 20% lower than the risk threshold (0.05), which means risk states along the whole path remain tolerable. In addition, its path length is 10.2% longer than the minimal-length planner. As it aims to mitigate risks associated with the path to ensure safe deployment, although it could sacrifice certain mission lengths.

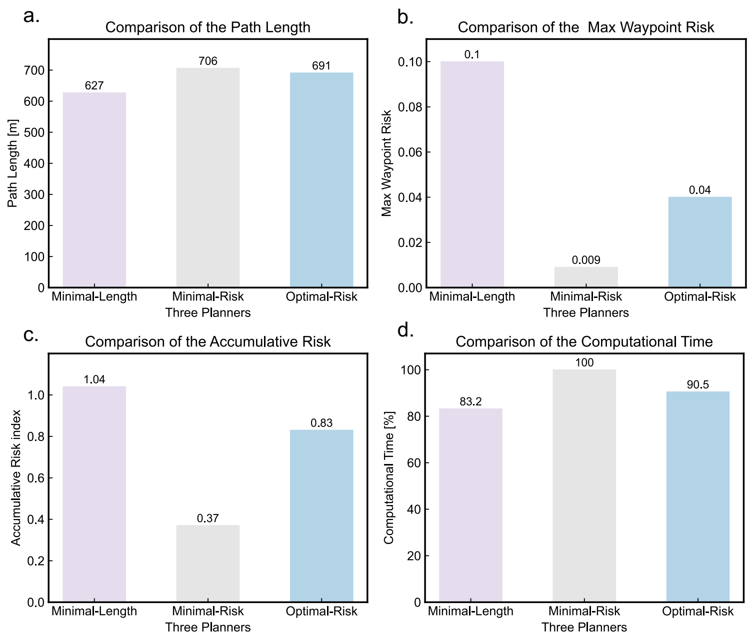

Fig. 4.8. Comparisons of the three planners including (a) path length, (b) max waypoint risk index, (c) accumulative risk index, and (d) normalized computational time.

In comparing the accumulated risk index in Fig. 4.8 (c), it is noteworthy that the minimal-length planner attains the largest value of 1.04, which is nearly triple that of the minimal-risk planner (0.37). However, the minimal-risk planner achieves the minimum accumulative risks at the expense of routing length, and in turn, the searching time could substantially increase along with an increasing number of waypoints. In this case, the computational time of the minimal-risk planner in finding a solution could also grow correspondingly, which reaches the maximum amongst these three planners, as shown in Fig. 4.8 (d). In contrast, the proposed Risk-A* planner performs moderately well, namely, its accumulative risk index is decreased by 20.2% compared with the minimal-length planner, whilst its computational time is 9.5% shorter than the minimal-risk planner.

Based on the above analyses, it can be concluded that: (1) The minimal-length planner outperforms in both the routing length and computational time. However, it overlooks the risk associated with the path, and as a result, the waypoint risk index exceeds a predefined risk threshold, which is unacceptable in terms of the vehicle′s safety requirement in real implementation. (2) The minimal-risk path is clearly over-conservative. Although it has the lowest waypoint risk index, it comes at a cost of the path distance, which further leads to the increasing computational time. Such a path could be infeasible in practice as it might fail to meet the criteria of available energy consumption for the vehicle. (3) The Risk-A* planner is a safer bet that exhibits good performance in avoiding risky regions along a path. It also achieves a balance between the involved risks, the path length, and computational efficiency. At the same time, it satisfies the precondition of operating below a risk tolerance threshold to ensure safe navigation.

4.4.4.2 Influences of different risk thresholds on the Risk-A* planner

Determination of a risk threshold is also an important issue for planning an AUV route. Impacts of various risk thresholds on the proposed Risk-A* planner were investigated. Fig. 4.9 plots the resulting paths under four different risk thresholds in the same environment. When the tolerable risk threshold gradually decreases, which refers to a higher safety requirement for the vehicle that demands more rigorous risk tolerance, the resulting path gets longer and the AUV moves further away from potential high-risky regions to attain the acceptable risk level, which consequently wastes additional route lengths.

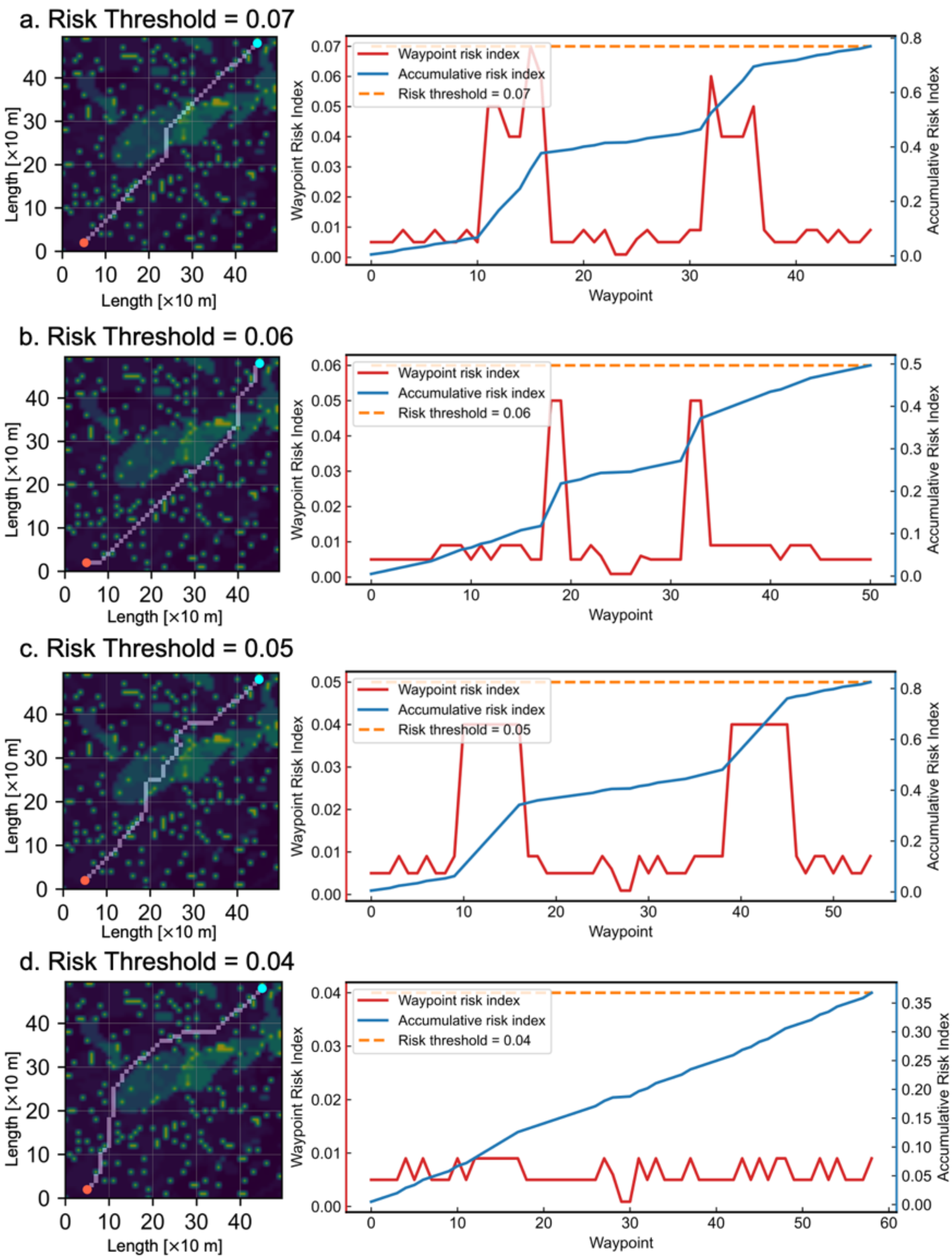

Fig. 4.9. Obtained paths, waypoint risk indices, and accumulative risk indices under different risk thresholds.

Particularly, Fig. 4.10 compares the path length, max risk index, accumulative risk index, and the normalized computational time under four risk thresholds. As shown in Fig. 4.10 (a), with decreasing risk threshold from 0.07 to 0.04, the path length increases from 650 m to 706 m with a changing rate of 8.6%. This implies that it is possible to achieve a higher safety level with a reduced risk threshold while only slightly degrading its length optimality. Similarly, the computational time in Fig. 4.10 (d) shows the same trend, which consumes 7.6% longer time when the risk threshold reduces from 0.07 to 0.04. In Fig. 4.10 (b), the max waypoint risk index drops gradually with the decreasing risk thresholds. It is noteworthy in Fig. 4.10 (c) that the accumulative risk index under the risk threshold of 0.05 is higher than that under the risk threshold of 0.06. This manifests a particular situation that should be considered in realistic mission planning, as a path with a lower risk tolerance could require more path lengths to avoid risky regions, and in turn, the accumulative risks could substantially increase along with the increasing traversed waypoints.

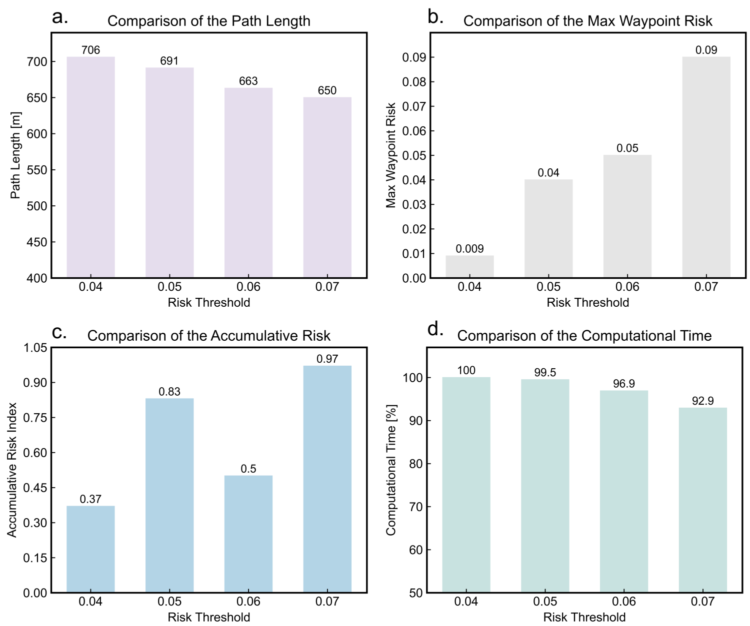

Fig. 4.10. Comparisons under different risk thresholds including (a) path length, (b) max waypoint risk index, (c) accumulative risk index, and (d) normalized computational time.

Therefore, the safest path does not indicate an optimal solution in practice, because it may sacrifice the mission length and deteriorate the computational efficiency at the same time. This prompts an insight to adjust the risk threshold for achieving a trade-off between an acceptable risk tolerance and the mission efficiency.

4.4.5 Limitations and future work

Limitations of this chapter were discussed below. This work only considered static environmental conditions and obstacles for global path planning of AUVs. It is desirable to conduct such offline mission planning beforehand given known environmental information. However, static global path planning requires accurate environmental predictions prior to a mission, which is difficult to achieve in reality, and it is possible that only limited environmental information can be obtained for a target mission area. In addition, ambient environmental conditions, such as ocean currents and oil spills themselves, can change dynamically, which subsequently causes the risk of vehicle loss to varying accordingly. The possibility of colliding with moving obstacles also exists. In such cases, global path planning designed for static environments cannot handle the unpredictable situations that may emerge, and re-planned solutions will be required to account for dynamic environmental observations. Hence, future research should explore a hybrid risk-based architecture for AUVs′ autonomous mission planning to combine static global planning and dynamic local re-planning, which is essential for the real-life decision making of AUV missions.

Furthermore, some recent research provided advanced methods for model validation for marine robotic systems (Albarakati et al., 2021; Liu et al., 2022). These studies considered multiple simulation scenarios with various vehicle maneuvers in practical environments. They provided insights to bridge the gap between pure computer-based simulations and real experimental validation. For potential experimental simulations, other key parameters besides the path length could be considered, such as the vehicle velocity, turning maneuvers, travel time, and energy consumption, which can be affected by ambient environmental conditions as well. Analyses from multiple perspectives of the simulations could enhance the feasibility of the planner, especially for multi-objective problems. An accurate estimation of AUVs navigational data is also crucial for safe path planning. The use of multiple sensors′ data could be beneficial for high-fidelity validation in practical environments in the future.

4.5 Conclusion

In this chapter, a systematic risk-based path planning approach for AUVs operating in an oil spill environment was proposed. The risk of vehicle loss was incorporated into a classic global planning problem of AUVs. A BN-based risk model was developed for probabilistic prediction of risk states given various environmental observations. The established risk model was then employed to generate a spatially-distributed risk map covering a potential mission area. Subsequently, an A* algorithm was applied to plan a Risk-A* path through the risk map by combining costs of mission lengths and risk indices. The proposed path planner aims to avoid high-risk regions to ensure safer operations, whilst achieving a relatively shorter path length. A case study using a Slocum G1 Glider in an oil spill environment around Baffin Bay was conducted to demonstrate the effectiveness of the proposed planner. Key findings from the case study results were highlighted below:

(1) The proposed BN-based risk model can forecast risk states of vehicle loss given

comprehensive spill environments. Its probabilistic reasoning enhances the accuracy for further path searching and risk-based decision making. The generated risk map based on BN reasoning intuitively presents the spatial distributions of high-risk regions in a gridded mission area, which provides insights of risk mitigation through obstacle avoidance and waypoint selections.

(2) Comparisons between the Risk-A* planner with two classic path planners (i.e., minimal-length planner and minimal-risk planner) have indicated that a trade-off exists between the routing length, associated risks, and computational efficiency along a path. The proposed Risk-A* planner outperforms in risk mitigation by avoiding potential risky regions and obstacles, whilst it is highly competitive in terms of path distance and computational time.

(3) Different risk thresholds can affect the performance of Risk-A* path planning. A lower tolerable risk threshold, which refers to a higher safety requirement, can increase the mission length and consume more computational time. In this case, considering a particular scenario during an oil detection mission, a lower risk threshold can drag the vehicle away from the most highly-concentrated oil regions, which causes the vehicle to miss nearby plumes with rich information and thereby degrading its detection efficiency. Hence, the risk threshold should be modulated to achieve a trade-off between safety performance and mission efficiency.

(4) The developed risk-based planner can be practical in realistic AUV implementation. Although this chapter only investigated the off-line global path planning for AUVs with static environmental conditions, it is a potential precomputing policy to save the computational memory for a vehicle, and it is a worthwhile investigation for preventing AUV loss at the path planning stage prior to a mission. In addition, this chapter considered a two-dimensional

trajectory of AUVs, which is particularly useful for missions in detecting oil spills released by vessels without significant depth changes. The approach could also be applied for AUV path planning in tracking oil spills from reservoirs. For this scenario, the vehicle would have to dive to higher depths. To capture this scenario, both the risk model and the path searching algorithm should be updated to take a 3D problem into consideration. A modification would be required to our methodology to include the 3D body dynamics property of the AUV.

Future work based on this chapter should incorporate dynamic risks into the path planning framework for AUVs. To this end, a hybrid risk-based path planner combining both static global planning and dynamic local re-planning for AUVs should be investigated.

Chapter 5. Hybrid Risk-based Path Planning for Autonomous Underwater Vehicles in Dynamic Environments

5.1 Introduction

As introduced in Chapter 4, path planning is an important issue for AUVs to plan a feasible and safe route in uncertain environments. To make AUV systems more risk-aware during path planning, it is crucial to take the vehicle's risk state into account. Risk-aware path planning is a critical technique for AUVs. It refers to planning an optimal path for the AUV from its initial position to the target while considering the navigational risks along the path simultaneously (Chen et al., 2022).

Former studies have investigated risk-aware path planning methods for AUVs to achieve safer navigation. (Pereira et al., 2011) proposed a minimum risk planner for a glider AUV, taking the surfacing risks into account. As an extension of their work, a risk-aware path planner was designed for AUVs to mitigate the collision risk with ships and land (Pereira et al., 2013). (Hegde et al., 2016b) identified the collision risk indicators for AROVs, which assisted in finding risky waypoints during path planning. (Lefebvre et al., 2016) presented a hierarchical A* approach for global path planning, which addressed the collision risk of AUVs. (Yan et al., 2022) applied a whale optimization algorithm to address the AUV 3D planning problem. This algorithm is inspired by imitating the bubble-net hunting behavior of humpback whales to obtain an optimal global solution with a fast convergence speed. The proposed planner is able to effectively avoid risky mission areas and achieve the shortest distance while consuming minimal energy. (Zhang et al., 2022) tackled AUV path tracking with real-time obstacle avoidance using reinforcement learning. The risk thresholds were incorporated into reward functions to generate a collision-free path. In our former work (Chen et al., 2022), we proposed a path planning framework for AUVs using a Risk-A* algorithm, which is an adapted A* approach that incorporates the risk of vehicle loss under an oil spill environment.

In general, path planning methodologies can be roughly divided into global path planning, local path planning, and hybrid path planning. Global path planning aims to find a globally optimal path with known environmental information. It is usually performed in a large-scale mission area. A variety of global path planning algorithms for AUVs have been investigated, including the Dijkstra algorithm (Dijkstra, 1959), A* algorithm (Hart et al., 1968), rapidly exploring random trees (RRT) (Karaman et al., 2011), to name a few. It is desirable to conduct global path planning prior to a mission. However, it requires complete and accurate environmental information, which is difficult to collect in reality. In addition, ambient surrounding conditions can change fast and moving obstacles also exist. In this case, global path planning cannot handle unpredictable situations and react rapidly.

In the contrast, local path planning searches for a locally optimal solution under unknown or changing environments (Cheng et al., 2021). It relies on real-time environmental observation from sensors for fast reactions and path adjustment. A number of local path planning algorithms have been proposed, such as the dynamic window approach (DWA) (Fox et al., 1997), the artificial potential field (APF) (Vadakkepat et al., 2000), and the vector field histogram (VFH) (Borenstein and Koren, 1991). Despite these local path planning algorithms possessing high computational efficiency and real-time performance, only applying local path planning may lead to the local optimum problem and cause the vehicle to fail to reach its target.

Therefore, it is essential to combine a global planner and a local planner into a hybrid architecture. A hybrid path planner can balance the computational complexity and real-time reaction to unforeseen changes. (Nakhaeinia et al., 2015) proposed a hybrid path planner for mobile robot navigation in an unknown dynamic environment, where the global planner generated a collision-free path with the shortest distance, while the local planner produced safe and time-minimal paths. (Chen et al., 2019) presented a hybrid path planning algorithm for unmanned surface vessels (USV), which combines the A* algorithm to generate a global path with the DWA method to avoid local dynamic obstacles.

Despite much progress having been made in AUV path planning, limited research has been done to design a tailored hybrid path planner for AUVs, especially taking a risk-aware strategy into consideration. Therefore, the overall objective of this chapter is to propose a hybrid risk-aware decision making strategy for AUVs. The proposed strategy is expected to achieve risk identification from a control perspective, and bridge real-time risk modelling with risk-aware path planning to realize more intelligent and safer deployment of AUVs. Specifically, the risk state of the vehicle during navigation is rigorously estimated based on an online risk model. The predicted risk index is integrated into a hybrid path planning module to achieve real time risk-aware decision making.

The structure of this chapter is organized as follows. Section 5.2 elaborates the details of the proposed hybrid risk-aware decision making methodology. Section 5.3 designs a case study using the ecoSUBm5 AUV in the Baffin Bay area and Section 5.4 presents the simulation results.

Section 5.5 concludes this study.

5.2 Methodology: development of a hybrid risk-based decision making strategy

The overall framework of the proposed method consists of five modules, as shown in Fig. 5.1. Environmental observation aims to provide the mission map and environmental data, which serve as the input for the online risk analysis model. The online risk model is developed based on the systems theoretical process analysis (STPA) model for risk identification and the Bayesian network (BN) for risk prediction. The global path planner can generate an optimal global path based on the Risk-A* algorithm, which is realized in Chapter 4. A local path generator using the dynamic window algorithm (DWA) is designed to assist in avoiding dynamic obstacles. The detail of each step is elaborated in the following subsections.

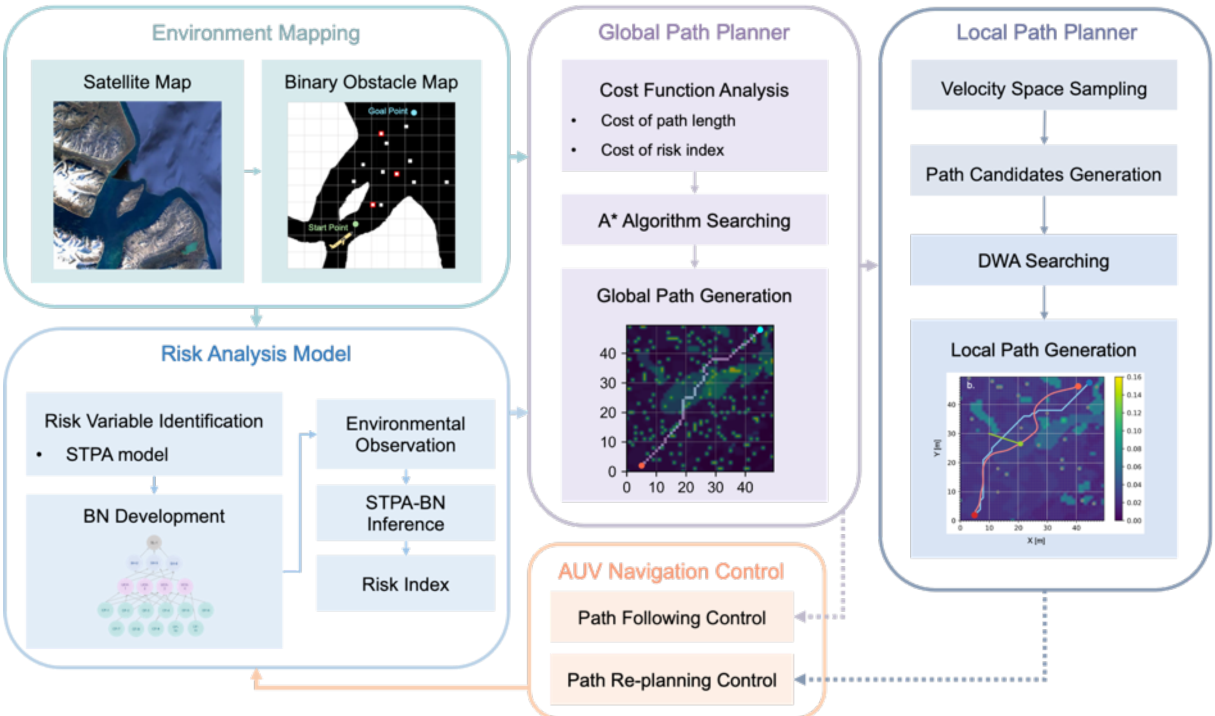

Fig. 5.1. The overall flowchart of the proposed methodology.

5.2.1 Environmental observation and situation awareness

Situation awareness based on the onboard sensors is important for observing the ambient environment and path planning for the vehicle. The global environmental map is obtained from a gridded satellite map of the mission area.

5.2.2 Development of the STPA-BN risk analysis model

An autonomous system features advanced sensory perception, situation awareness, path planning and replanning capabilities, and can be classified as a deliberative control system utilizing the feedback loops of sense, model, plan, and action to make decisions (Utne et al., 2020). Given that autonomous systems are highly dependent on complex software, the software-intensive feature makes it difficult to apply conventional risk analysis methods, many of which decompose the system into components while not considering the hazard of system behavior. Previous studies provided a number of risk models for AUV operations (Thieme et al., 2015b; Brito and Griffiths, 2016). However, only a few of the aforementioned studies have integrated and implemented the risk analysis model as part of the control system. In addition, several former studies considered a risk in the collision avoidance module of the AUV (Hegde et al., 2016b; Lefebvre et al., 2016). However, the risk was addressed as a general parameter, and a rigorous risk model is lacking. By observing the limitations of the current literature, it is essential to integrate the risk analysis model into the control system to achieve risk-aware decision making for AUV platforms.

(Rasmussen, 1997) stated that risk management should be considered as a control mechanism to ensure that system processes are within a safe operational envelope. Based on this principle, (Leveson, 2011) has proposed the STPA method to identify the hazards for complex control systems, in which safety is considered as a control problem of a system instead of a component failure problem, and accidents are caused by inadequate control or inadequate enforcement of safety constraints (Bensaci et al., 2023).

Due to the superiority of the STPA in risk identification from the control perspective, this method has been applied as a hazard analysis technique for multiple autonomous systems, including autonomous ships (Wróbel et al., 2018b, a; Chaal et al., 2022; Yang and Utne, 2022), maritime autonomous surface ships (MASS) (Thieme et al., 2018; Utne et al., 2020), autonomous vessels (Valdez Banda et al., 2019), and multi-mobile robotic systems (Bensaci et al., 2023). These former studies have demonstrated the effectiveness of the STPA framework in capturing the hazards associated with system component interaction and unsafe behaviors of an autonomous system. They also highlighted the potential of STPA in mitigating the risk and guiding the design for autonomous systems. However, the original STPA method is a purely qualitative technique for hazard analysis, and it has not yet taken quantitative risk estimation into consideration (Bjerga et al., 2016).

In order to address this limitation of the STPA method, several studies have combined STPA with the BN model, in which the STPA was used for hazard identification for an autonomous system, while the BN model was applied for estimating the system risk state. As clarified in the former chapters, BN is a probabilistic tool for risk analysis under uncertainty. It is a graphical model composed of a directed acyclic graph, where each node denotes a random variable and arrows represent causal relationships among nodes (Afenyo et al., 2017). The dependency degrees among variables can be captured using conditional probabilities. According to (Thieme et al., 2018), BN is a powerful technique for risk modelling and estimation regarding an autonomous system, such as autonomous ships, and should be incorporated as a part of the risk model of the system. Specifically, (Utne et al., 2020) outlined a general framework by combining the STPA and BN for online risk modelling for autonomous ships, based on which (Johansen and Utne, 2022; Johansen et al., 2023) extended and integrated the STPA within a BN model to enable real-time supervisory risk control for autonomous ships in changing conditions. The proposed hybrid risk model provided the basis for selecting appropriate control and machinery modes. More latterly, (Wang et al.) extended the application for reliability assessment of autonomous vehicles. The authors modelled the safety control structure via the STPA framework and constructed the BN model to assess the system reliability. (Chaal et al., 2022) proposed a hybrid framework to ensure ship safety, in which the STPA was used for hazard analysis and identification of risk control operations, while the BN model was employed for estimating the system risks. The authors highlighted the possibility of integrating the STPA and BN to cover most of the steps of risk assessment for ships. These studies proved that the combination of STPA and BN can mutually compensate by permitting quantitative risk estimation and prioritizing the risk mitigation control actions.

Therefore, considering the advantages of combining STPA and BN for risk analysis of complex control systems, the STPA-BN framework is selected for risk identification and risk estimation for an AUV platform in this chapter. The purpose of developing the STPA-BN risk model is to assist in path selection and decision making during AUV navigation. The developed risk model aims to predict the real-time risk state of the vehicle. Fig. 5.2 shows the flowchart of the proposed STPA-BN model for risk analysis, which applies STPA in conjunction with the BN model. Firstly, environmental mapping and situation awareness based on onboard sensors are applied for assessing ambient conditions. Then, the STPA method is applied for hazard analysis for AUVs. The outcomes of the STPA are then utilized as the basis for developing the BN model. According to (Leveson and Thomas, 2018), the STPA results mainly include the losses, system-level hazards, control structure, unsafe control actions (UCAs), causal scenarios, and safety constraints or requirement. Among the outcomes, the control structure serves only for the STPA analysis, while other outcomes are subsequently used for BN analysis. The predicted risk index from the BN enables the path planning module in Section 5.2.3 to make risk-aware decisions for the vehicle during navigation.

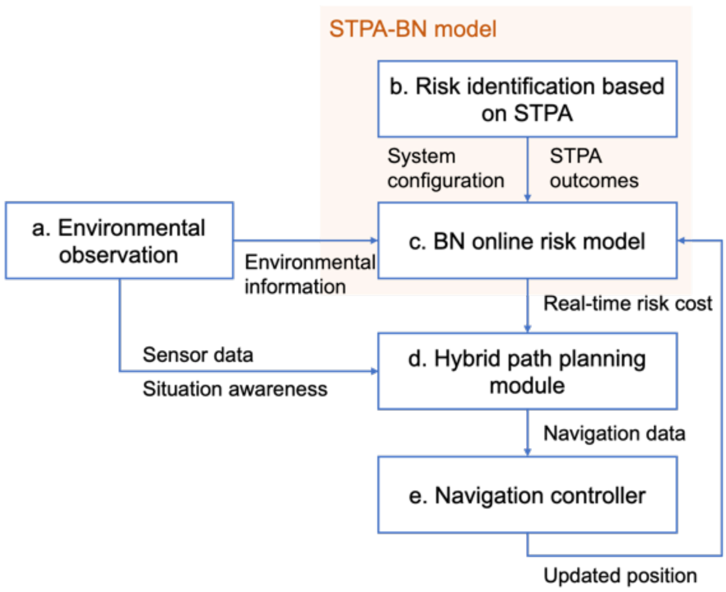

Fig. 5.2. Overall process of integrating risk analysis results into decision making module.

5.2.2.1 Risk identification based on the STPA model

The first step of the proposed STPA-BN risk analysis model is risk identification through STPA. The STPA model mainly consists of four steps. The detailed implementation process of STPA is presented by (Leveson, 2011; Leveson and Thomas, 2018).

a. Define the system boundary and analysis purpose

The system boundary and the analysis purpose should be firstly defined. The definition of the system boundary impacts the scope of the overall analysis, which should specify the system components, sub-systems, system context, ambient environment, and how they could interact with each other. In general, the analysis purpose includes the identification of the system loss and system-level hazards.

b. Develop the control structure of the system

A control structure of a system refers to an ensemble of feedback control loops that shows control interactions among system components. In this step, the control structure is developed to identify different controllers, their control actions to enforce the safety constraints, and control variables that describe the state of the control process.

c. Identify the unsafe control actions (UCAs)

UCAs can be defined as unsafe control actions which violate safety constraints and cause system-level hazards (Johansen and Utne, 2022). In this stage, the control structure is examined to determine UCAs that can lead to losses and hazards identified in the first step. In general, there are four kinds of UCAs: (i) a control action that, if provided, causes a hazard; (ii) a control action that, if not provided, causes a hazard; (iii) a control action that, if provided too late or too early, causes a hazard; (iv) a control action that, if applied for a too long or too short time, causes a hazard.

d. Identify causal factors and safety requirements

The objective of this step is to identify the underlying causes of UCAs defined in the former step. The causal factors are further applied to determine the safety constraints. Possible causal factors may include controller failures, inadequate control algorithms, wrong control inputs, inadequate process models, and so on.

In summary, the outcomes of STPA contain the system-level hazards, the UCAs that can lead to the hazards, and the causal factors that could lead to the UCAs. Based on this identification, the safety constraints that can prevent unsafe scenarios and secure safer operations are further provided. The outcomes obtained from STPA provide a basis for developing the BN-based risk model in the next step.

5.2.2.2 Online risk prediction based on the BN model

Based on the outcomes of STPA, the BN model for risk analysis can be developed. The process of mapping the BN structure from STPA outcomes is shown in Fig. 5.3. In the top-down BN structure, the top node represents the system loss which is identified in the first step of the STPA. Subsequently, the system-level hazard nodes that lead to the top node are shown as the intermediate nodes in the BN, which are further linked to their parent nodes of UCAs. Finally, the causal factors that lead to each UCA are identified as input nodes in the bottom level of the STPA.

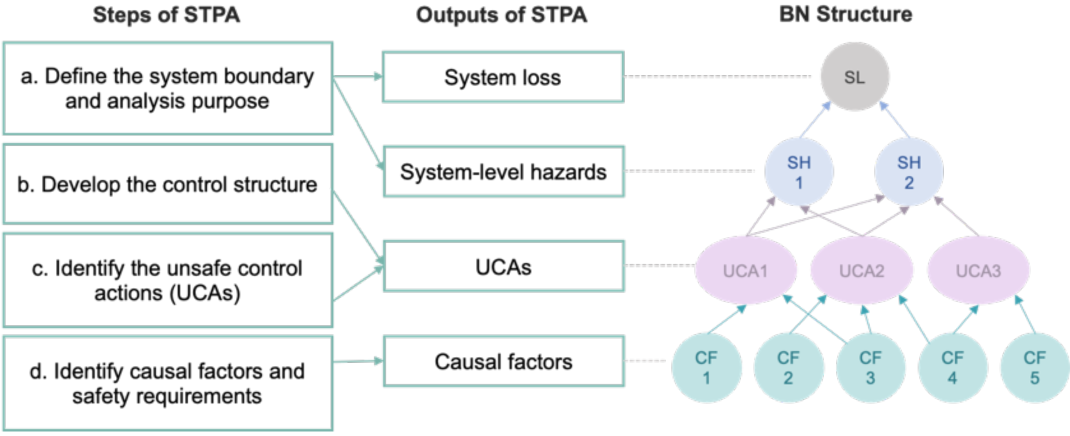

Fig. 5.3. Mapping the BN structure from the STPA outcomes.

5.2.3 Development of hybrid path planners

The core idea of the proposed hybrid path planner is as follows. Firstly, the Risk-A* which was proposed in Chapter 4 is firstly applied to generate an optimal global path as a planned route for the vehicle to follow. Once dynamic obstacles occur and the collision risk exceeds a predefined risk threshold, the local path planner based on the DWA algorithm could be triggered to generate a local collision-free trajectory. After the collision risk is mitigated to an acceptable level, the vehicle continues to track the remaining global path until reaching the target.

5.2.3.1 Global path planner based on the Risk-A* algorithm

The details of the process of applying the Risk-A* algorithm to generate a global path were elaborated in Chapter 4. Based on it, the output of the global path planner is a Risk-A* global path for the vehicle to follow.

5.2.3.2 Local path planner based on the DWA algorithm

The local path planner is a part of the hybrid path planner for AUVs in this study. It is applied to generate a locally optimal path for the vehicle to avoid dynamic obstacles. The adapted DWA algorithm is used in this section to generate the local path. DWA is a velocity-space-based approach used in robotics for motion planning and control under an uncertain environment. It was originally proposed in the application of obstacle avoidance for indoor robots (Fox et al., 1997). The DWA is intended to search for a feasible path in a velocity space consisting of the surge velocity and the rotational rate (Jian et al., 2020). The DWA algorithm mainly includes three steps. It firstly samples a desired velocity search space composed of multiple velocity pairs (u, r), where u denotes the forward velocity and r is the rotational rate. Each velocity pair is then used to generate a trajectory for a certain time interval. The trajectory is generated by simulating the vehicle's motion over time, considering its kinematics and other constraints. Finally, the generated trajectories are evaluated by the cost function, and the velocity pair corresponding to the optimal trajectory is selected as the reference command for the vehicle's controller.

DWA is widely used in different agents to realize autonomous obstacle avoidance. (Shen et al., 2020) proposed a real-time obstacle avoidance method for AUVs based on the DWA. Since the original DWA with constant weights is limited to dealing with complex environments, their study incorporates reinforcement learning to learn the appropriate weights under different environments and optimizes the DWA. (Kobayashi and Motoi, 2022) reported a novel local pp method by combining the DWA with virtual manipulators for the mobile robot. (Dobrevski and

Skočaj, 2020) proposes an adaptive DWA approach for local navigation of the mobile robot. It uses the deep convolutional neural network to dynamically update the weight parameters of the DWA considering the sensor readings. (Liu et al., 2021) developed a global dynamic path planning fusion algorithm combining the Jump-A* algorithm and the DWA to improve the global optimality of a robot. (Jian et al., 2020) demonstrates a hybrid pp strategy for AUVs by combining a modified DWA and the RRT* algorithm. The proposed planner can automatically evaluate the collision risk and switch from RRT* to DWA when dynamic obstacles are approaching.

5.2.3.2.1 Define the velocity search space

Defining a velocity search space is the precondition of applying the DWA. The velocity search space consists of two parts. A set of possible velocities V_s is firstly defined in Eq. (5-1), indicating the velocity range that the AUV can reach considering the kinematic constraints. Since the AUV is a symmetrical platform, its maximum and minimum angular velocities are assumed to have the same amplitude in opposite directions.

$$V_s = \{(u, r) |\ u \in [u_{min}, u_{max}] \wedge r \in [-r_{max}, r_{max}]\} \tag{5-1}$$

where u_{min} and u_{max} are the minimum and maximum forward speeds, while r_{max} is the maximum rotational rate.

The second velocity space called dynamic window V_d is defined in Eq. (5-2), implying the velocity that the AUV can actually achieve in a time interval after the acceleration (Eriksen et al., 2016; Chen et al., 2019).

$$V_d = \{(u,r) \in R \times R | u \in [u_c - \dot{u}_{min}\Delta t, u_c + \dot{u}_{max}\Delta t] \wedge r \in [r_c - \dot{r}_{max}\Delta t, r_c + \dot{r}_{max}\Delta t]\} \tag{5-2}$$

where u_c and r_c are the current surge speed and yaw rate, $\dot{u}_{min}$ is the maximum backward acceleration, $\dot{u}_{max}$ is the maximum forward acceleration, $\dot{r}_{max}$ is the maximum turning acceleration, and Δt denotes the time step.

Therefore, the overall velocity search space V_r can be determined as:

$$V_r = V_s \cap V_d \tag{5-3}$$

5.2.3.2.2 Trajectory prediction

After the velocity search space is generated, each feasible velocity pair can be used to predict a local trajectory in a certain time interval considering the kinematics constraints of AUVs. Assuming that the vehicle moves in the two-dimensional earth coordinate frame with the x-axis pointing to the north direction and the y-axis pointing to the east direction. The posture of the vehicle includes the global position (x, y) and the heading angle θ within the range of $(-\pi, \pi)$. This study considers a simplified kinematic model to update the vehicle state after a time step Δt as follows:

$$\begin{cases} x_{t+1} = x_t + u_t \Delta t \cos\theta_t \\ y_{t+1} = y_t + u_t \Delta t \sin\theta_t \\ \theta_{t+1} = \theta_t + r_t \Delta t \end{cases} \tag{5-4}$$

By defining the kinematics model of the AUV, the local trajectories can be predicted in a time period $T = n \cdot \Delta t$.

5.2.3.2.3 Cost function analysis

The predicted local trajectories are evaluated by the cost function, and the trajectory that minimizes the cost function is selected as the optimal trajectory (Shen et al., 2020). The velocity pair of the optimal trajectory is served as the reference velocities of the vehicle, and thereby the vehicle can create a locally collision-free path to avoid dynamic obstacles.

The overall cost function in this study mainly considers four parts as defined in Eq. (5-5), which is the weighted sum of the four types of costs. The first part $dist_{goal}(u,r)$ calculates the Euclidean distance between the vehicle and the local target to force the vehicle toward the local goal. The second cost $dist_{goal}(u,r)$ is the Euclidean distance between the vehicle and the nearest obstacle. The third part $vel(u,r)$ denotes the velocity cost of the vehicle, which is the difference between the maximum forward speed in a local trajectory and the current forward speed of the vehicle. To enhance the safety navigation performance of the AUV, the risk cost $risk(u,r)$ predicted from the STPA-BN model is incorporated as the fourth part of the cost function. The risk cost is an essential term to ensure safe navigation along the local path.

$$G(u,r) = \alpha \cdot dist_{goal}(u,r) + \beta \cdot \frac{1}{dist_{ob}(u,r)} + \gamma \cdot vel(u,r) + \delta \cdot risk(u,r) \tag{5-5}$$
$$s.t.\ (u,r) \in V_r$$

where α, β, γ, and δ are constant weights of the cost function.

5.2.4 Development of the navigation controller

The pure pursuit controller is selected as the navigational controller in this study. The generated optimal path is composed of a set of discrete waypoints. Pure pursuit is an effective algorithm for a vehicle following a path defined by waypoints (Coulter, 1992; Samuel et al., 2016). The core idea of this method is to find the closest waypoint around the vehicle, and then steer the vehicle towards that waypoint given the estimated desired heading. Given that the pure pursuit algorithm is computationally efficient and easy to implement, it is adopted in this study for path following for AUVs.

5.3 Case study: considering an oil spill scenario in Baffin Bay

In the case study, an ecoSUBm5 AUV operating in an oil spill scenario in Baffin Bay is considered to demonstrate the effectiveness of the proposed method. Our former work (Chen et al., 2022) has clarified the difficulties of AUVs operating in an oil spill environment and discussed the importance of risk-based decision making to assist in safer navigation. In addition, the former study has demonstrated the effectiveness of the proposed Risk-A* algorithm in controlling risks and moderating the path length. It should be noted that this case study assumed the environmental data obtained from onboard sensors can be accurately measured and directly used. Moreover, it is assumed that the time delay of data converting can be neglected.

5.3.1 Mission profile description

As described in Chapter 4, the mission area in this case study is selected as an open water area around Scott Inlet (71.10941 N, -71.10576 W), which is on the east coast of Baffin Island where oil seeps are naturally present.

5.3.2 Risk identification from the STPA model

Considering the operating characteristics and historical accidents of AUVs. Three types of system losses for AUVs are identified, as listed in Table 5.1. The three undesired system losses are ranked according to their severity.

Table 5.1. System losses of AUVs.

System loss	Description
SL-1 Vehicle loss or unrepairable damage	Complete loss of the physical vehicle or an AUV being damaged and unrepairable for future missions.
SL-2 Severe damage, mission failure, mission abort	Inability to complete the mission.
SL-3 Mitigable damage, mission degraded, mission delayed	Can be fixed in the next planned maintenance.

According to determined system losses, potential system-level hazards that could lead to a system loss are identified, as shown in Table 5.2. A total of seven system hazards are identified, covering most of the technical hazards that an AUV could possibly suffer during deployment in an oil spill environment.

Table 5.2. System-level hazards of AUVs operating in an oil spill environment.

Identifier	System-level hazard	Related loss

SH-1	Integrity failure	SL-1, SL-2
SH-2	Collision with ships or underwater obstacles	SL-1, SL-2, SL-3
SH-3	Emergency system failure	SL-1, SL-2
SH-4	Communication system failure	SL-1, SL-2, SL-3
SH-5	Undesired path deviation	SL-1, SL-2, SL-3
SH-6	Invisibility of the vehicle	SL-1, SL-2, SL-3
SH-7	Buoyancy control failure	SL-1, SL-2, SL-3

Although a number of UCAs remain to be identified in a realistic situation, the risk analysis model would become rapidly complicated to evaluate if all of them were involved. Therefore, this study focuses on four typical UCAs relating to path planning and navigational control of AUVs, as listed in Table 5.3, to facilitate the validation of the proposed framework.

Table 5.3. Identified UCAs and their causal factors.

UCAs	Related System-level Hazard	Causal Factors
UCA-1 Control module does not provide appropriate speed	SH-5 Undesired path deviation SH-6 Invisibility of the vehicle	CF-1 Current speed CF-2 Wrong waypoint generation CF-3 Limited power capacity CF-4 Insufficient environmental information for accurate path prediction

UCA-2 Control module does not provide appropriate yaw	SH-5 Undesired path deviation SH-6 Invisibility of the vehicle	CF-1 Current speed CF-2 Wrong waypoint generation CF-3 Limited power capacity CF-4 Insufficient environmental information for accurate path prediction CF-5 Failure of steering system
UCA-3 Navigation system provides inaccurate position and heading	SH-5 Undesired path deviation SH-6 Invisibility of the vehicle	CF-1 Current speed CF-4 Insufficient environmental information for accurate path prediction CF-6 Depth sensor failure CF-7 Current speed sensor failure CF-8 Sensor contamination caused by dense oil
UCA-4 Sensor system does not identify obstacles timely	SH-2 Collision with ships or underwater obstacles	CF-9 Delay of sensor data converting CF-10 Acoustic sensor failure CF-11 Dynamic obstacles

Among the causal factors, several nodes are defined as monitoring nodes, which could be monitored or measured during the mission by onboard sensors. These nodes assist in environmental observation and situation awareness in rapidly changing conditions. The monitoring nodes and potential employed sensors are summarized in Table 5.4.

Table 5.4. Monitoring nodes and employed sensors.

Monitored Node	Employed Sensor
CF-1 Current Speed	ADCP/DVL
CF-8 Sensor contamination caused by dense oil	Fluorometer
CF-11 Dynamic obstacles	Sonar

5.3.3 Development of the STPA-BN risk analysis model

The STPA outputs are used as the basis to develop the BN risk model. The structure of the developed BN risk model is shown in Fig. 5.4. For simplicity, this case study only considered the most severe system loss as the top node, namely, the vehicle loss or unrepairable damage. The occurrence probability of the top node can be specified as a risk index that could assist in further path planning and decision making.

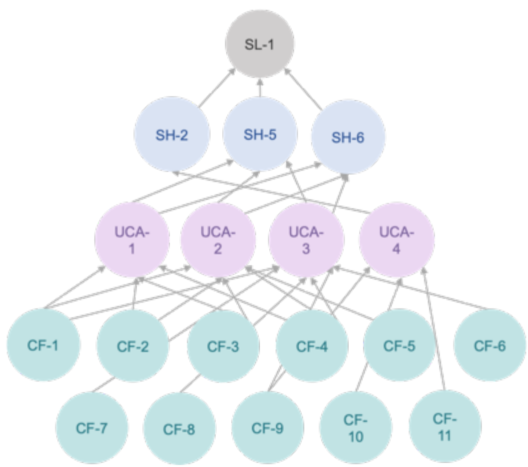

Fig. 5.4. The developed BN model.

In order to reduce the complexity of BN reference, the states of BN nodes are discretized into no more than three states. It is noted that a more comprehensive BN model can be expanded by adding nodes and their states, following the same process as this case study. A full description of BN nodes is defined as follows. Among the BN nodes, several monitoring nodes, namely, CF-1 current speed and CF-8 Sensor contamination caused by dense oil have three states of [Low, Medium, High], while other nodes only have two states of [Occur, Not occur]. The prior probability of each state of the BN node and conditional probabilities among nodes are determined according to domain experts′ judgements.

5.3.4 Risk map generation

On the basis of obtained environmental information and STPA-BN reasoning results, a risk map in terms of the probability of SL-1 in the mission area can be generated and illustrated in Fig. 5.5. This risk map intuitively presents high-risk regions which the AUV should avoid, where the numbers on the scale represent risk indices. For instance, locations with obstacles have the highest risk index, which can always prevent the vehicle from selecting an obstacle as a waypoint.

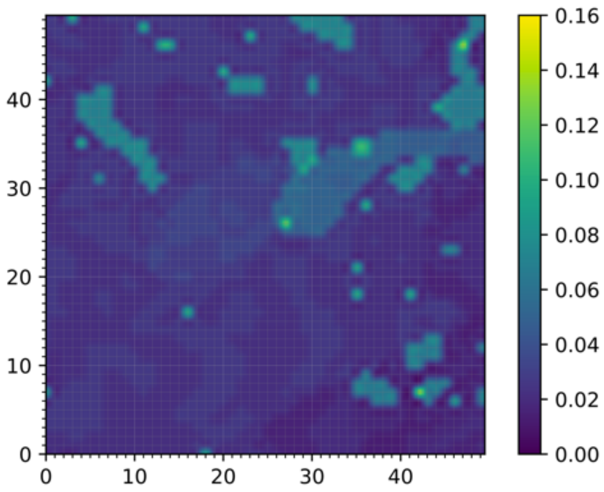

Fig. 5.5. Risk map generated from the STPA-BN reasoning results.

5.4 Simulation results and discussion

5.4.1 Simulation setup

In this section, the proposed hybrid risk-aware path planning strategy is simulated in the Python environment. The simulation is investigated to test the proposed method in a realistic environment with consideration of real environmental information, the real-time risk state of the vehicle, and the dynamic obstacles. The specification of the applied ecoSUBm5 AUV is summarized in Table 5.5.

Table 5.5. The specification of the ecoSUBm5 AUV.

Parameter	Value [Unit]
Vehicle length	1 [m]
Hull diameter	1.46 [m]
Weight in air	12 [kg]

Depth range	500 [m]
Cruising speed	1 [m/s]
Yaw rate	10-40 [degree/s]

The global map is generated by rasterizing the satellite map of the mission area in Baffin Bay, converting the world space into a binary array map. The size of the selected mission area is set as 50 m × 50 m. The whole search space is discretized into grids with the resolution for each grid being 1 m × 1 m, namely, the minimum distance between two adjacent waypoints was 1 m. The start and goal positions are set as (5 m, 2 m) and (45 m, 48 m) respectively in coordinates. To verify that the hybrid risk-aware planner can flexibly avoid dynamic obstacles, a dynamic obstacle with a constant forward velocity is added to the mission area. The dynamic obstacle is set to interfere in the predefined global path of the vehicle. The radii of the vehicle and the moving obstacle are set to be 0.5 m, to prevent the obstacle from approaching too close to the vehicle.

The schematic flowchart of the hybrid path planning simulation is presented in Fig. 5.6. Once the vehicle detects a dynamic obstacle and the distance between them is less than the safety distance of 10 m, the local path planner is triggered. In this case, the vehicle switches from following the global path to following a local optimal trajectory for obstacle avoidance. Once the dynamic obstacle moves far away from the vehicle and their distance exceeds the safety distance of 10 m, the vehicle will continue to follow the global path.

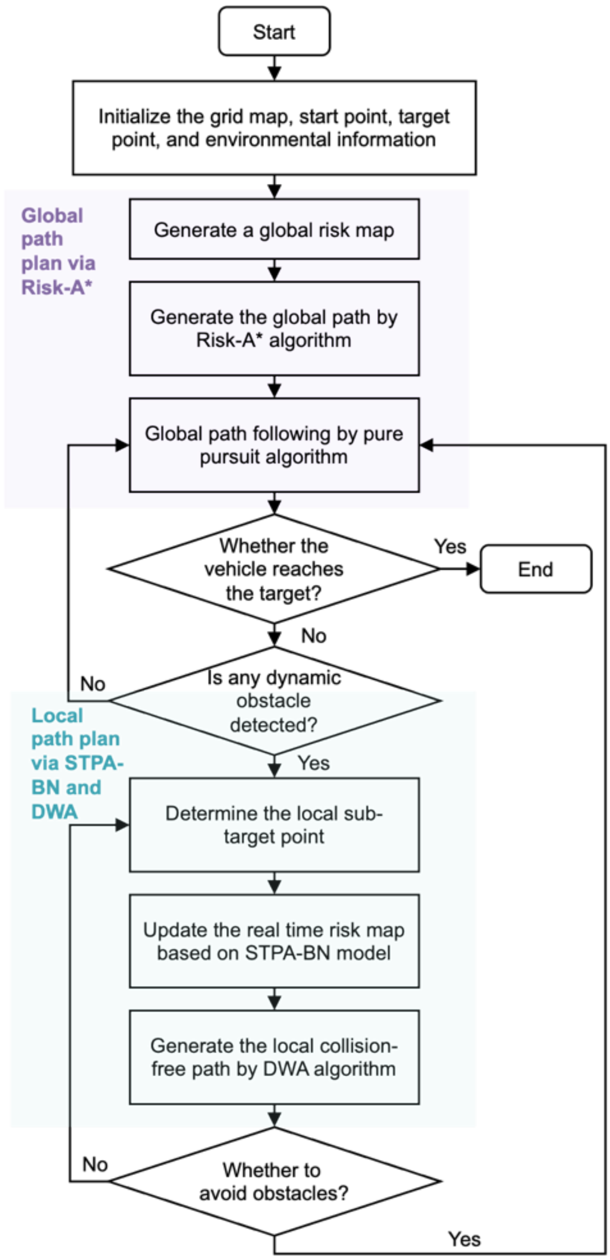

Fig. 5.6. Schematic flowchart of the hybrid path planning strategy.

5.4.2 Risk-aware hybrid path planning

The global path planner firstly plans an optimal global path using the Risk-A* algorithm, which can be obtained from Chapter 4, as shown in Fig. 5.7. In a normal scenario without dynamic obstacles, the vehicle will follow the generated global path using the pure pursuit controller.

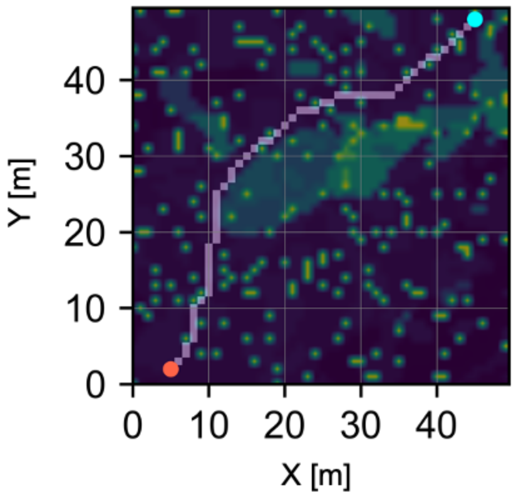

Fig. 5.7. The global path obtained from Chapter 4.

Despite that the global path can be obtained by the Risk-A* algorithm, only following the global path cannot avoid dynamic obstacles. Therefore, local path planning is simulated.

To validate that the proposed risk-aware path planning strategy can better assist in safe navigation, simulations under two different scenarios are implemented for comparative analysis: The first scenario does not consider the real-time risk cost for local path planning, while the second scenario involves the risk cost as a term of the cost function. For simplicity, the forward speed of the dynamic obstacle is held constant. The weights of various parameters in the cost function are defined under two scenarios. In the first scenario, the parameters are specified as $\alpha = 0.02$, $\beta = 0.41$, $\gamma = 0.01$, $\delta = 0$, $\Delta t = 0.2s$, and $T = 2s$. In the second scenario with the risk cost taken into consideration, $\delta = 0.56$ while other parameters remain the same. The allocation of weight value is based on expert knowledge, which can be adjusted according to the willingness to take greater risks and reduce other costs. To test the obstacle avoidance ability of the vehicle, 23 static obstacles and 1 moving obstacle are considered.

5.4.2.1 Scenario 1: Without the risk cost considered

The simulated path planning process of the ecoSUBm5 AUV under Scenario 1 is shown in Fig. 5.8. The symbols and color codes shown in Fig. 5.8 (a) are specified as follows. Five types of nodes are represented with different colors, including static obstacles, a dynamic obstacle, the start position, the target position, and the current position of the vehicle in real time. Four kinds of curves are shown with different colors, including the obtained global path, the historical trajectory of the vehicle that has traveled, the optimum local trajectory predicted by the DWA, and the historical trajectory of the dynamic obstacle. Once the distance between the vehicle and the target is shorter than 3 m, the target is assumed to be reached and the mission is complete.

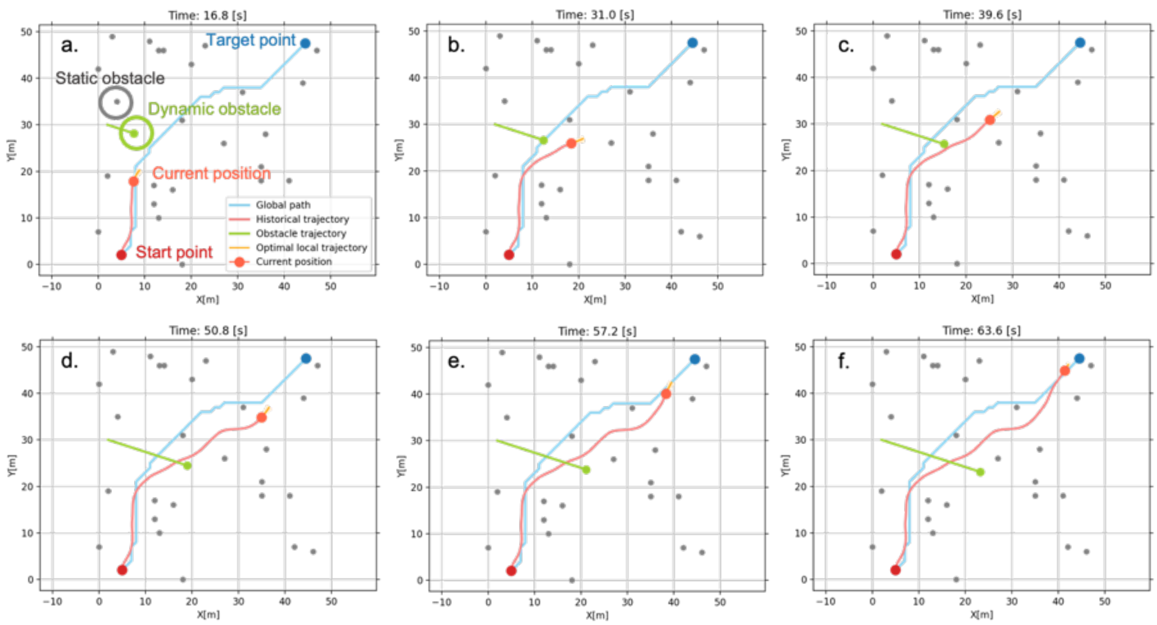

Fig. 5.8. Simulated path planning process under Scenario 1.

It can be seen that the vehicle kept following the global path from the start position until the time of 16.8 s in Fig. 5.8 (a). On this occasion, the vehicle detected a moving obstacle and the distance between them was less than the predefined safety distance of 10 m, and therefore, the DWA local planner was triggered. Fig. 5.8 (b) shows that the vehicle gave up following the global path and switched to follow a local optimal path obtained by the DWA to avoid the approaching moving obstacle. After successfully avoiding the moving obstacle, instead of immediately returning back to the global path, the vehicle made the decision to continually re-plan the local path, as shown in Figs. 5.8 (c) and (d). The reason is that the vehicle ran into a cluster of static obstacles at this moment, and there was a higher collision probability if it returned to the global path. At the time of 57.2 s in Fig. 5.8 (e), the vehicle has moved far away from all the obstacles, with their distance exceeding the safety distance. In other words, the collision risk was lifted. Therefore, the vehicle switched back to follow the global path and finally reached the target in Fig. 5.8 (f).

5.4.2.2 Scenario 2: With the risk cost considered

The simulated path planning process of the ecoSUBm5 AUV under Scenario 1 is shown in Fig. 5.9. It can be seen that Figs. 5.9 (a) and (b) show the process of global path following and dynamic obstacle avoidance, which is similar to Scenario 1. However, from the time of 42.2 s in Fig. 5.9 (c), the vehicle chose to detour around the static obstacles. It should be noted in Fig. 5.9 (e) at the time of 57.8 s, the vehicle successfully avoided all obstacles and reached the safety distance from them. However, the vehicle continued to detour instead of sailing back to the global path. At the time of 65.4 s in Fig. 5.9 (f), the vehicle reached the target after a detour.

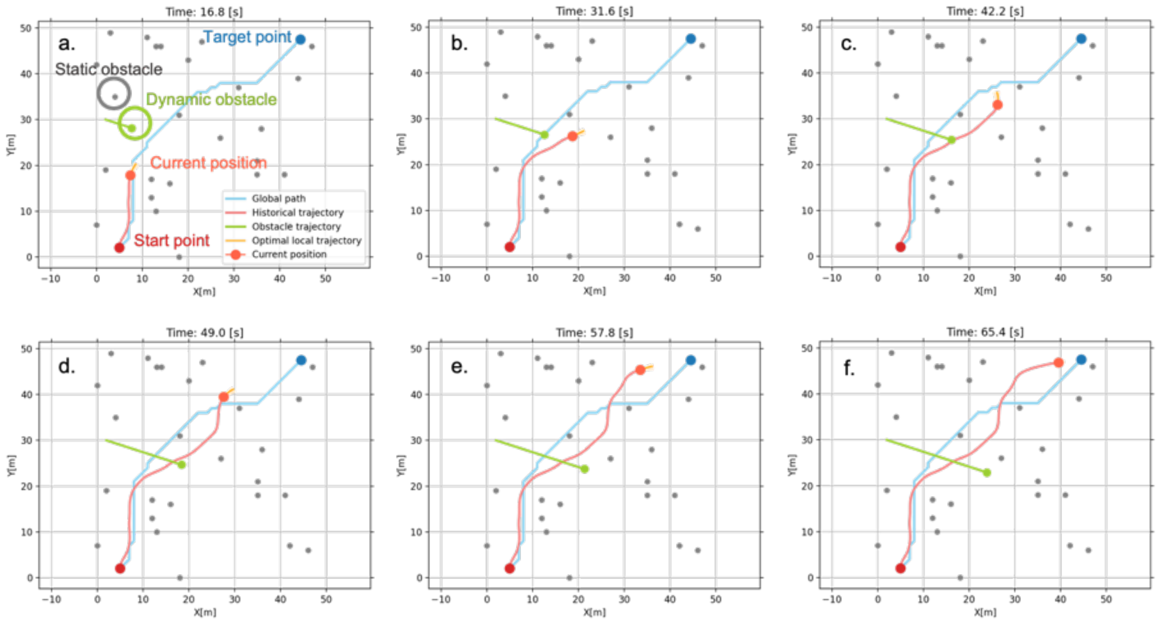

Fig. 5.9. Simulated path planning process under Scenario 2.

5.4.2.3 Comparison of the risk state under two scenarios

The obtained final paths under the two scenarios are presented in Fig. 5.10 (left column), which are overlapping on the same risk map. During the global path following and local path adaptation, the risk state of the vehicle is updated in real-time based on the developed STPA-BN risk model. The data of measurable nodes are dynamically monitored and transferred as the input for the risk model. Accordingly, Fig. 5.10 (right column) visualizes the changing waypoint risk index and the accumulative risk index along the path under the two scenarios. The estimated risk index at each time point represents the probability of "SL-1 vehicle loss or damage" under the current environmental conditions.

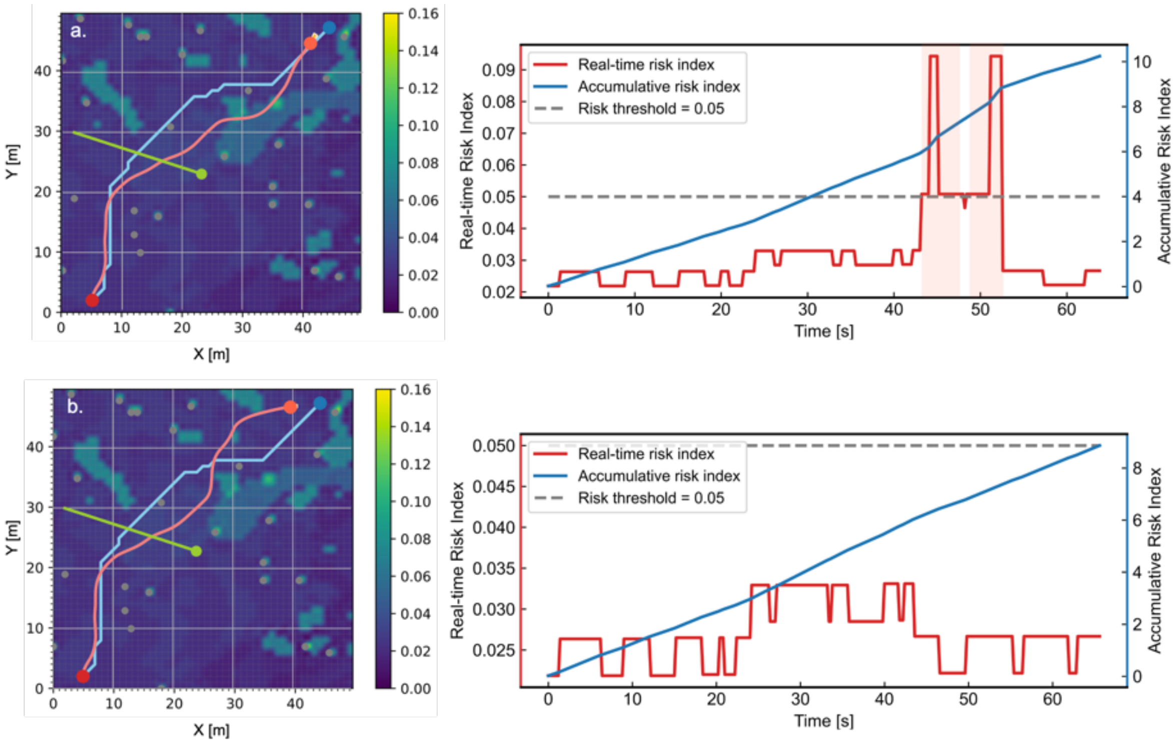

Fig. 5.10. Obtained final paths, waypoint risk indices, and accumulative risk indices under (a) Scenario 1 and (b) Scenario 2.

It can be seen that with the location and the ambient environmental conditions changing, the risk state of the vehicle also varies accordingly. As shown in Fig. 5.10 (a), without considering the risk cost predicted by STPA-BN, candidate waypoints are potentially selected for the local trajectory, no matter how risky they are. For example, the risk state from 43.4 s to 47.8 s in the local path rises to an unacceptable level that exceeds the predefined risk threshold of 0.05. In this case, the vehicle was directly running into a high-risk region according to the risk map. The path planner without the risk taken into account fails to select a safer waypoint to mitigate the risk state, and the vehicle could have a major chance of being lost during this mission. In contrast, with the risk cost considered, the performance of avoiding high risk regions can be significantly improved, as shown in Fig. 5.10 (b). The vehicle made a detour to avoid the high-risk region, and thereby the waypoint risk index remained lower than the risk threshold of 0.05.

Based on the comparative analysis of simulations of scenario 1 and scenario 2, it can be seen that the proposed hybrid path planner embedding the risk analysis model has better risk-aware abilities. It can not only avoid static and dynamic obstacles in real time, but also can be aware of risky regions and select safer trajectories in a timely manner. The simulation results demonstrate the optimum and effectiveness of the proposed strategy.

5.5 Conclusion

In this study, a risk-aware hybrid path planning strategy for AUVs operating in challenging environments is proposed. The risk factors of vehicle loss are identified from a control perspective using the STPA framework. The risk state of the vehicle during navigation is rigorously estimated based on an online STPA-BN model. The predicted risk index is integrated into a hybrid path planning module to achieve real time risk-aware decision making. The proposed risk-aware path planning strategy that considers the risk cost during cruising exhibits better performance in avoiding risky regions compared with the traditional DWA algorithm which neglects the risk cost. It helps to select safer waypoints in real time, and at the same time, it mitigates the risk level within a tolerable threshold to ensure safe navigation.

The limitations of this study are observed. Since the original DWA algorithm uses constant weights in the cost function, it lacks flexibility to handle complex situations with an increasing number of dynamic obstacles. In future work, an advanced DWA algorithm should be introduced to learn and adjust the weights of the cost function, which should overcome the shortcomings of the traditional DWA and improve the applicability of the proposed path planner in multiple environments. In addition, the proposed strategy will be carried out in field trials to further validate its effectiveness.

Chapter 6. Conclusions and Future Directions

This chapter concludes the research progress performed in this thesis and highlights the key findings of individual chapters. It also provides a summary of the overall research outcomes, discusses the limitations of the current work, and specifies the directions for future research.

6.1 Conclusions

Risk analysis and safety-based decision making is a critical issue for autonomous underwater vehicles (AUVs) operating in dynamic underwater environments. The primary objective of this research was to investigate systematic risk analysis approaches and safety-based decision making strategies for the AUV system in challenging marine environments. The expected research outcomes of this thesis addressed the following research questions:

(i) What is the current state-of-the-art for the domain of risk analysis for AUVs? What are the critical risk factors and evolving risk analytical models? What are existing research gaps and future research trends in this domain?

(ii) What are the main inherent technical failures of AUVs? How can they be impacted by environmental conditions? How is it possible to predict the risk level of an AUV platform considering the non-linear relationships among inherent technical failures and complex environmental variables?

(iii) How is it possible to use the estimated risk state for safer navigation for AUVs? How can a design of a risk-based mission planning strategy for AUVs aid in global navigation and decision making?

(iv) How is it possible to address the real-time mission planning problem considering the dynamic risks and moving obstacles in realistic operating environments for AUVs?

The key findings from this thesis are summarized as follows:

Through an extensive literature review, it is found that the systematic identification of risk factors and their causal relationships is vital for further risk analysis. Most of the early research focused on technical factors of AUVs, relying on historical performance data. Whereas in current trends, environmental factors, human factors, and their interactive impacts are increasingly receiving attention. Furthermore, it is evident that quantitative methods have been rapidly implemented in recent years to enhance the accuracy and to handle the uncertainties of risk analysis of AUVs. However, former studies still rely heavily on expert knowledge, which may introduce judgmental bias. Lastly, future challenges for risk analysis for AUVs may focus on addressing dynamic risk analysis, scarce historical data, intelligent risk analysis, and multi-vehicles risk analysis.

Based on the dependence analysis in Chapter 3, the most critical environmental variables contributing to the loss of an autonomous underwater glider (AUGs) were identified, including a large water density gradient (E6), large current speed (E7), and large ship density (E3), which deserve constant attention in the environmental monitoring and risk mitigation process. The predict inference of the copula Bayesian network (CBN) can continuously update the occurrence probability of AUG loss given new observations of environmental conditions. Case study results proved that the risk level of AUG operations can be mitigated by reducing the occurrence probabilities of key risk factors. Moreover, a narrow probability interval of these factors can minimize the prediction uncertainties, which gave insights into deploying the vehicle in a relatively gentle environment where the ambient conditions change moderately. In addition, according to the diagnose inference of the CBN model, the posterior probability of each risk variable can be obtained given a certain state of AUG loss. Hence, by defining an acceptable risk level of AUG loss, environmental conditions can be adaptively adjusted to achieve the safety requirement. Moreover, applications considering a Slocum G1 Glider operating in the Holyrood water region validated that the proposed CBN model is effective for risk prediction both over time and space, which indicated that the proposed risk model can be implemented to prevent risky occasions and areas in advance of a mission. In addition, risk mitigation measures can be provided according to the above findings, such as reducing the surfacing times for AUGs in the water column with busy shipping, and cruising away from deep-water regions with a large density gradient or with a close distance to the seafloor.

Chapter 4 provides a systematic risk-based path planning approach for AUVs operating in an oil spill environment. The proposed BN-based risk model can forecast risk states of vehicle loss given comprehensive spill environments. Its probabilistic reasoning enhances the accuracy for further path searching and risk-based decision making. The generated risk map based on BN reasoning intuitively presents the spatial distributions of high-risk regions in a gridded mission area, which provides insights of risk mitigation through obstacle avoidance and waypoint selections. In addition, comparisons between the Risk-A* planner with two classic path planners (i.e., minimal-length planner and minimal-risk planner) have indicated that a trade-off exists between the routing length, associated risks, and computational efficiency along a path. The proposed Risk-A* planner outperforms in risk mitigation by avoiding potential risky regions and obstacles, whilst it is highly competitive in terms of path distance and computational time. Moreover, different risk thresholds can affect the performance of Risk-A* path planning. A lower tolerable risk threshold, which refers to a higher safety requirement, can increase the mission length and consume more computational time. In this case, considering a particular scenario during an oil detection mission, a lower risk threshold can drag the vehicle away from the most highly-concentrated oil regions, which causes the vehicle to miss nearby plumes with rich information and therefore degrades its detection efficiency. Hence, the risk threshold should be modulated to achieve a trade-off between safety performance and mission efficiency. In summary, the developed risk-based planner can be practical for realistic AUV implementation. It is a worthwhile investigation for preventing AUV loss at the path planning stage prior to a mission.

Chapter 5 designs a risk-ware hybrid path planning strategy for AUVs operating in challenging environments. The risk factors of vehicle loss are identified from a control perspective using the systems theoretical process analysis (STPA) model. The risk state of the vehicle during navigation is rigorously estimated based on an online STPA-BN model. The predicted risk index is integrated into a hybrid path planning module to achieve real time risk-aware decision making. The proposed risk-aware path planning strategy that considers the risk cost during cruising exhibits better performance in avoiding risky regions compared with the traditional DWA algorithm which neglects the risk cost. It helps to select safer waypoints in real time, and at the same time, it mitigates the risk level to within a tolerable threshold to ensure safe navigation.

6.2 Future directions

The current work aims to address risk analysis and safety-based decision making strategies for AUVs in harsh marine environments. Several limitations of the current study are observed and can be further addressed in future work:

Chapter 3 only employed the Gaussian copula function to model the correlation relationships among risk variables. Future work could explore different kinds of copula functions (i.e., Archimedean copula functions) to describe the dependencies more accurately. Furthermore, due to insufficient measured data, the case study combined measured environmental data with assumed environmental conditions, which could compromise the accuracy of risk prediction. In future work, real-time environmental data measured by multiple sensors should be incorporated to improve assessment accuracy. Lastly, this chapter provided an offline risk assessment method for AUGs, which could be extended to an online decision network for setpoint selection and path control given the current predicted risk level.

Chapter 4 and Chapter 5 both considered a two-dimensional trajectory of the AUVs, which is particularly useful for missions in detecting oil spills released by vessels without significant depth changes. The approach could also be applied for AUV path planning in tracking oil spills from reservoirs. For this scenario, the vehicle would have to dive to higher depths. To capture this scenario, both the risk model and the path searching algorithm should be updated to take the 3D problem into consideration. A modification would be required to the methodology to include the 3D body dynamics properties of the AUV. In addition, in the case of path planning, it is also important to consider the vehicle′s mechanical features in the path planning, such as the minimum turn radius of the vehicle.

Another limitation of Chapter 5 is that the original dynamic window approach (DWA) uses constant weights in the cost function, it lacks flexibilities to handle complex situations with an increasing number of dynamic obstacles. In future work, an advanced DWA algorithm should be introduced to learn and adjust the weights of the cost function, which should overcome the shortcomings of the traditional DWA and improve the applicability of the proposed path planner in multiple environments.

Furthermore, some recent research provided advanced methods for model validation for marine robotic systems (Albarakati et al., 2021; Liu et al., 2022). These studies considered multiple simulation scenarios with various vehicle maneuvers in practical environments. They provided insights to bridge the gap between pure computer-based simulations and real experimental validation. For potential experimental simulations, other key parameters besides the path length could be considered, such as the vehicle velocity, turning maneuvers, travel time, and energy consumption, which can be affected by ambient environmental conditions as well. Analyses from multiple perspectives of the simulations could enhance the feasibility of the planner, especially for multi-objective problems. An accurate estimation of AUVs navigational data is also crucial for safe path planning. The use of multiple sensors′ data could be beneficial for high-fidelity validation in practical environments in the future. In addition, the proposed strategy should be carried out in field trials to further validate its superiorities.

Appendix

Table. A1. Classification of literature regarding the risk analysis of AUVs.

No.	Literature	Risk Factor Identification			Risk Analysis Method		Mission Type	Mission area	Consequence Type
		Technical Factor	Environmental Factor	Human Factor					
1	(Ortiz et al., 1999)	✓			Safety layers analysis	Qualitative	General mission	General area	AUV abnormal working
2	(Madsen et al., 2000)	✓			Tree diagram	Qualitative	Deep water and under ice mission	General area	Mission abort
3	(Griffiths et al., 2003)	✓			Kaplan-Meier survival model	Quantitative	Under sea ice mission	The Antarctic	AUV loss
4	(Griffiths and Trembanis, 2007)	✓			RMP	Semi-quantitative	Under sea ice and ice shelf mission	Polar regions	AUV loss
5	(Griffiths and Brito, 2008)		✓		BN	Quantitative	Under sea ice mission	Polar regions	AUV loss
6	(Bian et al., 2009a)	✓			Fuzzy FTA	Quantitative	General mission	General area	AUV abnormal working
7	(Bian et al., 2009b)	✓			FTA	Quantitative	General mission	General area	AUV abnormal working

8	(Brito et al., 2010)		✓		RMP, Kaplan-Meier survival model	Quantitative	Under sea ice and ice shelf mission	The Antarctic	AUV loss
9	(Meng and Qingyu, 2010)	✓			Safety measures analysis	Qualitative	General mission	Lake area	Battery failure, leakage, fishing net wrapped
10	(Kaminski et al., 2010)		✓		Fault Response Table	Qualitative	Under ice bathymetric surveys	The Arctic	AUV loss
11	(Brito and Griffiths, 2011)	✓	✓		Markov chain	Quantitative	General mission	General area	AUV loss
12	(Griffiths and Brito, 2011)	✓	✓		RMP, Markov chain	Quantitative	Under sea ice mission	Polar regions	AUV loss
13	(Ho et al., 2011)			✓	Human factor analysis	Qualitative	General mission	General area	Mission abort
14	(Brito et al., 2012)	✓			BN	Quantitative	Under sea ice mission	The Arctic	Operational risk
15	(Brito and Griffiths, 2012)	✓			SD	Quantitative	Multi-vehicles mission	General area	AUV loss
16	(Hu et al., 2013)	✓			FMECA, FTA	Quantitative	General mission	General area	AUV loss, mission abort
17	(Xu et al., 2013)	✓			FTA	Semi-quantitative	Deep-sea minerals exploration	Deep-sea hydrothermal area	Mission abort
18	(Pereira et		✓		Markov chain	Quantitative	Path planning	General area	AUV collision

	al., 2013)								
19	(Aslansefat et al., 2014a)	✓			FTA	Quantitative	General mission	General area	AUV abnormal working
20	(Brito et al., 2014b)	✓			Probability tree model	Quantitative	General mission	General area	Loss of communication
21	(Brito et al., 2014a)	✓			Kaplan-Meier survival model	Quantitative	Shallow water and deep-water glider mission	Shallow water, deep water	AUV collision
22	(Zhang et al., 2015)	✓			Grey relation analysis	Qualitative	General mission	General area	Thruster fault
23	(Thieme et al., 2015b)	✓	✓	✓	BN	Quantitative	General mission	General area	Mission abort
24	(Thieme et al., 2015a)	✓	✓	✓	Risk management framework, human reliability analysis, FTA, ETA	Quantitative	Seafloor mapping	Coastal area	AUV loss, mission abort
25	(Brito and Griffiths, 2016)		✓		BN, Kaplan-Meier survival model	Quantitative	Under sea ice mission	the Antarctic	AUV loss
26	(Hegde et al., 2016a)	✓	✓		Risk indicator model	Quantitative	Subsea IMR operation, path planning	General area	AUV collision
27	(Harris et al., 2016)	✓			FMEA, FTA, Markov chain	Quantitative	Multi-vehicles mission	General area	AUV loss

28	(Brito, 2016)	✓			FTA	Quantitative	General mission	General area	Glider mission abort
29	(Yu et al., 2017)	✓	✓		Bow-tie	Quantitative	IMR operation of offshore oil and gas platform	General area	AUV collision
30	(Xiang et al., 2017)	✓			FTA	Quantitative	General mission	General area	Failure of onboard system
31	(Hegde et al., 2018)	✓	✓	✓	BN	Quantitative	Subsea IMR operation	Åsgard field, Norway	Mission abort
32	(Brito et al., 2018)			✓	ETA	Quantitative	Adaptive mission planning	General area	Mission failure
33	(Brito and Griffiths, 2018)	✓			BN	Quantitative	General mission	General area	Mission abort, AUV loss
34	(Brito and Chang, 2018)	✓			FTA	Quantitative	General mission	General area	AUV loss
35	(Hegde et al., 2019)	✓	✓		Safety envelop, Octree method	Semi-quantitative	Subsea IMR operation, path planning	General area	AUV collision
36	(Loh et al., 2019)	✓	✓	✓	Fuzzy set theory	Semi-quantitative	Under sea ice mission	The Antarctic	AUV loss
37	(Bremnes et al., 2019)	✓	✓		BN	Quantitative	Under ice altitude control	The Arctic	AUV loss
38	(Loh et al.,	✓		✓	FuSDRA	Quantitative	Under sea ice	The	AUV loss

	2020a)						mission	Antarctic	
39	(Loh et al., 2020b)	✓	✓	✓	FuSDRA	Quantitative	Under sea ice mission	The Antarctic	AUV loss
40	(Loh et al., 2020c)			✓	SD	Quantitative	Under sea ice mission	The Antarctic	AUV loss
41	(Xu et al., 2020)	✓		✓	FuSDRA	Quantitative	Under sea ice mission	The Antarctic	AUV loss
42	(Yang et al., 2020)	✓	✓		BN	Quantitative	Under sea ice mission	The Antarctic	AUV damage

References

Afenyo, M., Khan, F., Veitch, B., Yang, M., 2017. Arctic shipping accident scenario analysis using Bayesian Network approach. Ocean Engineering 133, 224-230. doi:https://doi.org/10.1016/j.oceaneng.2017.02.002

Akhtar, M.J., Utne, I.B., 2014. Human fatigue's effect on the risk of maritime groundings–A Bayesian Network modeling approach. Safety Science 62, 427-440. doi:https://doi.org/10.1016/j.ssci.2013.10.002

Albarakati, S., Lima, R.M., Theußl, T., Hoteit, I., Knio, O., 2021. Multiobjective Risk-Aware Path Planning in Uncertain Transient Currents: An Ensemble-Based Stochastic Optimization Approach. IEEE Journal of Oceanic Engineering 46 (4), 1082-1098. doi:https://doi.org/10.1109/JOE.2021.3063196

Allotta, B., Pugi, L., Reatti, A., Corti, F., 2017. Wireless power recharge for underwater robotics, 2017 IEEE International Conference on Environment and Electrical Engineering and 2017 IEEE Industrial and Commercial Power Systems Europe (EEEIC / I&CPS Europe), pp. 1-6.

Alvarez, A., Caffaz, A., Caiti, A., Casalino, G., Gualdesi, L., Turetta, A., Viviani, R., 2009. Fòlaga: A low-cost autonomous underwater vehicle combining glider and AUV capabilities. Ocean Engineering 36 (1), 24-38. doi:https://doi.org/10.1016/j.oceaneng.2008.08.014

Amin, M.T., Khan, F., Ahmed, S., Imtiaz, S., 2021. A data-driven Bayesian network learning method for process fault diagnosis. Process Safety and Environmental Protection 150, 110-122. doi:https://doi.org/10.1016/j.psep.2021.04.004

An, E., Dhanak, M.R., Shay, L.K., Smith, S., Van Leer, J., 2001. Coastal oceanography using a small AUV. Journal of Atmospheric Oceanic technology 18 (2), 215-234. doi:https://doi.org/10.1175/1520-0426(2001)018<0215:COUASA>2.0.CO;2

Anderlini, E., Salavasidis, G., Harris, C.A., Wu, P., Lorenzo, A., Phillips, A.B., Thomas, G., 2021. A remote anomaly detection system for Slocum underwater gliders. Ocean Engineering 236, 109531. doi:https://doi.org/10.1016/j.oceaneng.2021.109531

Aslansefat, K., Latif-Shabgahi, G., Kamarlouei, M., 2014a. A strategy for reliability evaluation and fault diagnosis of Autonomous Underwater Gliding Robot based on its Fault Tree. International Journal of Advances in Science Engineering Technology 2 (4), 83-89.

Aslansefat, K., Latif-Shabgahi, G.R., Kamarlouei, M., 2014b. A Strategy for Reliability Evaluation and Fault Diagnosis of Autonomous Underwater Gliding Robot based on its Fault Tree. International Journal of Advances in Science, Engineering and Technology (IJASEAT) 2, 83-89.

Bachmayer, R., De Young, B., Williams, C., Bishop, C., Knapp, C., Foley, J., 2006. Development and deployment of ocean gliders on the Newfoundland Shelf, Proceedings of the Unmanned Vehicle Systems Canada Conference.

Bai, X., Lam, J.S.L., 2022. Portfolio value-at-risk estimation for spot chartering decisions under changing trade patterns: A copula approach. Risk Analysis n/a (n/a). doi:https://doi.org/10.1111/risa.13989

Bandhauer, T.M., Garimella, S., Fuller, T.F., 2011. A critical review of thermal issues in lithium-ion batteries. Journal of the Electrochemical Society 158 (3), R1. doi:https://doi.org/10.1149/1.3515880

Bao, J., Li, D., Qiao, X., Rauschenbach, T., 2020. Integrated navigation for autonomous underwater vehicles in aquaculture: A review. Information Processing in Agriculture 7 (1), 139-151. doi:https://doi.org/10.1016/j.inpa.2019.04.003

Bedford, T., Daneshkhah, A., Wilson, K.J., 2016. Approximate Uncertainty Modeling in Risk Analysis with Vine Copulas. Risk Analysis 36 (4), 792-815. doi:https://doi.org/10.1111/risa.12471

Bellingham, J., Cokelet, E.D., Kirkwood, W.J., 2008. Observation of warm water transport and mixing in the Arctic basin with the ALTEX AUV, 2008 IEEE/OES Autonomous Underwater Vehicles. IEEE, pp. 1-5.

Bensaci, C., Zennir, Y., Pomorski, D., Innal, F., Lundteigen, M.A., 2023. Collision hazard modeling and analysis in a multi-mobile robots system transportation task with STPA and SPN. Reliability Engineering & System Safety 234, 109138. doi:https://doi.org/10.1016/j.ress.2023.109138

Bian, X., Mou, C., Yan, Z., Xu, J., 2009a. Reliability analysis of AUV based on fuzzy fault tree, 2009 International Conference on Mechatronics and Automation. IEEE, pp. 438-442.

Bian, X., Mou, C., Yan, Z., Xu, J., 2009b. Simulation model and fault tree analysis for AUV, 2009 International Conference on Mechatronics and Automation. IEEE, pp. 4452-4457.

Bjerga, T., Aven, T., Zio, E., 2016. Uncertainty treatment in risk analysis of complex systems: The cases of STAMP and FRAM. Reliability Engineering & System Safety 156, 203-209. doi:https://doi.org/10.1016/j.ress.2016.08.004

Borenstein, J., Koren, Y., 1991. The vector field histogram-fast obstacle avoidance for mobile robots. IEEE transactions on robotics and automation 7 (3), 278-288.

Bound, M., 2019. Expedition blogs. Retrieved from https://oceanwide-expeditions.com/.

Bremnes, J.E., Norgren, P., Sørensen, A.J., Thieme, C.A., Utne, I.B., 2019. Intelligent Risk-Based Under-Ice Altitude Control for Autonomous Underwater Vehicles, OCEANS 2019 MTS/IEEE SEATTLE. IEEE, Seattle, WA, USA, pp. 1-8.

Bremnes, J.E., Thieme, C.A., Sørensen, A.J., Utne, I.B., Norgren, P., 2020. A Bayesian approach to supervisory risk control of AUVs applied to under-ice operations. Marine Technology Society Journal 54 (4), 16-39. doi:https://doi.org/10.4031/MTSJ.54.4.5

Brito, M., Griffiths, G., 2016. A Bayesian approach for predicting risk of autonomous underwater vehicle loss during their missions. Reliability Engineering & System Safety 146, 55-67. doi:https://doi.org/10.1016/j.ress.2015.10.004.

Brito, M., Griffiths, G., Ferguson, J., Hopkin, D., Mills, R., Pederson, R., MacNeil, E., 2012. A behavioral probabilistic risk assessment framework for managing autonomous underwater vehicle deployments. Journal of Atmospheric Oceanic technology 29 (11), 1689-1703. doi:https://doi.org/10.1175/JTECH-D-12-00005.1

Brito, M., Smeed, D., Griffiths, G., 2014a. Underwater glider reliability and implications for survey design. Journal of Atmospheric Oceanic technology 31 (12), 2858-2870. doi:https://doi.org/10.1175/JTECH-D-13-00138.1

Brito, M.P., 2016. Uncertainty management during hybrid autonomous underwater vehicle missions, 2016 IEEE/OES Autonomous Underwater Vehicles (AUV). IEEE, Tokyo, pp. 278-285.

Brito, M.P., Chang, M.Y., 2018. On the Reliability of Experts' Assessments for Autonomous

Underwater Vehicle Risk of Loss Prediction: Are Optimists better than Pessimists? Proceedings International Conference on Probabilistic Safety Assessment and Management (PSAM14), 12.

Brito, M.P., Griffiths, G., 2011. A Markov chain state transition approach to establishing critical phases for AUV reliability. IEEE Journal of Oceanic Engineering 36 (1), 139-149. doi:https://doi.org/10.1109/JOE.2010.2083070

Brito, M.P., Griffiths, G., 2012. A systems dynamics framework for risk management of multiple autonomous underwater vehicles. 11th International Probabilistic Safety Assessment and Management Conference and the Annual European Safety and Reliability Conference 2012 (PSAM11 ESREL 2012), 2093-2101.

Brito, M.P., Griffiths, G., 2018. Updating autonomous underwater vehicle risk based on the effectiveness of failure prevention and correction. Journal of Atmospheric Oceanic technology 35 (4), 797-808. doi:https://doi.org/10.1175/JTECH-D-16-0252.1

Brito, M.P., Griffiths, G., Challenor, P., 2010. Risk analysis for autonomous underwater vehicle operations in extreme environments. Risk Analysis: An International Journal 30 (12), 1771-1788. doi:https://doi.org/10.1111/j.1539-6924.2010.01476.x

Brito, M.P., Griffiths, G., Trembranis, A., 2008. Eliciting expert judgment on the probability of Loss of an AUV operating in four environments. Southampton, UK: National Oceanography Centre Southampton Research and Consultancy Report 48.

Brito, M.P., Lewis, R.S., Bose, N., Griffiths, G., 2018. Adaptive autonomous underwater vehicles: An assessment of their effectiveness for oceanographic applications. IEEE Transactions on Engineering Management 66 (1), 98-111. doi:https://doi.org/10.1109/TEM.2018.2805159

Brito, M.P., Smeed, D.A., Griffiths, G., 2014b. Analysis of causation of loss of communication with marine autonomous systems: A probability tree approach. Methods in Oceanography 10, 122-137. doi:https://doi.org/10.1016/j.mio.2014.07.003

Brito, M.P., Stevenson, M., Bravo, C., 2022. Subjective machines: Probabilistic risk assessment based on deep learning of soft information. Risk Analysis. doi:https://doi.org/10.1111/risa.13930

Cai, Y., Golay, M.W., 2022. A dynamic Bayesian network-based emergency decision-making framework highlighting emergency propagations: Illustrated using the Fukushima nuclear accidents and the Covid-19 pandemic. Risk Analysis 00 (n/a), 1-18. doi:https://doi.org/10.1111/risa.13928

Camilli, R., Reddy, C.M., Yoerger, D.R., Mooy, B.A.S.V., Jakuba, M.V., Kinsey, J.C., McIntyre, C.P., Sylva, S.P., Maloney, J.V., 2010. Tracking Hydrocarbon Plume Transport and Biodegradation at Deepwater Horizon. Science 330 (6001), 201-204. doi:https://doi.org/10.1126/science.1195223

Caress, D.W., Thomas, H., Kirkwood, W.J., McEwen, R., Henthorn, R., Clague, D.A., Paull, C.K., Paduan, J., Maier, K.L., Reynolds, J., 2008. High-resolution multibeam, sidescan, and subbottom surveys using the MBARI AUV D. Allan B. Marine habitat mapping technology for Alaska, 47-69.

Čepin, M., Mavko, B., 2002. A dynamic fault tree. Reliability Engineering & System Safety 75 (1), 83-91. doi:https://doi.org/10.1016/S0951-8320(01)00121-1

Chaal, M., Bahootoroody, A., Basnet, S., Valdez Banda, O.A., Goerlandt, F., 2022. Towards system-theoretic risk assessment for future ships: A framework for selecting Risk Control Options. Ocean Engineering 259, 111797. doi:https://doi.org/10.1016/j.oceaneng.2022.111797

Chen, A.T., Abe, N.D., Mullen, C.R., Gilbert, C.C., 1987. Contamination Sensitivity And Control Of Optical Sensors. SPIE, pp. 97-126.

Chen, T., Wong, Y.D., Shi, X., Yang, Y., 2021a. A data-driven feature learning approach based on Copula-Bayesian Network and its application in comparative investigation on risky lane-changing and car-following maneuvers. Accident Analysis & Prevention 154, 106061. doi:https://doi.org/10.1016/j.aap.2021.106061

Chen, X., Bose, N., Brito, M., Khan, F., Millar, G., Bulger, C., Zou, T., 2022. Risk-based path planning for autonomous underwater vehicles in an oil spill environment. Ocean Engineering 266, 113077. doi:https://doi.org/10.1016/j.oceaneng.2022.113077

Chen, X., Bose, N., Brito, M., Khan, F., Thanyamanta, B., Zou, T., 2021b. A Review of Risk Analysis Research for the Operations of Autonomous Underwater Vehicles. Reliability Engineering & System Safety 216, 108011. doi:https://doi.org/10.1016/j.ress.2021.108011

Chen, Z., Zhang, Y., Zhang, Y., Nie, Y., Tang, J., Zhu, S., 2019. A Hybrid Path Planning Algorithm for Unmanned Surface Vehicles in Complex Environment With Dynamic Obstacles. IEEE Access 7, 126439-126449. doi:10.1109/ACCESS.2019.2936689

Cheng, C., Sha, Q., He, B., Li, G., 2021. Path planning and obstacle avoidance for AUV: A review. Ocean Engineering 235, 109355. doi:https://doi.org/10.1016/j.oceaneng.2021.109355

Claus, B., Bachmayer, R., Williams, C.D., 2010. Development of an Auxiliary Propulsion Module for an Autonomous Underwater Glider. Proceedings of the Institution of Mechanical Engineers, Part M: Journal of Engineering for the Maritime Environment 224 (4), 255-266. doi:https://doi.org/10.1243/14750902JEME204

Coulter, R.C., 1992. Implementation of the pure pursuit path tracking algorithm. Carnegie-Mellon UNIV Pittsburgh PA Robotics INST.

Coupé, V.M.H., Peek, N., Ottenkamp, J., Habbema, J.D.F., 1999. Using sensitivity analysis for efficient quantification of a belief network. Artificial Intelligence in Medicine 17 (3), 223-247. doi:https://doi.org/10.1016/S0933-3657(99)00024-X

Dhont, D., Jatiault, R., Lattes, P., 2019. Combined Use of SAR and Underwater Gliders for Oil Seeps Detection, IGARSS 2019 - 2019 IEEE International Geoscience and Remote Sensing Symposium, pp. 7865-7868.

Dijkstra, E.W., 1959. A note on two problems in connexion with graphs. Numerische Mathematik 1 (1), 269-271. doi:https://doi.org/10.1007/BF01386390

DiPinto, L., 2019. Three-dimensional mapping of dissolved hydrocarbons and oil droplets using a REMUS-600 autonomous underwater vehicle. Report to Bureau of Safety and Environmental Enforcement (BSEE).

Doble, M.J., Forrest, A.L., Wadhams, P., Laval, B.E., 2009. Through-ice AUV deployment: Operational and technical experience from two seasons of Arctic fieldwork. Cold Regions Science Technology 56 (2-3), 90-97. doi:https://doi.org/10.1016/j.coldregions.2008.11.006

Dobrevski, M., Skočaj, D., 2020. Adaptive Dynamic Window Approach for Local Navigation, 2020 IEEE/RSJ International Conference on Intelligent Robots and Systems (IROS), pp. 6930-6936.

Dowdeswell, J.A., Evans, J., Mugford, R., Griffiths, G., McPhail, S., Millard, N., Stevenson, P., Brandon, M.A., Banks, C., Heywood, K.J.J.o.G., 2008. Autonomous underwater vehicles (AUVs) and investigations of the ice–ocean interface in Antarctic and Arctic waters. 54 (187), 661-672. doi:https://doi.org/10.3189/002214308786570773

Du, L., Goerlandt, F., Kujala, P., 2020. Review and analysis of methods for assessing maritime waterway risk based on non-accident critical events detected from AIS data. Reliability Engineering & System Safety 200, 106933. doi:https://doi.org/10.1016/j.ress.2020.106933

Eichhorn, M., 2009. A new concept for an obstacle avoidance system for the AUV "SLOCUM Glider" operation under ice, OCEANS 2009-EUROPE. IEEE, pp. 1-8.

Elidan, G., 2010a. Copula Bayesian Networks, Advances in Neural Information Processing Systems (NIPS), Vancouver, pp. 559-567.

Elidan, G., 2010b. Copula Bayesian networks, Proceedings of the 23rd International Conference on Neural Information Processing Systems - Volume 1. Curran Associates Inc., Vancouver, British Columbia, Canada, pp. 559–567.

Eriksen, B.O.H., Breivik, M., Pettersen, K.Y., Wiig, M.S., 2016. A modified dynamic window algorithm for horizontal collision avoidance for AUVs, 2016 IEEE Conference on Control Applications (CCA), pp. 499-506.

Eusgeld, I., Nan, C., Dietz, S., 2011. "System-of-systems" approach for interdependent critical infrastructures. Reliability Engineering & System Safety 96 (6), 679-686. doi:https://doi.org/10.1016/j.ress.2010.12.010

Fan, S., Woolsey, C.A., 2014. Dynamics of underwater gliders in currents. Ocean Engineering 84, 249-258. doi:https://doi.org/10.1016/j.oceaneng.2014.03.024

Ferguson, J., 2008. Adapting AUVs for use in under-ice scientific missions, OCEANS 2008. IEEE, Quebec City, QC, pp. 1-5.

Forrest, A., Hamilton, A., Schmidt, V., Laval, B., Mueller, D., Crawford, A., Brucker, S., Hamilton, T., 2012. Digital terrain mapping of Petermann Ice Island fragments in the Canadian high arctic, 21st IAHR International Symposium on Ice. , pp. 1-12.

Forrester, J.W., 1997. Industrial dynamics. Journal of the Operational Research Society 48 (10), 1037-1041. doi:https://doi.org/10.1057/palgrave.jors.2600946

Fossen, T.I., 2012. HOW TO INCORPORATE WIND, WAVES AND OCEAN CURRENTS IN THE MARINE CRAFT EQUATIONS OF MOTION. IFAC Proceedings Volumes 45 (27), 126-131. doi:https://doi.org/10.3182/20120919-3-IT-2046.00022

Fox, D., Burgard, W., Thrun, S., 1997. The dynamic window approach to collision avoidance. IEEE Robotics & Automation Magazine 4 (1), 23-33. doi:https://10.1109/100.580977

Ghadhab, M., Junges, S., Katoen, J.-P., Kuntz, M., Volk, M., 2019. Safety analysis for vehicle guidance systems with dynamic fault trees. Reliability Engineering & System Safety 186, 37-50. doi:https://doi.org/10.1016/j.ress.2019.02.005

Govender, I.H., Sahlin, U., O'Brien, G.C., 2022. Bayesian Network Applications for Sustainable Holistic Water Resources Management: Modeling Opportunities for South Africa. Risk Analysis 42 (6), 1346-1364. doi:https://doi.org/10.1111/risa.13798

Griffiths, G., Bose, N., Ferguson, J., Blidberg, D., 2007a. Insurance for autonomous underwater vehicles. Underwater Technology 27 (2), 43-48. doi:https://doi.org/10.3723/175605407782724870

Griffiths, G., Brito, M., 2008. Predicting risk in missions under sea ice with autonomous underwater vehicles, 2008 IEEE/OES Autonomous Underwater Vehicles. IEEE, pp. 1-7.

Griffiths, G., Brito, M.P., 2011. Risk management for autonomous underwater vehicles operating under ice, OTC Arctic Technology Conference. Offshore Technology Conference.

Griffiths, G., Collins, K., 2007. Masterclass in AUV technology for Polar science: collaborative Autosub science in extreme environments. Proceedings of the International Masterclass, March 2006, National Oceanography Centre, Southampton, UK. Society for Underwater Technology.

Griffiths, G., Jones, C., Ferguson, J., Bose, N., 2007b. Undersea gliders. Journal of Ocean Technology 2 (2), 64-75.

Griffiths, G., Millard, N., McPhail, S., Stevenson, P., Challenor, P., 2003. On the reliability of the Autosub autonomous underwater vehicle. Underwater Technology 25 (4), 175-184. doi:https://doi.org/10.3723/175605403783101612

Griffiths, G., Trembanis, A., 2007. Towards a risk management process for autonomous underwater vehicles. Masterclass in AUV technology for polar science, 103-118.

Guo, C., Khan, F., Imtiaz, S., 2019. Copula-based Bayesian network model for process system risk assessment. Process Safety and Environmental Protection 123, 317-326. doi:https://doi.org/10.1016/j.psep.2019.01.022

Guo, Y., Liu, H., Fan, X., Lyu, W., 2021. Research Progress of Path Planning Methods for Autonomous Underwater Vehicle. Mathematical Problems in Engineering 2021, 8847863. doi:https://doi.org/10.1155/2021/8847863

Gwyther, D.E., Spain, E., King, P., Guihen, D., Williams, G.D., Evans, E., Cook, S., Richter, O., Galton-Fenzi, B.K., Coleman, R., 2020. Cold ocean cavity and weak basal melting of the Sørsdal ice shelf revealed by surveys using autonomous platforms. Journal of Geophysical Research: Oceans 125 (6), e2019JC015882. doi:https://doi.org/10.1029/2019JC015882

Haimes, Y.Y., 2009. On the complex definition of risk: A systems-based approach. Risk Analysis: An International Journal 29 (12), 1647-1654. doi:https://doi.org/10.1111/j.1539-6924.2009.01310.x

Harris, C.A., Phillips, A.B., Dopico-Gonzalez, C., Brito, M.P., 2016. Risk and reliability modelling for multi-vehicle marine domains, 2016 IEEE/OES Autonomous Underwater Vehicles (AUV). IEEE, Tokyo, pp. 286-293.

Hart, P.E., Nilsson, N.J., Raphael, B., 1968. A Formal Basis for the Heuristic Determination of Minimum Cost Paths. IEEE Transactions on Systems Science and Cybernetics 4 (2), 100-107. doi:https://10.1109/TSSC.1968.300136

Hashemi, S.J., Khan, F., Ahmed, S., 2016. Multivariate probabilistic safety analysis of process facilities using the Copula Bayesian Network model. Computers & Chemical Engineering 93, 128-142. doi:https://doi.org/10.1016/j.compchemeng.2016.06.011

Hashemi, S.J., Khan, F., Ahmed, S., 2019. An Insurance Model for Risk Management of Process Facilities. Risk Analysis 39 (3), 713-728. doi:https://doi.org/10.1111/risa.13179

Hegde, J., Henriksen, E.H., Utne, I.B., Schjølberg, I., 2019. Development of safety envelopes and subsea traffic rules for autonomous remotely operated vehicles. Journal of Loss Prevention in the Process Industries 60, 145-158. doi:https://doi.org/10.1016/j.jlp.2019.03.006

Hegde, J., Rokseth, B., 2020. Applications of machine learning methods for engineering risk assessment–A review. Safety Science 122, 104492. doi:https://doi.org/10.1016/j.ssci.2019.09.015

Hegde, J., Utne, I.B., Schjølberg, I., 2016a. Development of collision risk indicators for autonomous subsea inspection maintenance and repair. Journal of Loss Prevention in the Process Industries 44, 440-452. doi:https://doi.org/10.1016/j.jlp.2016.11.002

Hegde, J., Utne, I.B., Schjølberg, I., Thorkildsen, B., 2018. A Bayesian approach to risk modeling of autonomous subsea intervention operations. Reliability Engineering & System Safety 175, 142-159. doi:https://doi.org/10.1016/j.ress.2018.03.019

Hegde, J., Utne, I.B., Schjølberg, I.J.J.o.L.P.i.t.P.I., 2016b. Development of collision risk indicators for autonomous subsea inspection maintenance and repair. 44, 440-452.

Ho, G., Pavlovic, N., Arrabito, R., 2011. Human factors issues with operating unmanned underwater vehicles, Proceedings of the Human Factors and Ergonomics Society Annual Meeting. SAGE Publications Sage CA: Los Angeles, CA, pp. 429-433.

Hollinger, G.A., Pereira, A.A., Binney, J., Somers, T., Sukhatme, G.S., 2016. Learning uncertainty in ocean current predictions for safe and reliable navigation of underwater vehicles. Journal of Field Robotics 33 (1), 47-66. doi:https://doi.org/10.1002/rob.21613

Hossain, N.U.I., Nur, F., Hosseini, S., Jaradat, R., Marufuzzaman, M., Puryear, S.M., 2019. A Bayesian network based approach for modeling and assessing resilience: A case study of a full service deep water port. Reliability Engineering & System Safety 189, 378-396. doi:https://doi.org/10.1016/j.ress.2019.04.037

Hu, Z., Yang, Y., Lin, Y., 2013. Failure analysis for the mechanical system of autonomous underwater vehicles, 2013 International Conference on Quality, Reliability, Risk, Maintenance, and Safety Engineering (QR2MSE). , pp. 943-948.

Huang, W., Zhang, Y., Kou, X., Yin, D., Mi, R., Li, L., 2020. Railway dangerous goods transportation system risk analysis: An Interpretive Structural Modeling and Bayesian Network combining approach. Reliability Engineering & System Safety 204, 107220. doi:https://doi.org/10.1016/j.ress.2020.107220

Hwang, J., Bose, N., Fan, S., 2019. AUV Adaptive Sampling Methods: A Review. Applied Sciences 9 (15), 3145. doi:https://doi:10.3390/app9153145

Hwang, J., Bose, N., Nguyen, H.D., Williams, G., 2020. Acoustic Search and Detection of Oil

Plumes Using an Autonomous Underwater Vehicle. Journal of Marine Science and Engineering 8 (8), 618. doi:https://doi:10.3390/jmse8080618

Jäger, W.S., Christie, E.K., Hanea, A.M., den Heijer, C., Spencer, T., 2018. A Bayesian network approach for coastal risk analysis and decision making. Coastal Engineering 134, 48-61. doi:https://doi.org/10.1016/j.coastaleng.2017.05.004

Jenkins, A., Dutrieux, P., Jacobs, S.S., McPhail, S.D., Perrett, J.R., Webb, A.T., White, D., 2010. Observations beneath Pine Island Glacier in West Antarctica and implications for its retreat. Nature Geoscience 3 (7), 468-472. doi:https://doi.org/10.1038/ngeo890

Ji, C., Beegle-Krause, C.J., Englehardt, J.D., 2020. Formation, Detection, and Modeling of Submerged Oil: A Review. Journal of Marine Science and Engineering 8 (9), 642. doi:https://doi:10.3390/jmse8090642

Jian, X., Zou, T., Vardy, A., Bose, N., 2020. A Hybrid Path Planning Strategy of Autonomous Underwater Vehicles, 2020 IEEE/OES Autonomous Underwater Vehicles Symposium (AUV), pp. 1-6.

Johansen, T., Blindheim, S., Torben, T.R., Utne, I.B., Johansen, T.A., Sørensen, A.J., 2023. Development and testing of a risk-based control system for autonomous ships. Reliability Engineering & System Safety 234, 109195. doi:https://doi.org/10.1016/j.ress.2023.109195

Johansen, T., Utne, I.B., 2022. Supervisory risk control of autonomous surface ships. Ocean Engineering 251, 111045. doi:https://doi.org/10.1016/j.oceaneng.2022.111045

Johnson, N., Patron, P., Lane, D., 2007. The importance of trust between operator and AUV: Crossing the human/computer language barrier, OCEANS 2007-Europe. IEEE, pp. 1-6.

Johnson, N.A., Lane, D.M., 2011. Narrative monologue as a first step towards advanced mission debrief for AUV operator situational awareness, 2011 15th International Conference on Advanced Robotics (ICAR). IEEE, pp. 241-246.

Kaminski, C., Crees, T., Ferguson, J., Forrest, A., Williams, J., Hopkin, D., Heard, G., 2010. 12 days under ice–an historic AUV deployment in the Canadian High Arctic, 2010 IEEE/OES Autonomous Underwater Vehicles. IEEE, Monterey, CA, pp. 1-11.

Kammouh, O., Gardoni, P., Cimellaro, G.P., 2020. Probabilistic framework to evaluate the resilience of engineering systems using Bayesian and dynamic Bayesian networks.

Reliability Engineering & System Safety 198, 106813. doi:https://doi.org/10.1016/j.ress.2020.106813

Karaman, S., Walter, M.R., Perez, A., Frazzoli, E., Teller, S., 2011. Anytime Motion Planning using the RRT*, 2011 IEEE International Conference on Robotics and Automation, pp. 1478-1483.

Khakzad, N., 2015. Application of dynamic Bayesian network to risk analysis of domino effects in chemical infrastructures. Reliability Engineering & System Safety 138, 263-272. doi:https://doi.org/10.1016/j.ress.2015.02.007

Khakzad, N., Khan, F., Amyotte, P., 2011. Safety analysis in process facilities: Comparison of fault tree and Bayesian network approaches. Reliability Engineering & System Safety 96 (8), 925-932. doi:https://doi.org/10.1016/j.ress.2011.03.012

Khan, B., Khan, F., Veitch, B., 2020. A Dynamic Bayesian Network model for ship-ice collision risk in the Arctic waters. Safety Science 130, 104858. doi:https://doi.org/10.1016/j.ssci.2020.104858

Khan, F., Rathnayaka, S., Ahmed, S., 2015. Methods and models in process safety and risk management: Past, present and future. Process safety environmental protection 98, 116-147. doi:https://doi.org/10.1016/j.psep.2015.07.005

Kinsey, J.C., Yoerger, D.R., Jakuba, M.V., Camilli, R., Fisher, C.R., German, C.R., 2011. Assessing the Deepwater Horizon oil spill with the sentry autonomous underwater vehicle, 2011 IEEE/RSJ International Conference on Intelligent Robots and Systems, pp. 261-267.

Kleiner, A., Cheramie, J., Dean, J., Raye, R., 2011. Ice class AUV development, OTC Arctic Technology Conference. Offshore Technology Conference, Houston, Texas, USA.

Kobayashi, M., Motoi, N., 2022. Local Path Planning: Dynamic Window Approach With Virtual Manipulators Considering Dynamic Obstacles. IEEE Access 10, 17018-17029. doi:https://10.1109/ACCESS.2022.3150036

Kukulya, A., Plueddemann, A., Austin, T., Stokey, R., Purcell, M., Allen, B., Littlefield, R., Freitag, L., Koski, P., Gallimore, E., 2010. Under-ice operations with a REMUS-100 AUV in the Arctic, 2010 IEEE/OES Autonomous Underwater Vehicles. IEEE, Monterey, CA, pp. 1-8.

Lefebvre, N., Schjølberg, I., Utne, I.B., 2016. Integration of risk in hierarchical path planning of underwater vehicles. IFAC-PapersOnLine 49 (23), 226-231. doi:https://doi.org/10.1016/j.ifacol.2016.10.347

Leveson, N.G., 2011. Applying systems thinking to analyze and learn from events. Safety Science 49 (1), 55-64. doi:https://doi.org/10.1016/j.ssci.2009.12.021

Leveson, N.G., Thomas, J.P., 2018. STPA handbook. Cambridge, MA, USA.

Li, J., Kang, H., Park, G., Suh, J., 2017. Real Time Path Planning of Underwater Robots in Unknown Environment, 2017 International Conference on Control, Artificial Intelligence, Robotics & Optimization (ICCAIRO), pp. 312-318.

Li, M., Zhang, H., 2020. AUV 3D Path Planning Based On A Algorithm, 2020 Chinese Automation Congress (CAC), pp. 11-16.

Lin, C.-T., Wang, M.-J.J., 1997. Hybrid fault tree analysis using fuzzy sets. Reliability Engineering & System Safety 58 (3), 205-213. doi:https://doi.org/10.1016/S0951-8320(97)00072-0

Lippsett, L., 2010. RIPABE: the pioneering Autonomous Benthic Explorer is lost at sea. Oceanus 48 (1), 42-44.

Lisnianski, A., Elmakias, D., Laredo, D., Ben Haim, H., 2012. A multi-state Markov model for a short-term reliability analysis of a power generating unit. Reliability Engineering & System Safety 98 (1), 1-6. doi:https://doi.org/10.1016/j.ress.2011.10.008

Liu, L., Yao, J., He, D., Chen, J., Huang, J., Xu, H., Wang, B., Guo, J., 2021. Global Dynamic Path Planning Fusion Algorithm Combining Jump-A* Algorithm and Dynamic Window Approach. IEEE Access 9, 19632-19638. doi:https://10.1109/ACCESS.2021.3052865

Liu, W., Liu, Y., Bucknall, R., 2022. Filtering based multi-sensor data fusion algorithm for a reliable unmanned surface vehicle navigation. Journal of Marine Engineering & Technology, 1-17. doi:https://doi.org/10.1080/20464177.2022.2031558

Locorotondo, E., Cultrera, V., Pugi, L., Berzi, L., Pierini, M., Lutzemberger, G., 2021. Development of a battery real-time state of health diagnosis based on fast impedance measurements. Journal of Energy Storage 38, 102566. doi:https://doi.org/10.1016/j.est.2021.102566

Loh, T.Y., Brito, M.P., Bose, N., Xu, J., Nikolova, N., Tenekedjiev, K., 2020a. A hybrid fuzzy system dynamics approach for risk analysis of AUV operations. Journal of Advanced Computational Intelligence and Intelligent Informatics 24 (1), 26-39. doi:https://doi.org/10.20965/jaciii.2020.p0026

Loh, T.Y., Brito, M.P., Bose, N., Xu, J., Tenekedjiev, K., 2019. A Fuzzy-Based Risk Assessment Framework for Autonomous Underwater Vehicle Under-Ice Missions. Risk Analysis 39 (12), 2744-2765. doi:https://doi.org/10.1111/risa.13376

Loh, T.Y., Brito, M.P., Bose, N., Xu, J., Tenekedjiev, K., 2020b. Fuzzy system dynamics risk analysis (FuSDRA) of autonomous underwater vehicle operations in the Antarctic. Risk Analysis 40 (4), 818-841. doi:https://doi.org/10.1111/risa.13429

Loh, T.Y., Brito, M.P., Bose, N., Xu, J., Tenekedjiev, K., 2020c. Human Error in Autonomous Underwater Vehicle Deployment: A System Dynamics Approach. Risk Analysis 40 (6), 1258-1278. doi:https://doi.org/10.1111/risa.13467

Madsen, H.Ø., Christensen, P., Lauridsen, K., 2000. Securing the operational reliability of an autonomous mini-submarine. Reliability Engineering & System Safety 68 (1), 7-16. doi:https://doi.org/10.1016/S0951-8320(99)00077-0

Maksym, T., Singh, H., Bassett, C., Lavery, A., Freitag, L., Sonnichsen, F., Wilkinson, J., 2014. Oil Spill Detection and mapping under arctic sea ice using autonomous underwater vehicles. BSEE Contract E12PC00053.

Manley, J.E., 2007. The role of risk in auv development and deployment, OCEANS 2007-Europe. IEEE, pp. 1-6.

McPhail, S.D.P., Miles, 1998. Navigation and control of an autonomous underwater vehicle using a distributed, networked, control architecture. Oceanographic Literature Review 7 (45), 1240.

Meng, L., Qingyu, Y., 2010. Enhanced safety control and self-rescue system applied in AUV, 2010 International Conference on Intelligent Computation Technology and Automation. IEEE, pp. 212-215.

Merckelbach, L., 2013a. On the probability of underwater glider loss due to collision with a ship. Journal of Marine Science Technology 18 (1), 75-86. doi:https://doi.org/10.1007/s00773-012-0189-7

Merckelbach, L., 2013b. On the probability of underwater glider loss due to collision with a ship. Journal of Marine Science and Technology 18 (1), 75-86. doi:https://doi.org/10.1007/s00773-012-0189-7

Meyer, D., 2016. Glider Technology for Ocean Observations: A Review. Ocean Sci. Discuss. 2016, 1-26. doi:https://doi.org/10.5194/os-2016-40

Nakhaeinia, D., Payeur, P., Hong, T.S., Karasfi, B., 2015. A hybrid control architecture for autonomous mobile robot navigation in unknown dynamic environment, 2015 IEEE International Conference on Automation Science and Engineering (CASE), pp. 1274-1281.

Nelsen, R.B., 2006. An introduction to copulas. Springer Science & Business Media.

Oakey, G.N., Moir, P.N., Brent, T., Dickie, K., Jauer, C., Bennett, R., Williams, G., MacLean, B., Budkewitsch, P., Haggart, J., 2012. The Scott Inlet–Buchan Gulf oil seeps: actively venting petroleum systems on the northern Baffin margin offshore Nunavut, Canada, Canadian Society of Petroleum Geologists, Annual Convention, Calgary, Alberta.

Obeng, F., Domeh, V., Khan, F., Bose, N., Sanli, E., 2022. Analyzing operational risk for small fishing vessels considering crew effectiveness. Ocean Engineering 249, 110512. doi:https://doi.org/10.1016/j.oceaneng.2021.110512

Oliver, M.J., Breece, M.W., Fox, D.A., Haulsee, D.E., Kohut, J.T., Manderson, J., Savoy, T., 2013. Shrinking the haystack: using an AUV in an integrated ocean observatory to map Atlantic Sturgeon in the coastal ocean. Fisheries 38 (5), 210-216. doi:https://doi.org/10.1080/03632415.2013.782861

Ortiz, A., Proenza, J., Bernat, G., Oliver, G., 1999. Improving the safety of AUVs, Oceans' 99. MTS/IEEE. Riding the Crest into the 21st Century. Conference and Exhibition. Conference Proceedings (IEEE Cat. No. 99CH37008). IEEE, Seattle, WA, USA, pp. 979-984.

Pan, Y., Ou, S., Zhang, L., Zhang, W., Wu, X., Li, H., 2019. Modeling risks in dependent systems: A Copula-Bayesian approach. Reliability Engineering & System Safety 188, 416-431. doi:https://doi.org/10.1016/j.ress.2019.03.048

Pan, Y., Zhang, L., Koh, J., Deng, Y., 2021. An adaptive decision making method with copula Bayesian network for location selection. Information Sciences 544, 56-77. doi:https://doi.org/10.1016/j.ins.2020.07.063

Parasuraman, R., Miller, C.A., 2004. Trust and etiquette in high-criticality automated systems. Communications of the ACM 47 (4), 51-55. doi:https://doi.org/10.1145/975817.975844

Pärt, S., Kõuts, T., Vahter, K., 2017. Oil detection using oil sensors on autonomous underwater vehicles. D1.5. wp1: oil spill detection, monitoring, fate and distribution. Integrated Oil Spill Response Actions and Environmental Effects Project (GRACE).

Paté-Cornell, E., Dillon, R., 2001. Probabilistic risk analysis for the NASA space shuttle: a brief history and current work. Reliability Engineering & System Safety 74 (3), 345-352. doi:https://doi.org/10.1016/S0951-8320(01)00081-3

Paull, L., Saeedi, S., Seto, M., Li, H., 2014. AUV Navigation and Localization: A Review. IEEE Journal of Oceanic Engineering 39 (1), 131-149. doi:https://doi.org/10.1109/JOE.2013.2278891

Pearl, J., 1986. Fusion, propagation, and structuring in belief networks. Artificial Intelligence 29 (3), 241-288. doi:https://doi.org/10.1016/0004-3702(86)90072-X

Pebody, M., 2008. Autonomous underwater vehicle collision avoidance for under-ice exploration. Proceedings of the Institution of Mechanical Engineers, Part M: Journal of Engineering for the Maritime Environment 222 (2), 53-66. doi:https://doi.org/10.1243%2F14750902JEME81

Pereira, A.A., Binney, J., Hollinger, G.A., Sukhatme, G.S., 2013. Risk-aware path planning for autonomous underwater vehicles using predictive ocean models. Journal of Field Robotics 30 (5), 741-762. doi:https://doi.org/10.1002/rob.21472

Pereira, A.A., Binney, J., Jones, B.H., Ragan, M., Sukhatme, G.S., 2011. Toward risk aware mission planning for Autonomous Underwater Vehicles, 2011 IEEE/RSJ International Conference on Intelligent Robots and Systems, pp. 3147-3153.

Petillo, S.M., Schmidt, H., 2012. Autonomous and adaptive underwater plume detection and tracking with AUVs: Concepts, methods, and available technology. IFAC Proceedings Volumes 45 (27), 232-237. doi:https://doi.org/10.3182/20120919-3-IT-2046.00040

Pugi, L., Allotta, B., Pagliai, M., 2018. Redundant and reconfigurable propulsion systems to improve motion capability of underwater vehicles. Ocean Engineering 148, 376-385. doi:https://doi.org/10.1016/j.oceaneng.2017.11.039

Rachman, A., Ratnayake, R.M.C., 2019. Machine learning approach for risk-based inspection screening assessment. Reliability Engineering & System Safety 185, 518-532. doi:https://doi.org/10.1016/j.ress.2019.02.008

Ramoni, M., Sebastiani, P., 2001. Robust learning with missing data. Machine Learning 45 (2), 147-170. doi:https://doi.org/10.1023/A:1010968702992

Rasmussen, J., 1997. Risk management in a dynamic society: a modelling problem. Safety Science 27 (2), 183-213. doi:https://doi.org/10.1016/S0925-7535(97)00052-0

Rausand, M., 2013. Risk assessment: theory, methods, and applications. John Wiley & Sons.

Rausand, M., Høyland, A., 2003. System reliability theory: models, statistical methods, and applications. John Wiley & Sons.

Reich, D., Etkin, D., Rowe, G., Zamorski, S., 2016. Modeling oil spill trajectories in Baffin Bay and Lancaster Sound. WWF-Canada Oil Spill Modeling Report.

Reiss, C.S., Cossio, A.M., Walsh, J., Cutter, G.R., Watters, G.M., 2021. Glider-Based Estimates of Meso-Zooplankton Biomass Density: A Fisheries Case Study on Antarctic Krill (Euphausia superba) Around the Northern Antarctic Peninsula. Frontiers in Marine Science 8. doi:https://doi.org/10.3389/fmars.2021.604043

Riedmann, R.A., Gasic, B., Vernez, D., 2015. Sensitivity Analysis, Dominant Factors, and Robustness of the ECETOC TRA v3, Stoffenmanager 4.5, and ART 1.5 Occupational Exposure Models. Risk Analysis 35 (2), 211-225. doi:https://doi.org/10.1111/risa.12286

Roper, D., Harris, C.A., Salavasidis, G., Pebody, M., Templeton, R., Prampart, T., Kingsland, M., Morrison, R., Furlong, M., Phillips, A.B., McPhail, S., 2021. Autosub Long Range 6000: A Multiple-Month Endurance AUV for Deep-Ocean Monitoring and Survey. IEEE Journal of Oceanic Engineering 46 (4), 1179-1191. doi:https://10.1109/JOE.2021.3058416

Rositano, F., Piñeiro, G., Bert, F.E., Ferraro, D.O., 2017. A comparison of two sensitivity analysis techniques based on four bayesian models representing ecosystem services provision in the Argentine Pampas. Ecological Informatics 41, 33-39. doi:https://doi.org/10.1016/j.ecoinf.2017.07.005

Rothrock, D., Wensnahan, M., 2007. The accuracy of sea ice drafts measured from US Navy submarines. Journal of Atmospheric Oceanic technology 24 (11), 1936-1949. doi:https://doi.org/10.1175/JTECH2097.1

Rudnick, D.L., Davis, R.E., Eriksen, C.C., Fratantoni, D.M., Perry, M.J., 2004a. Underwater gliders for ocean research. Marine Technology Society Journal 38 (2), 73-84. doi:https://doi.org/10.4031/002533204787522703

Rudnick, D.L., Davis, R.E., Eriksen, C.C., Fratantoni, D.M., Perry, M.J.J.M.T.S.J., 2004b. Underwater gliders for ocean research. 38 (2), 73-84.

Rudnick, D.L., Zarokanellos, N.D., Tintoré, J., 2022. A Four-Dimensional Survey of the Almeria–Oran Front by Underwater Gliders: Tracers and Circulation. Journal of Physical Oceanography 52 (2), 225-242. doi:https://doi.org/10.1175/jpo-d-21-0181.1

Sahoo, A., Dwivedy, S.K., Robi, P.S., 2019. Advancements in the field of autonomous underwater vehicle. Ocean Engineering 181, 145-160. doi:https://doi.org/10.1016/j.oceaneng.2019.04.011

Salavasidis, G., Harris, C., McPhail, S., Phillips, A.B., Rogers, E., 2016. Terrain Aided Navigation for Long Range AUV operations at arctic latitudes, 2016 IEEE/OES Autonomous Underwater Vehicles (AUV). IEEE, Tokyo, pp. 115-123.

Samuel, M., Hussein, M., Mohamad, M.B., 2016. A review of some pure-pursuit based path tracking techniques for control of autonomous vehicle. International Journal of Computer Applications 135 (1), 35-38.

Seto, M.L., 2012. Marine robot autonomy. Springer Science & Business Media.

Shen, Y., Xu, H., Wang, D., Zhang, Y., Yan, T., He, B., 2020. Real-time Obstacle Avoidance for AUV Based on Reinforcement Learning and Dynamic Window Approach, Global Oceans 2020: Singapore – U.S. Gulf Coast, pp. 1-4.

Singh, Y., Sharma, S., Sutton, R., Hatton, D., Khan, A., 2018. A constrained A* approach towards optimal path planning for an unmanned surface vehicle in a maritime environment containing dynamic obstacles and ocean currents. Ocean Engineering 169, 187-201. doi:https://doi.org/10.1016/j.oceaneng.2018.09.016

Sklar, M., 1959. Fonctions de repartition a n dimensions et leurs marges. Publications de l'Institut de Statistique de L'Universite de Paris 8, 229-231.

Smith, R.N., Kelly, J., Sukhatme, G.S., 2012. Towards improving mission execution for autonomous gliders with an ocean model and kalman filter, 2012 IEEE International Conference on Robotics and Automation, pp. 4870-4877.

Song, G., Khan, F., Wang, H., Leighton, S., Yuan, Z., Liu, H., 2016. Dynamic occupational risk model for offshore operations in harsh environments. Reliability Engineering & System Safety 150, 58-64. doi:https://doi.org/10.1016/j.ress.2016.01.021

Strutt, J., 2006. Report of the inquiry into the loss of Autosub2 under the Fimbulisen. National Oceanography Centre Southampton, 39.

Sun, B., Li, Y., Wang, Z., Yang, D., Ren, Y., Feng, Q., 2021a. A combined physics of failure and Bayesian network reliability analysis method for complex electronic systems. Process Safety and Environmental Protection 148, 698-710. doi:https://doi.org/10.1016/j.psep.2021.01.023

Sun, Y., Chen, K., Liu, C., Zhang, Q., Qin, X., 2021b. Research on reliability analytical method of complex system based on CBN model. Journal of Mechanical Science and Technology 35 (1), 107-120. doi:https://doi.org/10.1007/s12206-020-1210-4

Szczerba, R.J., Galkowski, P., Glicktein, I.S., Ternullo, N., 2000. Robust algorithm for real-time route planning. IEEE Transactions on Aerospace and Electronic Systems 36 (3), 869-878. doi:https://10.1109/7.869506

Thieme, C.A., Utne, I.B., 2017. Safety performance monitoring of autonomous marine systems. Reliability Engineering & System Safety 159, 264-275. doi:https://doi.org/10.1016/j.ress.2016.11.024

Thieme, C.A., Utne, I.B., Haugen, S., 2018. Assessing ship risk model applicability to Marine Autonomous Surface Ships. Ocean Engineering 165, 140-154. doi:https://doi.org/10.1016/j.oceaneng.2018.07.040

Thieme, C.A., Utne, I.B., Schjølberg, I., 2015a. A risk management framework for unmanned underwater vehicles focusing on human and organizational factors, ASME 2015 34th International Conference on Ocean, Offshore and Arctic Engineering. American Society of Mechanical Engineers Digital Collection.

Thieme, C.A., Utne, I.B., Schjølberg, I., 2015b. Risk modeling of autonomous underwater vehicle operation focusing on the human operator. 25th European Safety and Reliability Conference, 3653–3660.

Ullah, B., Ovinis, M., Baharom, M.B., Ali, S.S.A., Khan, B., Javaid, M.Y., 2020a. Effect of waves and current on motion control of underwater gliders. Journal of Marine Science and Technology 25 (2), 549-562. doi:https://doi.org/10.1007/s00773-019-00660-1

Ullah, B., Ovinis, M., Baharom, M.B., Ali, S.S.A., Khan, B., Javaid, M.Y., 2020b. Effect of waves and current on motion control of underwater gliders. Journal of Marine Science Technology 25 (2), 549-562. doi:https://doi.org/10.1007/s00773-019-00660-1

Utne, I.B., Rokseth, B., Sørensen, A.J., Vinnem, J.E., 2020. Towards supervisory risk control of autonomous ships. Reliability Engineering & System Safety 196, 106757. doi:https://doi.org/10.1016/j.ress.2019.106757

Vadakkepat, P., Kay Chen, T., Wang, M.-L., 2000. Evolutionary artificial potential fields and their application in real time robot path planning, Proceedings of the 2000 Congress on Evolutionary Computation. CEC00 (Cat. No.00TH8512), pp. 256-263 vol.251.

Valdez Banda, O.A., Kannos, S., Goerlandt, F., van Gelder, P.H.A.J.M., Bergström, M., Kujala, P., 2019. A systemic hazard analysis and management process for the concept design phase of an autonomous vessel. Reliability Engineering & System Safety 191, 106584. doi:https://doi.org/10.1016/j.ress.2019.106584

Vinoth Kumar, S., Jayaparvathy, R., Priyanka, B.N., 2020. Efficient path planning of AUVs for container ship oil spill detection in coastal areas. Ocean Engineering 217, 107932. doi:https://doi.org/10.1016/j.oceaneng.2020.107932

Wadhams, P., Wilkinson, J.P., McPhail, S., 2006. A new view of the underside of Arctic sea ice. Geophysical Research Letters 33 (4). doi:https://doi.org/10.1029/2005GL025131

Wan, C., Yan, X., Zhang, D., Qu, Z., Yang, Z., 2019. An advanced fuzzy Bayesian-based FMEA approach for assessing maritime supply chain risks. Transportation Research Part E: Logistics and Transportation Review 125, 222-240. doi:https://doi.org/10.1016/j.tre.2019.03.011

Wang, F., Araújo, D.F., Li, Y.-F., Reliability assessment of autonomous vehicles based on the safety control structure. Proceedings of the Institution of Mechanical Engineers, Part O: Journal of Risk and Reliability 0 (0), 1748006X211069705. doi:https://10.1177/1748006x211069705

Wang, H., Liu, Z., Wang, X., Graham, T., Wang, J., 2021a. An analysis of factors affecting the severity of marine accidents. Reliability Engineering & System Safety 210, 107513. doi:https://doi.org/10.1016/j.ress.2021.107513

Wang, L., Pang, S., 2019. Chemical Plume Tracing using an AUV based on POMDP Source Mapping and A-star Path Planning, OCEANS 2019 MTS/IEEE SEATTLE, pp. 1-7.

Wang, S., Yang, M., Niu, W., Wang, Y., Yang, S., Zhang, L., Deng, J., 2021b. Multidisciplinary design optimization of underwater glider for improving endurance. Structural and Multidisciplinary Optimization 63 (6), 2835-2851. doi:https://doi.org/10.1007/s00158-021-02844-z

Wang, T., Dyer, J.S., Butler, J.C., 2016. Modeling Correlated Discrete Uncertainties in Event Trees with Copulas. Risk Analysis 36 (2), 396-410. doi:https://doi.org/10.1111/risa.12451

Wang, W., He, X., Li, Y., Shuai, J., 2022a. Risk analysis on corrosion of submarine oil and gas pipelines based on hybrid Bayesian network. Ocean Engineering 260, 111957. doi:https://doi.org/10.1016/j.oceaneng.2022.111957

Wang, Y., Bose, N., Thanyamanta, W., Bulger, C., Shaikh-Upadhye, S., 2022b. Adaptive control for follower gliders mapping underwater oil patches. Journal of Hazardous Materials 436, 129039. doi:https://doi.org/10.1016/j.jhazmat.2022.129039

Wang, Y., Bulger, C., Thanyamanta, W., Bose, N., 2021c. A Backseat Control Architecture for a Slocum Glider. Journal of Marine Science and Engineering 9 (5), 532. doi:https://doi.org/10.3390/jmse9050532

Wang, Y., Thanyamanta, W., Bulger, C., Bose, N., 2022c. Experimental study to make gas bubbles as proxies for oil droplets to test AUV detection of oil plumes. Applied Ocean Research 121, 103080. doi:https://doi.org/10.1016/j.apor.2022.103080

Wang, Z., Xiang, X., Yang, J., Yang, S., 2017. Composite Astar and B-spline algorithm for path planning of autonomous underwater vehicle, 2017 IEEE 7th International Conference on Underwater System Technology: Theory and Applications (USYS), pp. 1-6.

Waters, H., 2015. The robots that dare to explore Antarctica’s frozen ocean. Retrieved from https://www.vice.com/en/article/nzex4z/the-robots-that-dare-to-explore-antarcticas-frozen-ocean.

Webb, D.C., Simonetti, P.J., Jones, C.P., 2001. SLOCUM: an underwater glider propelled by environmental energy. IEEE Journal of Oceanic Engineering 26 (4), 447-452.

doi:https://10.1109/48.972077

White, H.K., Conmy, R.N., MacDonald, I.R., Reddy, C.M., 2016. Methods of Oil Detection in Response to the Deepwater Horizon Oil Spill. Oceanography 29 (3), 76-87.

Williams, G., Maksym, T., Wilkinson, J., Kunz, C., Murphy, C., Kimball, P., Singh, H., 2015. Thick and deformed Antarctic sea ice mapped with autonomous underwater vehicles. Nature Geoscience 8 (1), 61-67. doi:https://doi.org/10.1038/ngeo2299

Wróbel, K., Montewka, J., Kujala, P., 2017. Towards the assessment of potential impact of unmanned vessels on maritime transportation safety. Reliability Engineering & System Safety 165, 155-169. doi:https://doi.org/10.1016/j.ress.2017.03.029

Wróbel, K., Montewka, J., Kujala, P., 2018a. System-theoretic approach to safety of remotely-controlled merchant vessel. Ocean Engineering 152, 334-345. doi:https://doi.org/10.1016/j.oceaneng.2018.01.020

Wróbel, K., Montewka, J., Kujala, P., 2018b. Towards the development of a system-theoretic model for safety assessment of autonomous merchant vessels. Reliability Engineering & System Safety 178, 209-224. doi:https://doi.org/10.1016/j.ress.2018.05.019

Xiang, X., Jouvencel, B., Parodi, O., 2010. Coordinated Formation Control of Multiple Autonomous Underwater Vehicles for Pipeline Inspection. International Journal of Advanced Robotic Systems 7 (1), 3. doi:https://10.5772/7242

Xiang, X., Yu, C., Zhang, Q., 2017. On intelligent risk analysis and critical decision of underwater robotic vehicle. Ocean Engineering 140, 453-465. doi:https://doi.org/10.1016/j.oceaneng.2017.06.020

Xu, H., Li, G., Liu, J., 2013. Reliability analysis of an autonomous underwater vehicle using fault tree, 2013 IEEE International Conference on Information and Automation (ICIA). IEEE, pp. 1165-1170.

Xu, J., Loh, T.Y., Brito, M.P., Bose, N., Tenekedjiev, K., 2020. Policy recommendations for autonomous underwater vehicle operations through hybrid Fuzzy System Dynamics Risk Analysis (FuSDRA). Proceeding of the International Association of Maritime Universities Conference (IAMUC 2019), 143-149.

Yan, Z., Zhang, J., Zeng, J., Tang, J., 2022. Three-dimensional path planning for autonomous underwater vehicles based on a whale optimization algorithm. Ocean Engineering 250, 111070. doi:https://doi.org/10.1016/j.oceaneng.2022.111070

Yang, R., Utne, I., Liu, Y., Paltrinieri, N., 2020. Dynamic risk analysis of operation of the autonomous underwater vehicle (auv). The 30th European Safety and Reliability Conference and the 15th Probabilistic Safety Assessment and Management.

Yang, R., Utne, I.B., 2022. Towards an online risk model for autonomous marine systems (AMS). Ocean Engineering 251, 111100. doi:https://doi.org/10.1016/j.oceaneng.2022.111100

Yang, X., Haugen, S., 2016. Risk information for operational decision-making in the offshore oil and gas industry. Safety Science 86, 98-109. doi:https://doi.org/10.1016/j.ssci.2016.02.022

Yang, Y., Khan, F., Thodi, P., Abbassi, R., 2017a. Corrosion induced failure analysis of subsea pipelines. Reliability Engineering & System Safety 159, 214-222. doi:https://doi.org/10.1016/j.ress.2016.11.014

Yang, Y., Liu, Y., Wang, Y., Zhang, H., Zhang, L., 2017b. Dynamic modeling and motion control strategy for deep-sea hybrid-driven underwater gliders considering hull deformation and seawater density variation. Ocean Engineering 143, 66-78. doi:https://doi.org/10.1016/j.oceaneng.2017.07.047

Yao, X., Wang, F., Wang, J., Zhao, J., 2018. Time-optimal Path Planning to Solve Motion Direction Restrict with Lower Computational Cost, 2018 37th Chinese Control Conference (CCC), pp. 5245-5250.

Yazdi, M., Kabir, S., 2017. A fuzzy Bayesian network approach for risk analysis in process industries. Process Safety and Environmental Protection 111, 507-519. doi:https://doi.org/10.1016/j.psep.2017.08.015

Yazdi, M., Khan, F., Abbassi, R., 2021. Microbiologically influenced corrosion (MIC) management using Bayesian inference. Ocean Engineering 226, 108852. doi:https://doi.org/10.1016/j.oceaneng.2021.108852

Yazdi, M., Zarei, E., 2018. Uncertainty Handling in the Safety Risk Analysis: An Integrated Approach Based on Fuzzy Fault Tree Analysis. Journal of Failure Analysis and Prevention 18 (2), 392-404. doi:https://doi.org/10.1007/s11668-018-0421-9

Yu, M., Venkidasalapathy, J., Shen, Y., Quddus, N., Mannan, S.M., 2017. Bow-tie analysis of underwater robots in offshore oil and gas operations, Offshore Technology Conference. Offshore Technology Conference, Houston, Texas, USA.

Yu, Q., Liu, K., Yang, Z., Wang, H., Yang, Z., 2021. Geometrical risk evaluation of the collisions between ships and offshore installations using rule-based Bayesian reasoning. Reliability Engineering & System Safety 210, 107474. doi:https://doi.org/10.1016/j.ress.2021.107474

Yuan, Z., Khakzad, N., Khan, F., Amyotte, P., 2015. Risk Analysis of Dust Explosion Scenarios Using Bayesian Networks. Risk Analysis 35 (2), 278-291. doi:https://doi.org/10.1111/risa.12283

Zarei, E., Khan, F., Abbassi, R., 2022. A dynamic human-factor risk model to analyze safety in sociotechnical systems. Process Safety and Environmental Protection 164, 479-498. doi:https://doi.org/10.1016/j.psep.2022.06.040

Zeng, Z., Lian, L., Sammut, K., He, F., Tang, Y., Lammas, A., 2015. A survey on path planning for persistent autonomy of autonomous underwater vehicles. Ocean Engineering 110, 303-313. doi:https://doi.org/10.1016/j.oceaneng.2015.10.007

Zhang, C., Cheng, P., Du, B., Dong, B., Zhang, W., 2022. AUV path tracking with real-time obstacle avoidance via reinforcement learning under adaptive constraints. Ocean Engineering 256, 111453. doi:https://doi.org/10.1016/j.oceaneng.2022.111453

Zhang, H., Zhang, S., Wang, Y., Liu, Y., Yang, Y., Zhou, T., Bian, H., 2021. Subsea pipeline leak inspection by autonomous underwater vehicle. Applied Ocean Research 107, 102321. doi:https://doi.org/10.1016/j.apor.2020.102321

Zhang, M., Wang, Y., Xu, J., Liu, Z., 2015. Thruster fault diagnosis in autonomous underwater vehicle based on grey qualitative simulation. Ocean Engineering 105, 247-255. doi:https://doi.org/10.1016/j.oceaneng.2015.06.037

Zhang, Y., McEwen, R.S., Ryan, J.P., Bellingham, J.G., Thomas, H., Thompson, C.H., Rienecker, E., 2011. A peak-capture algorithm used on an autonomous underwater vehicle in the 2010 Gulf of Mexico oil spill response scientific survey. Journal of Field Robotics 28 (4), 484-496. doi:https://doi.org/10.1002/rob.20399

Zhou, Q., Wong, Y.D., Loh, H.S., Yuen, K.F., 2018. A fuzzy and Bayesian network CREAM model for human reliability analysis – The case of tanker shipping. Safety Science 105, 149-157. doi:https://doi.org/10.1016/j.ssci.2018.02.011

Zhou, T., Modarres, M., Droguett, E.L., 2021. Multi-unit nuclear power plant probabilistic risk assessment: A comprehensive survey. Reliability Engineering & System Safety 213, 107782. doi:https://doi.org/10.1016/j.ress.2021.107782

Zhu, K., Mu, L., Xia, X., 2021. An ensemble trajectory prediction model for maritime search and rescue and oil spill based on sub-grid velocity model. Ocean Engineering 236, 109513. doi:https://doi.org/10.1016/j.oceaneng.2021.109513

Zilko, A.A., Kurowicka, D., Goverde, R.M.P., 2016. Modeling railway disruption lengths with Copula Bayesian Networks. Transportation Research Part C: Emerging Technologies 68, 350-368. doi:https://doi.org/10.1016/j.trc.2016.04.018

Zwolak, K., Simpson, B., Anderson, B., Bazhenova, E., Falconer, R., Kearns, T., Minami, H., Roperez, J., Rosedee, A., Sade, H., Tinmouth, N., Wigley, R., Zarayskaya, Y., 2017. An unmanned seafloor mapping system: The concept of an AUV integrated with the newly designed USV SEA-KIT, OCEANS 2017 - Aberdeen, pp. 1-6.